



Norwegian University of  
Science and Technology

# Simulation and analysis of FCR operation of a Francis turbine

**Anna Holm Aftret**

Master of Energy and Environmental Engineering

Submission date: June 2017

Supervisor: Pål Tore Selbo Storli, EPT

Norwegian University of Science and Technology  
Department of Energy and Process Engineering



EPT-M-2017-02

**MASTER THESIS**

for

Student Anna Holm Aftret

Spring 2017

Simulation and analysis of FCR operation of a Francis turbine

*Simulering og analyse av FCR- drift av en Francisturbin***Background and objective**

The Nordic TSOs are about to implement new demands for delivery of primary governing, FCR (frequency containment reserves). Power plants may have to undergo qualification tests to participate in FCR-delivery. The tests contain simulations of step and sinusoidal frequency disturbance in governor. If the hydropower system and governor is qualified, this can give incentives for changing the governor parameters, in order to deliver more governing capacity.

Objective:

Develop a trustworthy numerical model, and simulate the qualification test for FCR delivery for a specified hydropower plant, and determine if the plant can comply with the qualification criteria for different modes of governing and grid stabilisation.

**The following tasks are to be considered:**

1. Literature review of system dynamics and hydraulic turbine governing
2. Simulate the test for qualification of FCR deliveries for different PID parameters using the current PID governor at the hydro power plant
3. Make a conclusion regarding the possibilities for the current plant to participate in the FCR delivery market
4. Investigate other governor setups in order to find if they are better in obtaining safe, stable and rapid governing of FCR operation
5. The previous project work and the future work in this thesis shall be described in a paper which will be presented at 7<sup>th</sup> International symposium on Current Research in Hydraulic Turbines (CRHT-VII) at Kathmandu University in April 2017

-- ” --

Within 14 days of receiving the written text on the master thesis, the candidate shall submit a research plan for his project to the department.

When the thesis is evaluated, emphasis is put on processing of the results, and that they are presented in tabular and/or graphic form in a clear manner, and that they are analysed carefully.

The thesis should be formulated as a research report with summary both in English and Norwegian, conclusion, literature references, table of contents etc. During the preparation of the text, the candidate should make an effort to produce a well-structured and easily readable report. In order to ease the evaluation of the thesis, it is important that the cross-references are correct. In the making of the report, strong emphasis should be placed on both a thorough discussion of the results and an orderly presentation.

The candidate is requested to initiate and keep close contact with his/her academic supervisor(s) throughout the working period. The candidate must follow the rules and regulations of NTNU as well as passive directions given by the Department of Energy and Process Engineering.

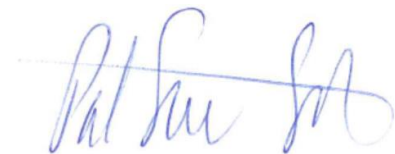
Risk assessment of the candidate's work shall be carried out according to the department's procedures. The risk assessment must be documented and included as part of the final report. Events related to the candidate's work adversely affecting the health, safety or security, must be documented and included as part of the final report. If the documentation on risk assessment represents a large number of pages, the full version is to be submitted electronically to the supervisor and an excerpt is included in the report.

Pursuant to "Regulations concerning the supplementary provisions to the technology study program/Master of Science" at NTNU §20, the Department reserves the permission to utilize all the results and data for teaching and research purposes as well as in future publications.

The final report is to be submitted digitally in DAIM. An executive summary of the thesis including title, student's name, supervisor's name, year, department name, and NTNU's logo and name, shall be submitted to the department as a separate pdf file. Based on an agreement with the supervisor, the final report and other material and documents may be given to the supervisor in digital format.

- Work to be done in lab (Water power lab, Fluids engineering lab, Thermal engineering lab)
- Field work

Department of Energy and Process Engineering, 15. January 2017



---

Pål-Tore Storli  
Academic Supervisor

Research Advisor: Jørgen Ramdal, Statkraft AS.

# Preface

This thesis was written at the Water Power laboratory in Trondheim, Department of Energy and Process Engineering at NTNU during the spring of 2017. It is my sincere wish that this thesis will be of aid in the frequency containment process project and be helpful for future students and people aiming to develop a simulation model of a hydro power plant. I really enjoyed working with this project and hope that readers of this document find it interesting.

I would like to thank my supervisor Pål-Tore Storli for always keeping his door open and welcoming questions and discussions. My co-supervisors Petter Lie and Jørgen Ramdal also deserves acknowledgement for answering my questions even at unfortunate times. The social environment at the Water Power lab has also been of great importance, and I would like to thank my fellow students for a memorable year.

Last, but not least, I would like to thank Jon-Inge for supporting me in my final year at NTNU.

Anna Holm Aftret  
Trondheim, 13 June 2017



# Abstract

In the Nordic power system, the frequency quality has decreased significantly over the years. One of the reasons for this is a superimposed periodic frequency oscillation with a time period of around 40-90 seconds, which may be due to the increasing amount of unregulated power in the Nordic grid [2]. To increase the frequency quality, a project was initiated to find measures to mitigate the oscillations. From this project, a set of qualification tests for primary governing was specified. Primary governing, also known as frequency containment reserves (FCR), is the first response to a change in frequency of the grid. For a unit to participate in the delivery of FCR, the plant has to pass the requirements set by the project group.

For this reason, Statkraft initiated that a simulation model of Songa hydro power plant should be developed, to perform the qualification tests and assess whether the plant can deliver FCR according to the new requirements. A simulation model was therefore constructed in MATLAB using the Method of Characteristics and equations describing the behaviour of the turbine and governor, as well as a generator connected to the grid.

Frequency containment reserves are divided into two categories, normal and disturbance. The FCR-N delivery is tested by applying a frequency step response and sine sweep. From these tests, the capacity, dynamic performance and stability can be determined from the power response of the unit. Based on the gain and phase of the sinusoidal response, a set of vectors in the complex plane, corresponding to a certain frequency time period, can be developed. These vectors are plotted with circles illustrating the requirements for the dynamic performance and stability. The criteria is fulfilled if the vectors point outside the circle. A final stability verification is performed by a Nyquist diagram obtained by multiplying the FCR-Vectors with a mathematical expression for the grid. The unit has sufficient stability if the Nyquist plot passes the point  $(-1, j0)$  on the right hand side, and if it bypasses a specified stability margin circle.

The capacity of the FCR-D delivery is determined by a step and ramp response sequence, where the recorded values are the steady-state power response, the active power and energy five seconds after the start of the ramp. To determine the stability, a Nyquist diagram is constructed by the FCR-Vectors and a FCR-D grid transfer function.

Performing the qualification tests on the simulation model of Songa hydro power plant, resulted in a FCR-N capacity of  $3.7MW$  at maximum load and  $4.6MW$  at minimum load, which correspond well to measurements performed at the actual plant. The FCR-N dynamic performance of the unit was shown to be satisfactory, but the stability was more difficult to determine as the stability circles and Nyquist plot came to differing conclusions. An investigation of the grid transfer function, defined by the project group, revealed that the conclusion on stability from the diagram is dependent on how the function is normalized. The FCR-D capacity, and dynamic performance, was negative for all simulations except for FCR-D downwards regulation at minimum load. The Nyquist stability requirement was not achieved for neither of the simulations.

Unfortunately, changing the governor settings did not lead to a more stable system according to the Nyquist stability criteria.





# Sammendrag

I de seneste årene, har frekvenskvaliteten i det nordiske nettet gått ned. En av grunnene til dette er en periodisk frekvensoscillasjon med en tidsperiode på 40-90 sekunder, som kan komme av en økende mengde uregulerbar kraft i det nordiske nettet. For å øke frekvenskvaliteten ble et prosjekt startet for å finne tiltak for å minske oscillasjonene. Fra dette prosjektet ble et sett med kvalifikasjonstester for primærregulering spesifisert. Primærregulering, også kjent som FCR, er den første responsen på en endring i nettfrekvens. For at en enhet skal ha mulighet til å delta i primærreservemarkedet, må den oppfylle kravene spesifisert av prosjektgruppen.

På grunn av dette, har Statkraft foreslått å utvikle en simuleringsmodell av Songa vannkraftverk. Gjennom modellen kan de utføre kvalifikasjonstestene og vurdere om enheten er kvalifisert i henhold til kravene. En simuleringsmodell ble derfor konstruert i MATLAB ved bruk av karakteristikkmetoden og ligninger som beskriver oppførselen til turbin og regulator, samt en generator koblet til nettet.

FCR er delt inn i to kategorier, normal og forstyrrelse. Levering av FCR-N blir testet ved frekvensstegresponser og sinussignaler. Fra disse testene kan kapasiteten, den dynamiske ytelsen, og stabiliteten bli bestemt fra effektresponsen til vannkraftverket. Basert på amplituden og fasen til sinussignalet kan et sett med vektorer i det komplekse plan, som korresponderer til en bestemt frekvenstidsperiode, bli utviklet. Disse vektorene er plottet med sirkler som illustrerer kravene til dynamisk ytelse og stabilitet. Kriteriet er oppfylt hvis vektorene peker ut av sirkelen. En endelig stabilitetsverifikasjon blir utført ved et Nyquistdiagram, konstruert ved å multiplisere FCR-Vektorene med et matematisk uttrykk for nettet. Enheten er stabil hvis Nyquistplottet passerer punktet  $(-1, j0)$  på høyre side, og hvis den unngår en spesifisert stabilitetsmarginsirkel.

Kapasiteten til FCR-D leveranse blir bestemt av steg- og rampetester, hvor de noterte verdiene er stabil effektrespons, aktiv effekt og energi fem sekunder etter rampen har startet. Stabiliteten blir bestemt ved et Nyquistdiagram konstruert med FCR-Vektorene og en FCR-D nettransferfunksjon.

Utførelsen av kvalifikasjonstestene på simuleringsmodellen av Songa vannkraftverk, resulterte i en FCR-N kapasitet på  $3.7MW$  ved maks last og  $4.6MW$  ved minimum last, verdier som korresponderer til målinger utført på det faktiske vannkraftverket. Den dynamiske ytelsen til FCR-N var tilfredsstillende, men det viste seg å være vanskeligere å bestemme stabiliteten da stabilitetssirkelene og Nyquistplottene viste forskjellig resultat. En undersøkelse av nettransferfunksjonen, definert av prosjektgruppen, avslørte at konklusjonen av stabilitet var avhengig av hvordan funksjonen ble normalisert. Kapasiteten, og den dynamiske ytelsen, til FCR-D var negativ for alle simuleringer, med unntak av FCR-D nedover regulering ved minimum last. Nyquistkriteriet ble ikke oppfylt for noen av simuleringene.

Dessverre viste seg at en endring av reguleringsparametrene ikke førte til et mer stabilt system, ifølge Nyquistkriteriet.

# Contents

<b>1</b>	<b>Introduction</b>	<b>1</b>
1.1	Songa hydro power plant . . . . .	1
1.2	Previous work . . . . .	2
<b>2</b>	<b>Theory</b>	<b>3</b>
2.1	Steady-state and transient flow . . . . .	3
2.2	Method of Characteristics . . . . .	4
2.2.1	Boundary conditions . . . . .	6
2.2.2	Surging devices . . . . .	6
2.2.3	Draft tube . . . . .	7
2.3	Francis turbine . . . . .	8
2.3.1	Velocity triangle . . . . .	9
2.3.2	Turbine model . . . . .	10
2.3.3	Connection with Method of Characteristics . . . . .	12
2.4	Generator . . . . .	13
2.5	Grid . . . . .	15
2.6	Governor . . . . .	16
2.6.1	Voltage governor . . . . .	17
2.6.2	Frequency governor . . . . .	17
2.7	Frequency control in the Nordic grid . . . . .	18
2.7.1	Frequency tests . . . . .	19
2.7.2	Step response and ramp tests . . . . .	19
2.7.3	Sinusoidal response tests . . . . .	22
<b>3</b>	<b>Building the model</b>	<b>27</b>
3.1	Waterway . . . . .	27
3.2	Turbine, generator, governor and grid . . . . .	29
<b>4</b>	<b>Results and discussion</b>	<b>30</b>
4.1	Maximum load . . . . .	31
4.1.1	FCR-N step response . . . . .	31
4.1.2	Sine sweep . . . . .	33
4.1.3	FCR-D upwards regulation . . . . .	38
4.1.4	FCR-D downwards regulation . . . . .	42
4.2	Minimum load . . . . .	45
4.2.1	FCR-N step response . . . . .	45
4.2.2	Sine sweep . . . . .	47
4.2.3	FCR-D upwards regulation . . . . .	51
4.2.4	FCR-D downwards regulation . . . . .	55
4.3	Governor tuning . . . . .	58
4.4	Discussion on stability . . . . .	65
4.5	Discussion on simulation model . . . . .	69
<b>5</b>	<b>Conclusion</b>	<b>72</b>

<b>6 Further Work</b>	<b>73</b>
<b>7 References</b>	<b>74</b>
<b>Appendix A MATLAB script</b>	<b>i</b>
<b>Appendix B Parameters Songa</b>	<b>xxviii</b>
<b>Appendix C Figures and values</b>	<b>xxix</b>
C.1 Full FCR-N Nyquist response . . . . .	xxix
C.2 Full ramp response . . . . .	xxx
C.3 Governor tuning . . . . .	xxxii
<b>Appendix D Expanding section</b>	<b>xxxiv</b>
<b>Appendix E Paper presented at CRHT-VII</b>	<b>xl</b>
<b>Appendix F Risk assessment</b>	<b>1</b>

# List of Figures

1	Songa Hydro power plant . . . . .	1
2	Method of Characteristic . . . . .	5
3	Francis turbine [7] . . . . .	8
4	Velocity triangle Francis turbine[7] . . . . .	9
5	The displacement angle between rotor and stator[20] . . . . .	13
6	The relationship between frequency and power on the grid[18] . . . . .	15
7	Frequency control of the Nordic grid [27] . . . . .	18
8	Step response test FCR-N [27] . . . . .	19
9	Step response test FCR-D upwards regulation [27] . . . . .	20
10	Ramp test FCR-D upwards regulation [28] . . . . .	21
11	Sinusoidal frequency response . . . . .	22
12	Example plot FCR-Vector and dynamic performance circle [28] . . . . .	24
13	Example Nyquist plot with stability circle [28] . . . . .	25
14	Generator output step response FCR-N at maximum load . . . . .	31
15	Bode plot maximum load . . . . .	34
16	Dynamic performance circles at maximum load . . . . .	35
17	Stability performance circles at maximum load . . . . .	36
18	Nyquist plot of FCR-N response at maximum load . . . . .	37
19	Generator output step response FCR-D up at maximum load . . . . .	38
20	Generator output ramp response FCR-D up at maximum load . . . . .	39
21	Nyquist plot FCR-D upwards maximum load . . . . .	41
22	Generator output step response FCR-D down at maximum load . . . . .	42
23	Generator output ramp response FCR-D down at maximum load . . . . .	43
24	Nyquist plot FCR-D down maximum load . . . . .	44
25	Generator output step response FCR-N at minimum load . . . . .	45
26	Bode plot minimum load . . . . .	47
27	Dynamic Performance circles at minimum load . . . . .	48
28	Stability Performance circles at minimum load . . . . .	49
29	Nyquist plot of FCR-N response at minimum load . . . . .	50
30	Generator output step response FCR-D up at minimum load . . . . .	51
31	Generator output ramp response FCR-D down at minimum load . . . . .	52
32	Nyquist plot FCR-D upwards minimum load . . . . .	54
33	Generator output step response FCR-D down at minimum load . . . . .	55
34	Generator output ramp response FCR-D down at minimum load . . . . .	56
35	Nyquist plot FCR-D down minimum load . . . . .	57
36	Governor parameter set from Vattenfall Program . . . . .	59
37	Step response different governing parameters . . . . .	62
38	Nyquist plot for different governor parameters . . . . .	63
39	Nyquist plot with Vattenfall grid transfer function . . . . .	66
40	Nyquist plot with static gain grid transfer function . . . . .	67
41	Amount of regulating power at Songa hydro power station [17] . . . . .	70
42	Full FCR-N Nyquist response maximum load . . . . .	xxix
43	Full FCR-N Nyquist response minimum load . . . . .	xxix
44	Full ramp response FCR-D downwards at maximum load . . . . .	xxx

45	Full ramp response FCR-D downwards at minimum load . . . . .	xxx
46	Full ramp response FCR-D upwards at maximum load . . . . .	xxxi
47	Full ramp response FCR-D upwards at minimum load . . . . .	xxxi
48	Full step response FCR-N different governing parameters . . . . .	xxxii

## List of Tables

1	Waterway parameters . . . . .	27
2	Simulation parameters . . . . .	30
3	Step response FCR-N maximum load . . . . .	31
4	Sinus response maximum load . . . . .	33
5	Step response FCR-D upwards maximum load . . . . .	38
6	Step response FCR-D downwards maximum load . . . . .	42
7	Step response FCR-N minimum load . . . . .	45
8	Sinus response minimum load . . . . .	47
9	Step response FCR-D upwards minimum load . . . . .	51
10	Step response FCR-D downwards minimum load . . . . .	55
11	Grid parameters . . . . .	58
12	Unit parameter utilized for governor tuning . . . . .	58
13	Governing parameters . . . . .	61
14	Full waterway parameters . . . . .	xxviii
15	Rated values turbine and generator . . . . .	xxviii

# Nomenclature

## Acronyms

$FCR$	Frequency containment reserve
$FCR - D$	Frequency containment reserve disturbance
$FCR - N$	Frequency containment reserve normal
$MOC$	Method of Characteristic
$NP$	Number of poles in generator
$TSO$	Transmission system operators

## Greek Symbols

$\alpha$	Angle between peripheral and absolute velocity	<i>radians</i>
$\beta$	Angle between peripheral and relative velocity	<i>radians</i>
$\delta$	Displacement angle	<i>radians</i>
$\epsilon$	Roughness factor	—
$\eta$	Efficiency	—
$\kappa$	Opening degree of guide vanes	—
$\omega$	Angular frequency of applied sinusoidal signal	<i>rad/s</i>
$\omega$	Rotational speed	<i>rad/s</i>
$\phi$	Magnetic flux of generator	<i>Vs</i>
$\psi$	Machine constant turbine	—
$\sigma$	Dimensionless self governing parameter	—
$\tilde{\omega}$	Dimensionless angular speed of rotation	—
$\varphi$	Grid phase angle	<i>radians</i>
$\xi$	Machine constant turbine	—

## Roman Symbols

$2D$	Backlash	<i>W</i>
$\Delta h$	Hydraulic losses in turbine	<i>m</i>
$\Delta t$	Time step	<i>s</i>
$\Delta x$	Length increment	<i>m</i>
$\tilde{q}_c$	Discharge where the angle of attack fits the inlet runner angle	—
$\tilde{q}$	Dimensionless flow	—

$A$	Area	$m^2$
$a$	Pressure propagation speed	$m/s$
$A_f$	Amplitude of sinusoidal frequency signal	$Hz$
$A_p$	Amplitude of sinusoidal power signal	$W$
$A_s$	Surface area	$m^2$
$B$	Constant utilized in MOC	$s/m^2$
$B_1$	Width of runner	$m$
$b_p$	Permanent droop	$\%$
$C$	Capacity	$W$
$c$	Absolute velocity	$m/s$
$C^+$	Characteristic equation MOC	—
$C^-$	Characteristic equation MOC	—
$C_M$	Characteristic constant MOC	$m$
$C_P$	Characteristic constant MOC	$m$
$c_t$	Servo motor velocity	$m/s$
$D$	Diameter	$m$
$E$	Induced voltage in generator	$V$
$e$	Error term	—
$e_N$	Normalization factor	$W/Hz$
$E_s$	Activated energy five seconds after start of ramp	$W$
$f$	Friction factor	—
$f_0$	Nominal grid frequency	$Hz$
$G$	Grid transfer function	—
$g$	Gravity	$m/s^2$
$H$	Head	$m$
$h$	Dimensionless head	—
$h_b$	Backlash scaling factor	—
$H_{grid}$	Inertia time constant	$s$
$HC$	Characteristic constant MOC	$m$
$I$	Current	$A$
$J$	Polar moment of inertia	$m^4$



$K$	Machine constant generator	—
$K_f$	Load frequency dependence	—
$K_p$	Proportional gain	—
$K_v$	Frequency governor value at Songa	—
$L$	Pipe length	$m$
$m_d$	Damping constant	—
$m_s$	Dimensionless starting torque	—
$N$	Number of pipe line parts	—
$P$	Power	$W$
$Q$	Flow	$m^3/s$
$R$	Constant utilized in MOC	$s^2/m^5$
$R_a$	Loss constant due to off-design effects	—
$R_e$	Reynolds number	—
$R_f$	Frictional loss constant	—
$R_m$	Mechanical loss constant	—
$s$	Laplace variable	$1/s$
$S_n$	Grid load	$MW$
$s_t$	Throttling dependency of angular speed of rotation	$m^2$
$T$	Time period of applied sinusoidal signal	$s$
$T_1$	Frequency governor value at Songa	$s$
$T_a$	Acceleration time of rotating masses	$s$
$T_d$	Derivative time	$s$
$T_f$	Filter constant	$s$
$T_g$	Generator torque	$Nm$
$T_i$	Integral time	$s$
$T_w$	Inflow time of masses of water	$s$
$u$	Peripheral velocity	$m/s$
$u_d$	Derivative term	—
$V$	Velocity	$m/s$
$x$	Real part of transfer function vector	—
$y$	Imaginary part of transfer function vector	—

## Subscripts

0	User-defined starting value
1	Starting point segment
2	End point segment
5sec	Value five seconds after initiation of ramp
<i>A</i>	Point before present point in time and space
<i>B</i>	Point after present point in time and space
<i>bit</i>	Bitdalsvatnet
<i>f</i>	Value of loss
<i>FCR – D</i>	Value of FCR-D
<i>FCR – N</i>	Value of FCR-N
<i>g</i>	Value of generator
<i>grid</i>	Value of grid
<i>h</i>	Hydraulic
<i>j</i>	Pipe exiting junction
<i>k</i>	Pipe entering junction
<i>m</i>	Meridian direction
<i>max</i>	Maximum value
<i>min</i>	Minimum value
<i>P</i>	Present point in time and space
<i>R</i>	Value of reservoir
<i>r</i>	Rated value
<i>songa</i>	Songavatnet
<i>ss</i>	Steady-state
<i>t</i>	Value of turbine
<i>tot</i>	Total
<i>u</i>	Tangent direction

# 1 Introduction

In the later years, the Nordic grid has experienced a decrease in frequency quality, registering several incidents where the frequency is outside the nominal range[2]. In order to deal with this problem, the Nordic TSO's are implementing new demands for delivery of primary governing. Primary governing, also known as FCR, is the first response to a frequency deviation in the grid, and should be activated within seconds [18]. A hydro power plant must, in accordance with the new demands, qualify to participate in the FCR market. The qualification consists of several tests to measure the stability and dynamic performance of the unit. [28]

The frequency oscillations in the grid are triggered by a load or generation variation. The amplitude and the period time of these oscillations are affected by the system parameters and the turbine governor settings [16]. Changing the settings of a regulator in the system, may therefore improve the frequency quality of the grid.

For these reasons, it is desirable to find a way to test the performance of a hydro power unit based on the new requirements. This thesis describes how a simulation model of Songa hydro power plant was built in Matlab, utilizing the Method of Characteristics for the waterway, and formulas describing the behaviour of the turbine, generator, governor and grid. The qualification tests will be stated and performed on the simulation model with the current regulator settings. Afterwards, the results will be reviewed and other governor settings will be investigated.

## 1.1 Songa hydro power plant

Songa hydro power plant has been in operation since 1964 and is located in Vinje, Telemark. The plant has two reservoirs, Songavatnet and Bitdalsvatnet, as well as eight stream intakes and a lower reservoir Totak. The plant has one Francis turbine installed with a rated power of 136 MW at 264 m rated head and discharge of  $52 \text{ m}^3/\text{s}$ .

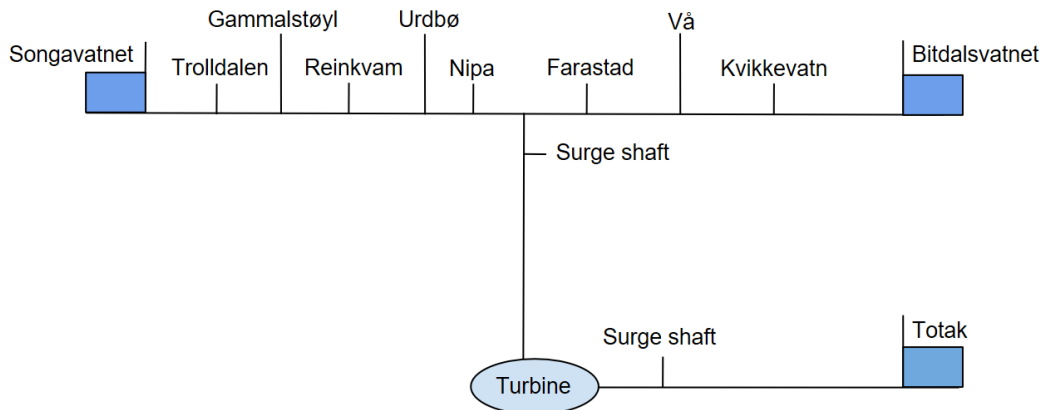


Figure 1: Songa Hydro power plant

## 1.2 Previous work

There has been written numerous theses on transient simulation of hydro power plants. The focus has, however, often been the turbine behaviour on a constant grid frequency or a sudden disconnection of the generator. In this thesis, the impact of a frequency change on the hydro power unit is studied.

To build the waterway in the simulation model, the Method of Characteristics, as described in Wylie and Streeter's "Fluid Transients" [33], is utilized. The losses in the system is modelled based on Haaland's formula, as outlined in [10].

A description of the behaviour of Francis turbines can be found in the books written by Hermod Brekke, ([6] and [7]). Torbjørn Nielsen theses, ([22], [23] and [19]), describe a method to simulate the behaviour of the turbine, based on Euler's equation. The latter report also contains a way of coupling with the Method of Characteristics. Generator and grid behaviour has been modelled after the thesis "Dynamic behaviour of governing turbines sharing the same electrical grid" by the same author. This thesis also contains a description of a frequency regulator, which is based on the transfer function of a hydro power unit with a PI governor. The author of this thesis, however, decided to develop a governing equation based on theory from control engineering, as described in [4] and [5].

Bjarne Vaage and Even Lillefosse Haugen also uses the Method of Characteristics and Torbjørn Nielsen's reports to simulate the behaviour of a hydro power plant in their master thesis, [31] and [12]. However, Haugen simulates a very simple unit with a gas chamber instead of a surge shaft. Vaage utilizes a surge shaft with varying geometry, but the simulation model is implemented in Simulink and not scripted in Matlab, as performed in this thesis. Both master theses simulate load rejection and frequency deviations to study the behaviour of a hydro power plant.

The qualification tests are described in a set of reports made by the prequalification working group on the FCP project, ([28], [27], [25] and [24]). Some background material of the tests are provided by reports written by Evert Agneholm, [2], M. Laasonen et al., [16] and the prequalification working group itself, [26].

Statkraft has also provided a report by Monica Lexholm of tests performed at Songa hydro power plant, [17]. The test were performed with the aim of validating a simple linear model of a hydro power unit.

## 2 Theory

This section will give an overview of the theory used to develop a simulation model of a hydro power plant. First, the general theory of fluid flow is explained, followed by a section on the Method of Characteristics. Thereafter, equations describing the behaviour of a Francis turbine is explained, as well as the grid and generator behaviour. A description of the voltage and frequency regulator in the system is also included. Lastly, the frequency control in the Nordic grid is explained, followed by a description of the qualification tests and requirements.

### 2.1 Steady-state and transient flow

Fluid flow can be categorized as either steady-state or transient. Steady-state flow occurs when the fluid properties are constant and does not change over time. In a hydro power plant, the properties of this state can be found by the energy equation [8]:

$$H_1 + \frac{V_1^2}{2g} = H_2 + \frac{V_2^2}{2g} + H_t + H_f \quad (2.1.1)$$

Where  $H$  is the pressure head and  $V$  the velocity. The head loss in the system,  $H_f$ , can be calculated by the Darcy-Weisbach equation[8]:

$$H_f = f \frac{L}{2gDA^2} Q^2 \quad (2.1.2)$$

The friction factor,  $f$ , is directly related to the wall shear stress and is dependent of the Reynolds number,  $Re$ , and the relative roughness,  $\epsilon/D$ , of the pipe. In this model, Haaland's explicit formula for the friction factor in turbulent flow is utilized[10]:

$$\frac{1}{\sqrt{f}} = -1.8 \log \left[ \frac{6.9}{Re} + \left( \frac{\epsilon}{3.7D} \right)^{1.11} \right] \quad (2.1.3)$$

When the power demand of the hydro power plant changes, so does the fluid properties of the flow. The fluid flow will change over time and transform into unsteady or transient mode, which is governed by the unsteady equation of motion and continuity.

The equation of motion states that the sum of forces is equal to the mass and acceleration of the fluid. In this thesis, a simplified form without the terms of lesser importance is used[33]:

$$g \frac{dH}{dx} + \frac{dV}{dt} + \frac{fV|V|}{2D} = 0 \quad (2.1.4)$$

The continuity equation expresses that the rate of mass into the control volume equals the rate of mass exiting the control volume, in addition to the accumulated mass within. On simplified form[8]:

$$\frac{dH}{dt} + \frac{a^2}{g} \frac{dV}{dx} = 0 \quad (2.1.5)$$

The pressure propagation speed,  $a$ , defines the elasticity of water in a closed conduit, therefore the wall and fluid properties are included in the term  $a^2$ . For fluid flow this parameter is approximately 1200  $m/s$  [21]. In order to solve the equations describing transient flow, the Method of Characteristics is utilized.

## 2.2 Method of Characteristics

The Method of Characteristics transforms the equation of motion 2.1.4 and the equation of continuity 2.1.5 into total differential equations,  $C^+$  and  $C^-$  characteristic equations[33]:

$$C^+ = \begin{cases} \frac{g}{a} \frac{dH}{dt} + \frac{dV}{dt} + \frac{fV|V|}{2D} = 0 & (2.2.1a) \\ \frac{dx}{dt} = +a & (2.2.1b) \end{cases}$$

$$C^- = \begin{cases} -\frac{g}{a} \frac{dH}{dt} + \frac{dV}{dt} + \frac{fV|V|}{2D} = 0 & (2.2.2a) \\ \frac{dx}{dt} = -a & (2.2.2b) \end{cases}$$

These equations are further integrated to finite difference equations that can be solved numerically:[33]

$$C^+ : H_P = C_P - BQ_P \quad (2.2.3)$$

$$C^- : H_P = C_M + BQ_P \quad (2.2.4)$$

Where [33]

$$C_M = H_A + BQ_A - RQ_A|Q_A| \quad (2.2.5)$$

$$C_P = H_B - BQ_B + RQ_B|Q_B| \quad (2.2.6)$$

and[33]

$$B = \frac{a}{gA} \quad (2.2.7)$$

$$R = \frac{f\Delta x}{2gDA^2} \quad (2.2.8)$$

The subscripts A and B refer to the points in space before and after point P in the previous time step:

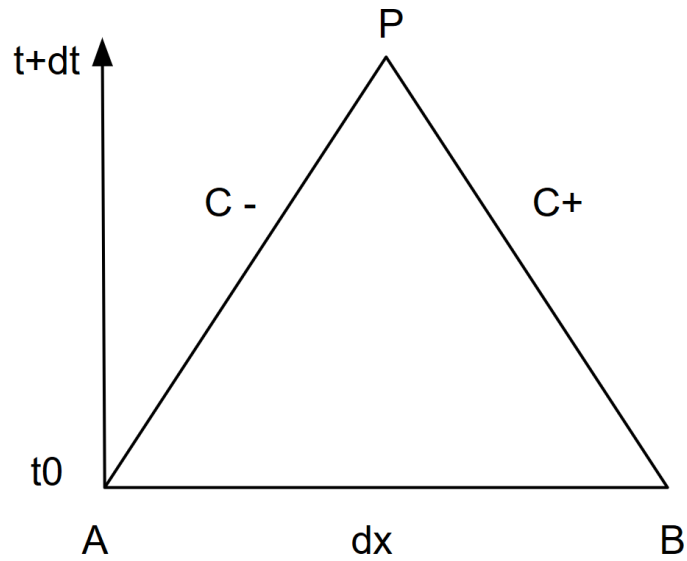


Figure 2: Method of Characteristic

A pipeline is divided into N parts[33]:

$$N = \frac{L}{\Delta x} \quad (2.2.9)$$

The length increment,  $\Delta x$ , of the system is therefore defined by the smallest pipe length, as the minimum value of N is 3. From  $\Delta x$ , the time step of the system can be established[33]:

$$\Delta t = \frac{\Delta x}{a} \quad (2.2.10)$$

For all interior points of a pipe line, the pressure can be calculated by combining equation 2.2.3 and equation 2.2.4:

$$H_P = \frac{C_P + C_M}{2} \quad (2.2.11)$$

After the pressure is found, the flow can be calculated by the same equations.

At the start and end point of the pipe line, a boundary condition needs to be properly defined as it conveys the behaviour and response of the fluid in the pipe line during the transient.

### 2.2.1 Boundary conditions

If the start or end point of a pipe line is an upstream or downstream reservoir, the head is defined accordingly [33]:

$$H_P = H_R \quad (2.2.12)$$

For pipes connecting in series or junction, the continuity equation must be fulfilled. Hence, the summation of flow into and out of the connection should be zero. The pressure head is also assumed to be the same for all pipes at the junction[33]:

$$H_P = \frac{\sum C_{Pj}/B_j + \sum C_{Mk}/B_k}{\sum (1/B)} \quad (2.2.13)$$

The subscript k refers to the pipes entering the junction and the subscript j refers to the pipes exiting. The flow is calculated as[33]:

$$Q_{Pj,N} = -\frac{H_P}{B_j} + \frac{C_{Pj}}{B_j} \quad (2.2.14)$$

$$Q_{Pk,1} = \frac{H_P}{B_k} - \frac{C_{Mk}}{B_k} \quad (2.2.15)$$

For pipes connecting in series, the flow in the two pipe lines is identical. Hence, the pressure head is found by setting equation 2.2.14 and equation 2.2.15 equal to one another. Thereafter, the discharge can be determined by the pressure head.

### 2.2.2 Surging devices

When the power changes, the pressure in front of the turbine increases. This pressure rise is proportional to the length/cross section area from the nearest free surface upstream of the turbine to the nearest free surface downstream of the turbine. To reduce this pressure, a surging device such as a surge shaft is introduced to the hydro power plant, to decrease the distance between the two free surfaces. A surge shaft in front of the turbine also improves the stability of the plant, as the penstock is allowed to extract water from the shaft during an increase of power, allowing the water from the reservoir to accelerate slower, thus reducing the pressure. [21]

In the Method of Characteristics, a surging device can be simulated as [21]:

$$H_P = H_A + \frac{\Delta t}{A_s} Q_A \quad (2.2.16)$$

This equation is also used for stream intakes.



### 2.2.3 Draft tube

After the turbine, the flow enters the draft tube, where the kinetic energy of the runner is transformed to pressure energy at the draft tube outlet[14]. In order to perform this transformation, the draft tube is designed as a straight cone at the inlet, which expands into an elliptical form towards the outlet[7]. In the model, the draft tube is therefore simulated as an expanding section:

$$Q_P = \frac{\frac{g}{a}(H_A - H_B) + \frac{1}{2}Q_B \left( \frac{1}{A_P} + \frac{1}{A_B} \right) + \frac{1}{2}Q_A \left( \frac{1}{A_P} + \frac{1}{A_A} \right)}{\frac{1}{A_P} + \frac{1}{2A_B} + \frac{1}{2A_A}} \quad (2.2.17)$$

$$H_P = H_A - \frac{a}{g} \left[ \frac{Q_P}{A_P} - \frac{Q_A}{A_A} - \frac{1}{2}(Q_P + Q_A) \left( \frac{1}{A_P} - \frac{1}{A_A} \right) \right] \quad (2.2.18)$$

$A_A$  and  $A_B$  are the area in the sections before and after point P.

The equations stated here are derived from the equation of motion and continuity for an expanding section. They differ from the ones stated in [33] as an error was found in the book. The full derivation of these equations can be found in appendix D.

## 2.3 Francis turbine

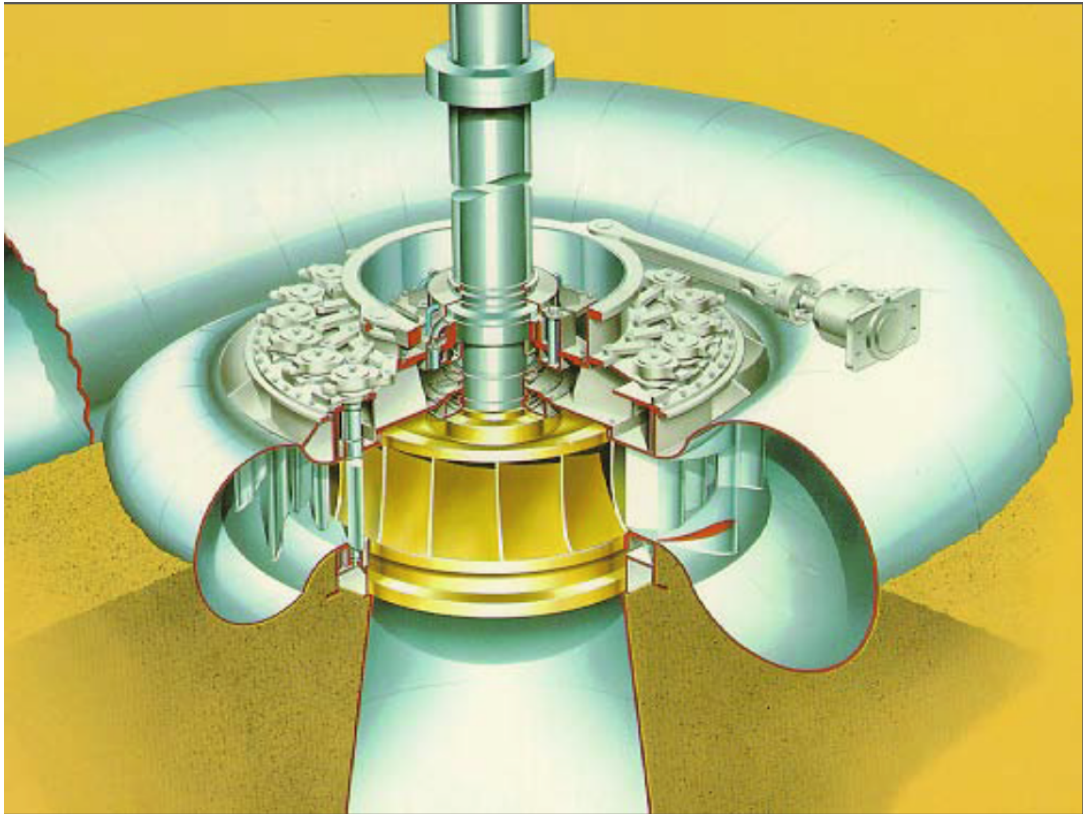


*Figure 3: Francis turbine [7]*

A Francis turbine is installed in the Songa hydro power plant. Francis turbines are usually utilized for medium to high head plants and consists of spiral casing, guide vanes, runner and shaft[14]. The shape of the spiral casing leads to a uniform flow, that is distributed equally to the guide vanes, which are the regulating components of the turbine. They control the amount of flow that enters the runner. In the runner, the hydraulic energy is transformed to rotational energy which is used by the shaft to produce electrical energy that is released to the grid.

In order to construct a simulation model of a hydro power plant with a Francis turbine, the velocity vectors of the guide vanes needs to be determined. These can be found by the main dimensions of the runner[7]:

### 2.3.1 Velocity triangle

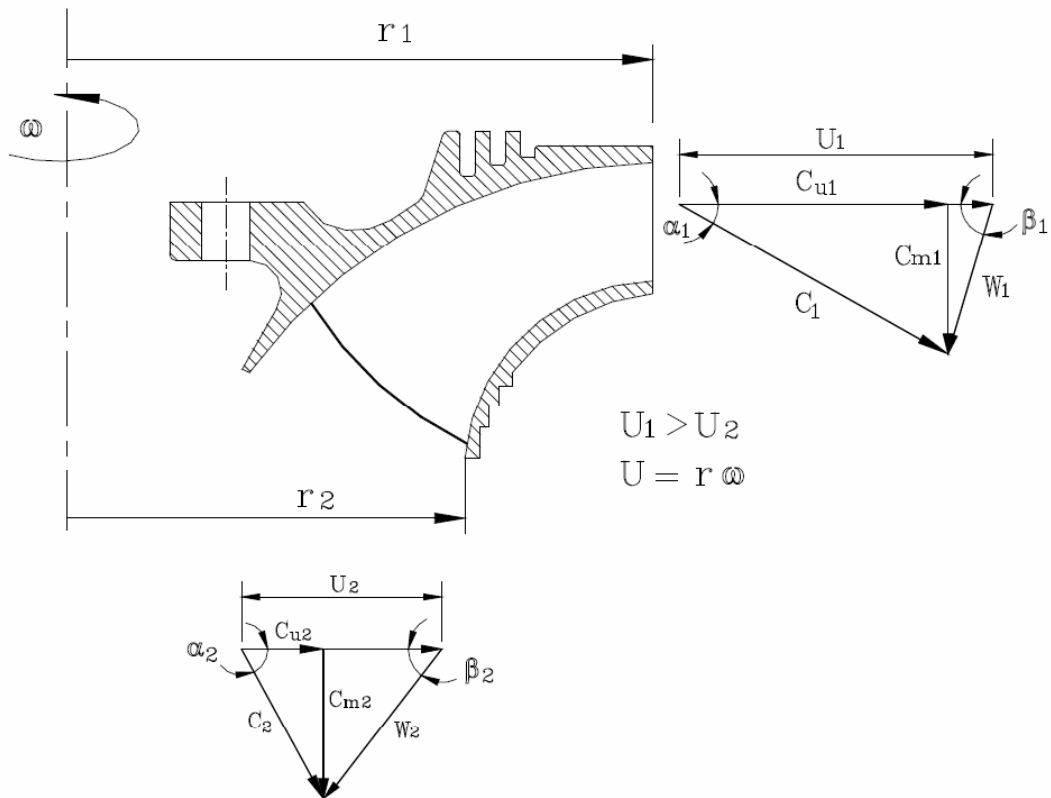


Figure 4: Velocity triangle Francis turbine[7]

At best efficiency point, the velocity vectors can be found by the rated values and geometry of the turbine [7]:

$$c_{m2r} = \frac{4 \cdot Q_r}{\pi D_2^2} \quad (2.3.1)$$

$$c_{m1r} = \frac{Q_r}{\pi D_1 B_1} \quad (2.3.2)$$

$$u_{1r} = 0.5 \omega_r D_1 \quad (2.3.3)$$

$$u_{2r} = 0.5 \omega_r D_2 \quad (2.3.4)$$

Euler's turbine equation states[7]:

$$\eta_h = \frac{1}{g H_r} (c_{u1r} u_{1r} - c_{u2r} u_{2r}) \quad (2.3.5)$$

At best efficiency point it is assumed that there is no swirl at the exit and therefore the value of  $c_{u2r}$  is zero. Equation 2.3.5 can then be used to find the value of  $c_{u1r}$ . To avoid that the inlet velocities are equal and that  $\beta_1$  is  $90^\circ$ , the value of the rated hydraulic efficiency,  $\eta_{hr}$ , is set to 0.96 [22].

By the use of trigonometry in figure 4, the angles between the velocities can be obtained[7]:

$$\tan \beta_{1r} = \frac{c_{m1r}}{u_{1r} - c_{u1r}} \quad (2.3.6)$$

$$\tan \beta_{2r} = \frac{c_{m2r}}{u_{2r}} \quad (2.3.7)$$

$$\tan \alpha_{1r} = \frac{c_{m1r}}{c_{u1r}} \quad (2.3.8)$$

### 2.3.2 Turbine model

To simulate dynamic behaviour of a hydro power plant, it is important to model the turbine correctly. The turbine defines the system flow and thus the change in pressure. In this thesis, a turbine model suggested by Torbjørn Nielsen in ([23], [22] and [19]) is utilized. In this model, the Euler turbine equation 2.3.5 is used to find two differential equations that represents the turbine behaviour. The input to the model is the turbine's main geometry, runner blade inlet and outlet angle, as well as the guide vane angle at best efficiency point [22]:

$$T_w \frac{d\tilde{q}}{dt} = h - \left( \frac{\tilde{q}}{\kappa} \right)^2 - \sigma(\tilde{\omega}^2 - 1) \quad (2.3.9)$$

$$T_a \frac{d\tilde{\omega}}{dt} = \tilde{q} (m_s - \psi\tilde{\omega}) \eta_h - \frac{T_g}{T_r} - R_m \tilde{\omega}^2 - m_d \frac{d\delta}{dt} \quad (2.3.10)$$

The equations are presented on dimensionless form, therefore the generator torque is normalized by a rated value, and the discharge, head and rotational speed is presented by:

$$\tilde{q} = \frac{Q}{Q_r}, \quad h = \frac{H}{H_r}, \quad \tilde{\omega} = \frac{\omega}{\omega_r} \quad (2.3.11)$$

$T_w$  and  $T_a$  are time constants representing the inflow time of masses of water and the acceleration time of the rotating masses [21].  $T_w$  is defined as the time it takes to accelerate the masses of water from zero to rated flow between the nearest free water surface upstream of the turbine to the nearest free surface downstream of the turbine [21]:

$$T_w = \frac{Q_r}{gH_r} \sum \frac{L}{A} \quad (2.3.12)$$

When there is a change in power demand on the grid, the power absorbed by the generator changes and an unbalanced torque on the turbine is created. To make up for this torque, the unit applies a net torque to change the speed. However, this change is not immediate, due to the polar moment of inertia of the rotating fluid and mechanical parts in the turbine and generator. This resistance to change have a stabilizing effect, as it gives the regulator more time to act. This effect is included in equation 2.3.10 by the time constant  $T_a$ .  $T_a$  is the time it takes to accelerate the turbine and generator from zero to angular speed, and is defined by the polar moment of inertia,  $J$ , as well as the rated speed and power of the system [33]:

$$T_a = J \frac{\omega_r^2}{P_r} \quad (2.3.13)$$

$m_s$  is the dimensionless starting torque, defined as  $m_s = t_s/t_r$  where  $t_s$  is the specific torque when the angular speed of rotation equals zero and  $t_r$  is the rated torque of the system. The following expression can be derived from the Euler equation and the velocity diagram [23]:

$$m_s = \xi \frac{\tilde{q}}{\kappa} (\cos \alpha_1 + \tan \alpha_{1r} \sin \alpha_1) \quad (2.3.14)$$

The guide vane angle  $\alpha_1$  can be obtained from the rated value of the angle and the opening degree of the guide vanes,  $\kappa$ [19]:

$$\alpha_1 = \arcsin(\kappa \sin \alpha_{1r}) \quad (2.3.15)$$

Machine constants describing the spin at the runner inlet,  $\xi$ , and the pressure number,  $\psi$ , are defined by the velocity vectors at the best efficiency point, as well as rated values for the hydraulic efficiency and head[23]:

$$\psi = \frac{u_{2r}^2}{gH_r}, \quad \xi = (\psi + \eta_{hr}) \cos \alpha_{1r} \quad (2.3.16)$$

The parameter  $\sigma$  represents the dimensionless self-governing of the turbine. It is calculated from  $s_t$ , which describes the throttling dependency of angular speed of rotation and is dependent of the geometry of the runner[23]:

$$s_t = \frac{1}{8} D_1^2 \left( 1 - \frac{D_2^2}{D_1^2} \right) \quad (2.3.17)$$

$$\sigma = \frac{s_t \omega_{ref}}{gH_r} \quad (2.3.18)$$

In equation 2.3.10,  $R_m$  represents the mechanical losses between the rotating and non-rotating parts in the system. This constant can be found by comparing the efficiency curve of the simulation model to the actual model and adjust accordingly.

The dampening effect on the torque, occurring when there is a change in the angle between the stator and rotor of the generator, is represented by the last term of equation 2.3.10, where  $m_d$  is a dampening constant.

The total efficiency of the turbine is found from the hydraulic efficiency[20]:

$$\eta_h = 1 - \frac{\Delta h}{h} \quad (2.3.19)$$

Where  $\Delta h$  is the hydraulic losses in the turbine [20]:

$$\Delta h = R_f \tilde{q}^2 + R_a (\tilde{q} - \tilde{q}_c)^2 \quad (2.3.20)$$

$R_f$  and  $R_a$  are loss constants describing the friction and the loss due to off-design effects such as wrong incident angles. These constants are found by comparing the efficiency curve of the actual system with the simulated one. As with the constant,  $R_m$ , these parameters must also be found by trial and error. The discharge at where the angle of attack fits the inlet runner angle,  $\tilde{q}_c$ , is found by the inlet velocity diagram[20]:

$$\tilde{q}_c = \tilde{\omega} \frac{1 + \cot \beta_1 \tan \alpha_{1r}}{1 + \cot \beta_1 \tan \alpha_1} \quad (2.3.21)$$

The total turbine efficiency is determined by rewriting the Euler equation 2.3.5:

$$\eta_{tot} = \frac{\tilde{q} \tilde{\omega} ((m_s - \psi \tilde{\omega}) \eta_h - R_m \tilde{\omega}^2)}{\tilde{q} h} \eta_r \quad (2.3.22)$$

### 2.3.3 Connection with Method of Characteristics

The equations describing the behaviour and response of the turbine is coupled with the rest of the hydro power system using the Method of Characteristics. The head over the turbine is found from [33]:

$$H_t = HC - B_t Q_P \quad (2.3.23)$$

Where

$$HC = C_{P1} - C_{M2} \quad (2.3.24)$$

$$B_t = B_1 + B_2 \quad (2.3.25)$$

The subscripts 1 and 2 refer to the pipe line before and after the turbine.  $C_{P1}$  and  $C_{M1}$  is found from equation 2.2.5 and 2.2.6.

To simulate the power plant while it is connected to the grid, these equations can be combined with formulas describing the generator and governor.

## 2.4 Generator

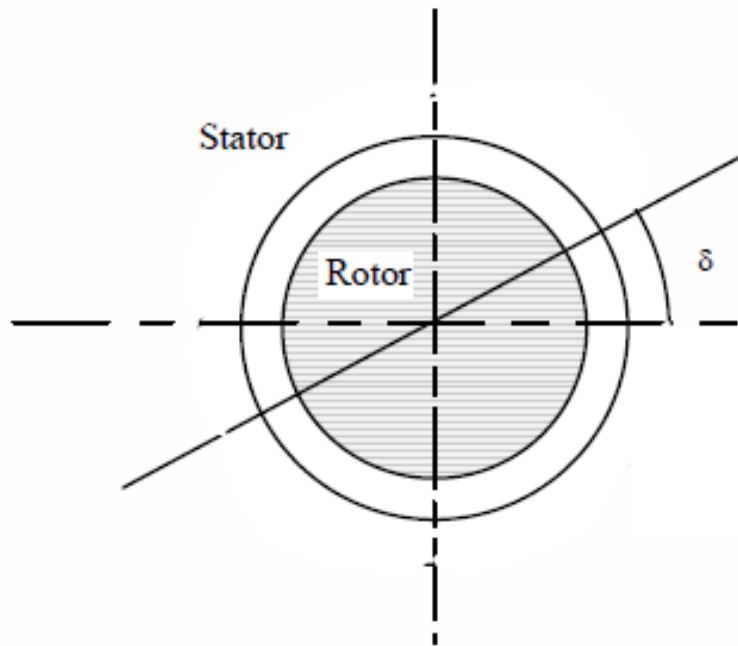


Figure 5: The displacement angle between rotor and stator[20]

In order to produce electrical energy that is delivered to the grid, the turbine runner is connected to a generator via a shaft. Here, the rotational energy from the runner is transformed to electrical energy.

A generator consists of a stator and a rotor. By applying a dc current to the rotor windings, the rotor transforms into an electromagnet. When the rotor is turned by the shaft, a rotating magnetic field is created within the machine. This rotating magnetic field induces a three-phase set of voltages in the windings of the stator. [9]

The magnitude of the voltage,  $E$ , induced in the generator, is dependent of the magnetic flux and the speed of rotation [9]:

$$E = K\phi \cdot \omega \quad (2.4.1)$$

$K$  and  $\phi$  defines the magnetic flux, where  $K$  is a machine constant [9]. The interaction between the rotating and static magnetic field produces a torque within the machine. This torque is a function of the electric current,  $I$ , the magnetic flux and a phase angle,  $\varphi$ , dependent on the property of the grid, which decides how much power the generator delivers to the power system [20]:

$$T_g = K\phi I \cos \varphi \quad (2.4.2)$$

The power produced by the generator depends on the angle between the magnetic fields of the rotor and the stator, the displacement angle  $\delta$ . The maximum power a generator can supply occurs at an angle of  $90^\circ$ . Using the relationship between power and torque, the torque induced in the generator is approximated as [20]:

$$\frac{T_g}{T_r} = \frac{\sin \delta}{\sin \delta_r} \quad (2.4.3)$$

When the electrical load of the grid changes, the displacement angle,  $\delta$ , will also change according to the relation [20]:

$$\frac{d\delta}{dt} = \frac{NP}{2} \omega_t - \omega_{grid} \quad (2.4.4)$$

This equation is valid for a transient period of a load change. When the generator is connected to the grid in steady-state operation, the angular speed of the grid,  $\omega_{grid}$ , will be equal to the angular speed of the turbine,  $\omega_t$ , multiplied with the number of pole pairs on the stator,  $NP$ .

A change in frequency of the power system can be simulated by the relation [9]:

$$\omega_{grid} = 2\pi f_{grid} \quad (2.4.5)$$



## 2.5 Grid

The grid connects several generators in parallel operation. The advantage of this procedure is that the grid can supply a bigger load and stabilize the system. In most applications, the grid frequency is defined by the generators in the power system and it is therefore an input to the hydro power plant [9].

When a generator is connected to the grid, the governor should be adjusted with a slight drooping characteristic between the speed of the turbine and the delivered power from the generator. Following, the speed of the turbine will decrease when the power increases. This characteristic is called speed droop and describes the load distribution between the generators connected to the grid. The speed of the turbine and the frequency of the grid is connected by equation 2.4.4, and therefore, the characteristic between frequency and power will result in a similar plot. This characteristic plays an essential role in the parallel operation of generators [9]

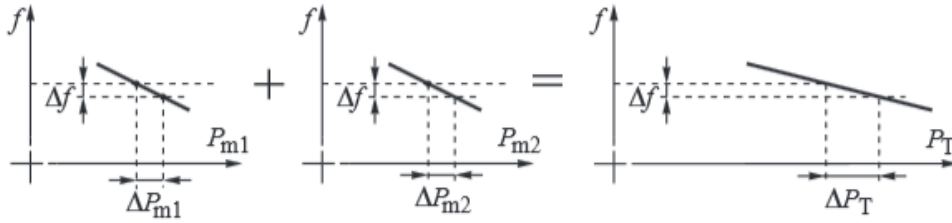


Figure 6: The relationship between frequency and power on the grid[18]

Equation 2.5.1 describes the droop,  $b_p$ , as the slope of the curve between power and frequency [18]:

$$b_p = -\frac{\Delta f_{grid}}{f_0} \frac{P_r}{\Delta P} \quad (2.5.1)$$

Where  $\Delta f_{grid}$  and  $\Delta P$  are changes in frequency and power, and  $f_0$  and  $P_r$  are the rated values of the grid and generator.

## 2.6 Governor

To ensure stability, the system is governed by a regulator. The regulator measures the input signal and compares it to a reference point. If a deviation exists, the regulator changes the control value until the error is minimal. Most governors utilized today are presented in the form of serial PID regulators[4]:

$$u(t) = \underbrace{K_p e(t)}_{\text{P-part}} + \underbrace{\frac{K_p}{T_i} \int_0^t e(t) dt}_{\text{I-part}} + \underbrace{K_p T_d \frac{d}{dt} e(t)}_{\text{D-part}} \quad (2.6.1)$$

In the equation above,  $u$  is the control variable and  $e$  is the error term or deviation from set point.

The different terms in the regulator plays different parts in the governing.

The proportional term increases the value of the control variable until the error term reaches a minimum. The p-part is, however, unable to provide zero deviation from set point. Considering the definition above, one can see that the P-part is zero only if the error term is zero. It is difficult to achieve zero deviation from set point and therefore the reference value will not be reached by the the P-term alone. The proportional term contributes to a faster regulation, but if the value of  $K_p$  is too large, the system will be unstable [13].

As long as the error term is non-zero. the integral term will increase and change the control variable. When the error is eliminated, the I-part is at a high enough value to ensure that the system stays at the set point. A large integral time,  $T_i$ , will provide a stable, but slow regulation. A decrease in this is parameter will make the governor faster, however, decreasing it too much can make the system unstable [5].

The D-part contributes to a faster regulation towards the set point by giving a positive contribution to the control variable in the case of an increasing error term. It also provides a dampening of the system towards the reference point by providing a negative contribution to the control variable if the error term is decreasing. If the value for  $T_d$  is chosen to be too large, oscillations will occur, and the system can reach instability [13].

However, the D-term has a tendency to increase the value of the noise on the measurement system. One way of reducing this noise is to implement a filter with a filter constant  $T_f$ . On Laplace form, the filter is implemented in the derivative part[13]:

$$u_d = \frac{K_p T_d s e}{1 + T_f s} \quad (2.6.2)$$

Using Laplace transformation and rearranging the equation, this term can be written in the time domain as [15]:

$$u_d = K_p T_d \frac{d}{dt} e(t) - T_f \frac{du_d}{dt} \quad (2.6.3)$$

Hydro power plants utilizes two governors, one for voltage regulation and one for frequency regulation.

### 2.6.1 Voltage governor

The voltage regulator's main task is to keep the voltage of the generator constant during load change. A difference between the output voltage and the desired reference voltage, leads to an adjustment of the magnetic flux of the generator [20].

In this thesis, the voltage governor is modelled as a PI-regulator on the form: [20]

$$\frac{dK\phi}{dt} = -\frac{K_{pg}}{E_r} \frac{dE}{dt} + \frac{K_{pg}}{T_{ig}E_r} \left( E_r + \frac{1}{b_{pg}I_r} (I - I_r) - E \right) \quad (2.6.4)$$

### 2.6.2 Frequency governor

The aim of the turbine governor is to keep the rotational speed constant by making sure the turbine mechanical torque is equal to the generator's electrical torque. A change in load on the generator will cause a difference between them. To compensate for this, the turbine adjusts the rotational speed by altering the opening into the runner. The power delivered from the turbine will then change until it is equal to the delivered power from the generator. [18]

To ensure stability, the governing system uses two negative feedback loops. The first one measures the speed towards the reference and regulates the opening if there is an error. The second makes sure the droop characteristics of the frequency and power is maintained. [18]

The error term,  $e$ , contains both the speed and the droop characteristic [18]:

$$e = \frac{\omega_r - \omega_t}{\omega_r} - b_p (\kappa_r - \kappa) \quad (2.6.5)$$

Using the PID regulator on serial form, as previously stated, and implementing the filter term, the equation for the frequency governor is:

$$\frac{d\kappa}{dt} = K_p e(t) + \frac{K_p}{T_i} \int_0^t e(t) dt + K_p T_d \frac{d}{dt} e(t) - T_f \frac{du_d}{dt} \quad (2.6.6)$$

## 2.7 Frequency control in the Nordic grid

The transmission system operators (TSOs) are responsible for the coordination of a reliable system operation and frequency control. Day by day, energy companies bid in how much power and how many generating units they can offer. As such, a daily operating schedule is planned. However, the actual power output is regularly monitored [18].

If a large unit is suddenly connected or disconnected to the system, there will be a distortion in the balance between the delivered power from the turbines and the consumed power by the grid. Initially, this imbalance is covered by the rotating rotors of the turbine and generator, causing a change in frequency of the system. In order to restore the nominal frequency, the turbine governor changes the opening of the guide vanes to increase or decrease the amount of flow into the runner, thus changing the power output from the generator. The action of the turbine governor due to frequency changes, when the reference values of the regulators are kept constant, is referred to as primary frequency control (FCR). The primary governing is the first response to a change in the system's demand of power. To ensure a safe system operation, primary control is installed at various geographical locations, evenly distributed around the system, to minimize the risk of overloading the transmission lines. The required time for the activation of this reserve should not be longer than a few seconds. To satisfy this condition, the units participating in the primary frequency containment reserve should be able to regulate power quickly. [18]

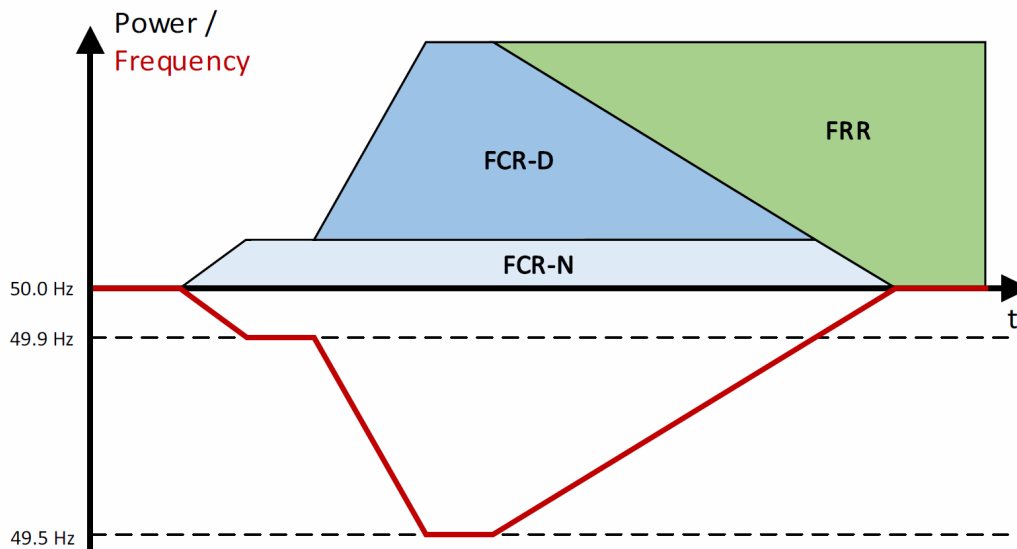


Figure 7: Frequency control of the Nordic grid [27]

After the primary governing, secondary control (FRR) is activated in order to return and keep the initial frequency. This activation is much slower than primary control, usually a couple of minutes, as the reference power on the turbine governing system must be changed in order to meet the power demand of the grid. [18]

### 2.7.1 Frequency tests

In accordance with new demands, a hydro power plant needs to pass a set of qualification tests to be able to deliver frequency containment reserves. These tests have been defined by the prequalification working group, aiming towards a common Nordic harmonization of the technical requirements for FCR delivery, to ensure a stable primary governing. All tests are performed while the hydro power plant is still connected to the grid. [27]

Frequency containment reserves can be divided into two categories; normal, FCR-N, and disturbance, FCR-D, where FCR-N is utilized for frequency deviations between 49.9 - 50.1 Hz. FCR-D is again divided into upwards regulation for deviations between 50.1 - 50.5 Hz, and downwards regulation for deviations between 49.9 - 49.5 Hz. To find the capacity and determine the performance and stability of the two types of frequency containment reserves, step, ramp and sinusoidal test are applied to the system.

### 2.7.2 Step response and ramp tests

The following step response is applied to find the capacity of the FCR-N delivery: [28]

50.00 → 50.05 → 50.00 → 49.90 → 50.00 → 50.10 → 50.00 [28]

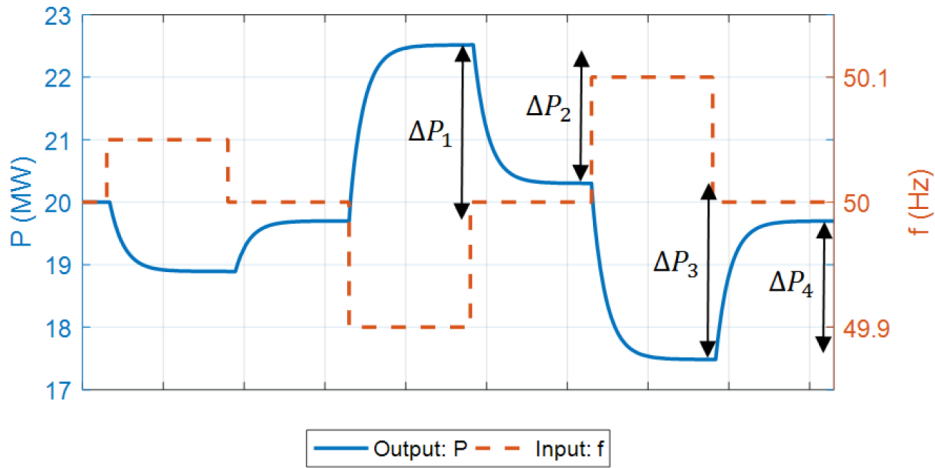


Figure 8: Step response test FCR-N [27]

From the step response, the average active power can be obtained: [27]

$$\Delta P = \frac{|\Delta P_1| + |\Delta P_3|}{2} \quad (2.7.1)$$

In hydro power plants, there exists a delay in the system, as the machinery does not immediately respond to changes. This delay is known as backlash and must be accounted for in real hydro power plants: [27]

$$2D = \frac{|\Delta P_1 - \Delta P_2| + |\Delta P_3 - \Delta P_4|}{2\Delta P} \quad (2.7.2)$$

Including the effect of backlash, the FCR-N capacity can be calculated from the power response: [27]

$$C_{FCR-N} = \frac{|\Delta P_1| + |\Delta P_3| - 2D}{2} \quad (2.7.3)$$

The FCR-D capacity is obtained from step and ramp response tests. For upwards regulation, the step response sequence is: [28]

49.90 → 49.70 → 49.90 → 49.50 → 49.90

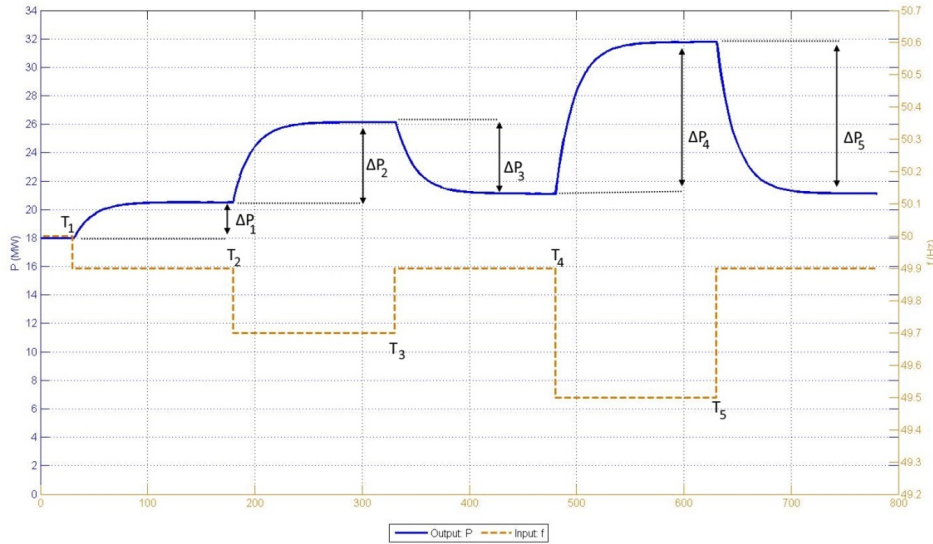


Figure 9: Step response test FCR-D upwards regulation [27]

From this sequence, the steady state FCR-D activation,  $\Delta P_{ss}$ , can be acquired from the frequency step from 49.9 to 49.5 Hz.

A frequency ramp starting from 49.9 Hz to 49.0 Hz with a slope of -0.3 Hz/s is performed on the system [28]:

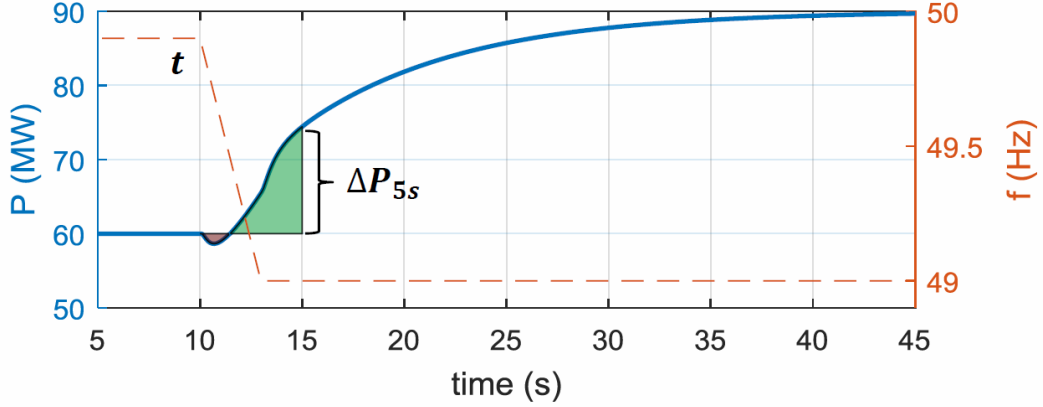


Figure 10: Ramp test FCR-D upwards regulation [28]

The active power from the ramp response is obtained five seconds after the initiation of the ramp,  $\Delta P_{5sec}$ . By integrating the area under the curve, the active energy within the five second limit can be acquired: [28]

$$E_s = \int_t^{t+5s} \Delta P(t) dt \quad (2.7.4)$$

Thus, the capacity of the FCR-D providing entity is calculated by utilizing values from the two tests: [28]

$$C_{FCR-D} = \min \left( \frac{\Delta P_{5sec}}{0.93}, \Delta P_{ss}, \frac{E_s}{1.8s} \right) \quad (2.7.5)$$

By applying a step response sequence of:

50.1 → 50.3 → 50.1 → 50.5 → 50.1 ,

and applying a mirrored ramp response with a slope of +0.3 Hz/s from 50.1 to 51.0 Hz, the capacity of the FCR-D downwards regulation can be obtained. [28]

### 2.7.3 Sinusoidal response tests

To test the stability and dynamic performance of the unit, the system is subjected to a sinusoidal signal at different time periods. The time periods are chosen based on the period times of the frequency oscillations observed in the power system. When the grid frequency is superimposed with a sinus signal, the active power response from the unit will also be a sinusoidal signal with the same frequency, but at a different amplitude and phase shift [16].

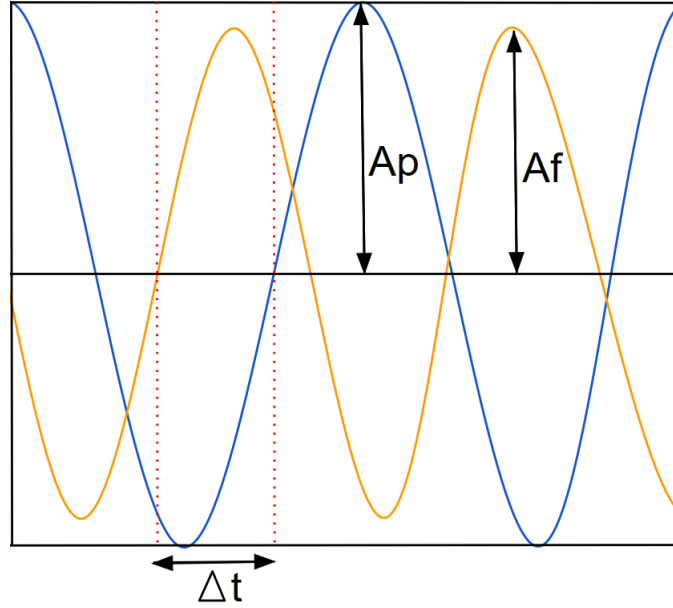


Figure 11: Sinusoidal frequency response

The applied time period can be represented by the angular frequency [27]:

$$\omega = \frac{2\pi}{T} \quad (2.7.6)$$

This angular frequency is superimposed on the nominal grid frequency with an amplitude of  $A_f$

$$f_{grid} = f_0 + A_f \sin(\omega t) \quad (2.7.7)$$

To verify that the unit complies with the dynamic performance and stability requirements, a mathematical expression for the unit needs to be developed. A set of time period specific transfer functions are therefore determined from the sine sweep. These transfer functions describe the dynamic behaviour of the unit, as well as the relationship between the frequency input and power response [27].

Each transfer function is defined by the magnitude and phase shift of the power output. The phase of the transfer function is calculated from the time difference between the input and output signal, as well as the applied time period of the frequency: [27]



$$Arg(F(j\omega)) = \Delta t \frac{360^\circ}{T} \quad (2.7.8)$$

The magnitude, or non-normalized gain, can be obtained from the sinusoidal power response, where  $A_p$  is the amplitude [27]:

$$|FCR(j\omega)| = \frac{A_p}{A_f} \quad (2.7.9)$$

In order to compare the results from the sine sweep to the requirements set by the pre-qualification working group, the magnitude found in equation 2.7.9 must be normalized. A normalization factor,  $e_N$ , is therefore obtained from the FCR-N step response tests. [27]

$$e_N = \frac{h_b \Delta P}{A_f} \quad (2.7.10)$$

Based on the value acquired in equation 2.7.2, the backlash of the system is represented by a backlash scaling factor,  $h_b$ . This value can be found in tables, and is not allowed to be over 0.3 pu [27].

From the normalization factor and equation 2.7.9, the normalized gain can be calculated [27]:

$$|F(j\omega)| = \frac{|FCR(j\omega)|}{e_N} \quad (2.7.11)$$

By tabulating the normalized gain and phase for each time period, the values can be used to construct a Bode diagram, where the gain and phase is plotted against the angular frequency.

The gain and phase can also be further developed to be expressed as FCR-Vectors, where the gain describes the length of the vector and the phase describes the angle between the vector and the real axis. To plot the vectors in the complex plane, the end points can be determined by[27]:

$$x = |F(j\omega)| \cdot \cos(Arg(F(j\omega))) \quad (2.7.12)$$

$$y = |F(j\omega)| \cdot \sin(Arg(F(j\omega))) \quad (2.7.13)$$

Where x is the real part of the vector and y the imaginary. The vectors are plotted from the origin to the end points.

To test the dynamic performance of the unit, the FCR-Vectors are plotted in the complex plane with a set of dynamic performance circles, specified by the prequalification working group. The circles are defined based on theory describing the frequency quality requirement, the net power disturbances in the Nordic synchronous area and the requirements of the power system [26]. To fulfill the criteria, the FCR-Vector must point outside the corresponding time period specific circle [28]:

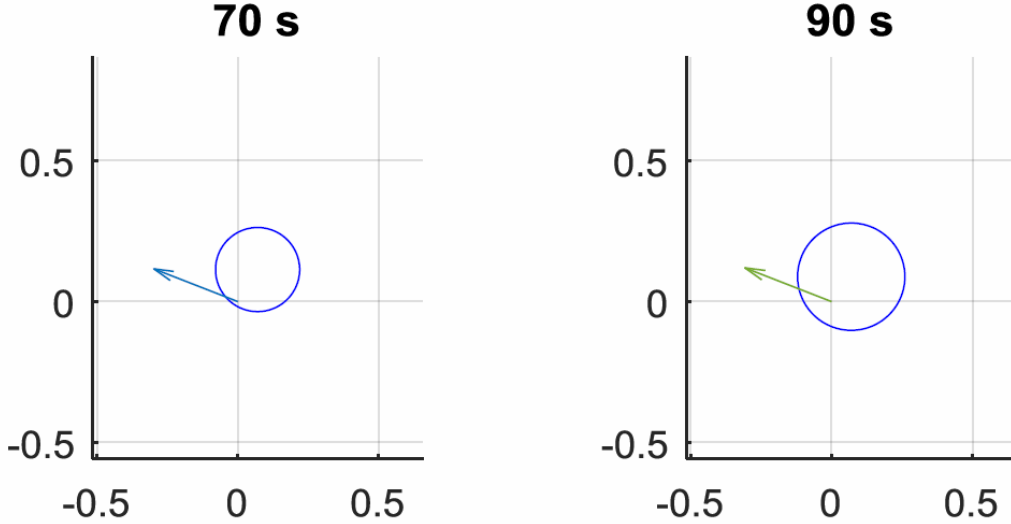


Figure 12: Example plot FCR-Vector and dynamic performance circle [28]

In the same manner as the system is tested against dynamic performance circles, it can also be tested against stability requirement circles. These circles are defined as the difference between a nominal grid and a less stable, worst-case grid with a low level of inertia and load frequency dependence [26]. The stability criteria is thus met if all FCR-vectors point outside the circles defined for each time period. [28]

However, the stability circles only ensures that the stability requirements are met at specific time periods, not that the system itself is stable. Therefore, a final stability verification must be performed by a Nyquist diagram.

To obtain the Nyquist diagram, the FCR-Vectors of the unit are multiplied with a transfer function representing a mathematical expression of the power system [27],

$$G(s)_{grid,FCR-N} = -\frac{600MW}{0.1Hz} \frac{f_0}{S_n} \frac{1}{2H_{grid}s + K_f f_0} \quad (2.7.14)$$

where  $f_0$  is the nominal grid frequency,  $S_n$  is the system loading,  $H_{grid}$  the inertia time constant and  $K_f$  is the load frequency dependence[26].

The Nyquist curve is then plotted for each angular frequency in the complex plane. To pass the stability criteria, the curve must pass the point  $(-1, j0)$  on the right hand side. In addition, a stability margin circle is defined with a center at the point  $(-1, j0)$  and a radius of 0.411 pu. The unit has sufficient stability as long as the curve does not enter this circle [27]

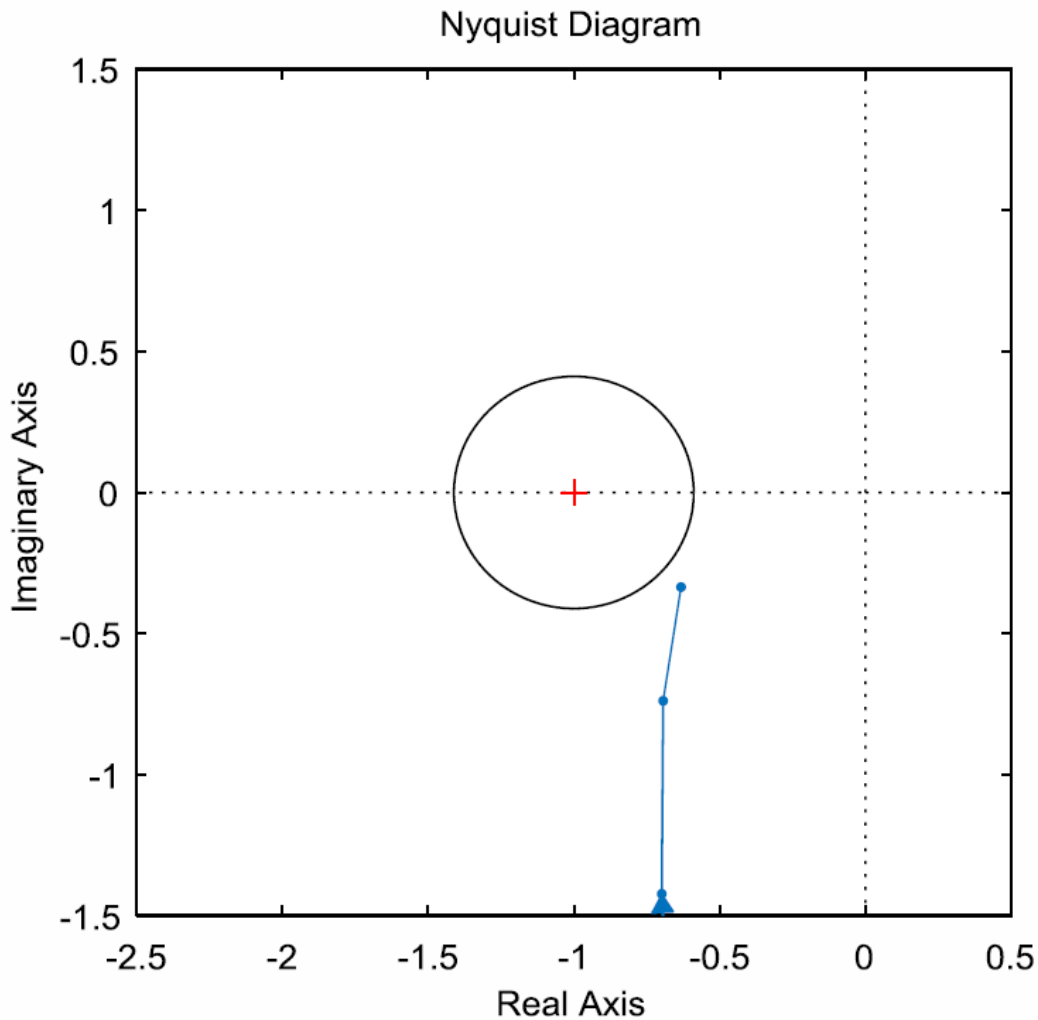


Figure 13: Example Nyquist plot with stability circle [28]

If the same governor settings are used to deliver FCR-D regulation as FCR-N regulation, the FCR-Vectors determined by the sine sweep can be used to establish the stability for the delivery of FCR-D. However, only the vectors representing the time periods between 10-50 seconds is utilized. The stability is determined by the use of a Nyquist diagram, obtained by multiplying the FCR-Vectors with a grid transfer function for FCR-D: [27]

$$G(s)_{grid,FCR-D} = -\frac{\Delta P_{ss}}{C_{FCR-D}} \frac{1450MW}{0.4Hz} \frac{f_0}{S_n} \frac{1}{2H_{grid}s + K_f f_0} \quad (2.7.15)$$

Due to the non-linear relationship between gate opening and active power, the volume of FCR will change with the loading. For this reason, all tests shall be performed at the maximum and minimum power set point where FCR shall be provided. In between these two extremes, the FCR capacity can be determined through interpolation. [16]

Before any qualification tests can be performed, a simulation model of a hydro power plant must be developed. The next section will therefore give a thorough description of how the model utilized in this thesis is built.

### 3 Building the model

To perform the simulations, a program was developed in MATLAB using numerical methods for solving the equations stated in the previous section.

#### 3.1 Waterway

Songa hydro power plant has a rather complicated waterway with two upper reservoirs and seven stream intakes. To model the plant correctly, parameters such as pipe length, area and diameter has been collected from technical drawings. In appendix B, all sections between stream intakes and reservoirs have been listed, as illustrated in figure 1. To give the reader an idea of the dynamics of the power plant, a summation of the pipe lengths and average area and diameter from reservoir to junction, have been provided in the table below:

Pipe distance	Length [m]	Area [m <sup>2</sup> ]	Diameter [m]
Songavatnet-Junction	9864	42	8
Bitdalsvatnet-Junction	10801	10	3
Penstock	327	7.5	3.1
Lower surge shaft-Totak	462	40	7.1

Table 1: Waterway parameters

The length increment of the simulated system,  $\Delta x$ , is determined by the smallest pipe length in the hydro power plant. Utilizing equation 2.2.9 and the smallest value of  $N$  dividing parts, equal to 3,  $\Delta x$  can be decided. For each pipe section, the same equation can be used to calculate the number of dividing parts,  $N$ , based on  $\Delta x$  and the pipe length. The smallest length increment also decides the time step of the simulation,  $\Delta t$ . This parameter can be determined by formula 2.2.10, where the pressure propagation speed,  $a$ , is set to  $1200\text{m/s}$  as described in [21]. In addition, the parameter  $N$  must be an integer. Therefore, the value of  $a$  is somewhat altered between a range of  $\pm 1\%$ .

Since Songa hydro power plant extracts water from two reservoirs, Bitdalsvatnet and Songavatnet, the distribution of flow between them must be determined. As described in the theory section, the pressure head is equal at an intersection point and all flow entering and exiting a junction must be zero. Therefore, two steady-state equations with loss, 2.1.1 and 2.1.2, from the reservoirs to the junction can be set to have equal pressure head, and the flow from Songavatnet can be determined by using the relation below, where  $Q_0$  is the user-defined discharge from junction to turbine:

$$Q_{songa} = Q_0 - Q_{bit}$$

After the distribution of flow have been established, the steady-state form of the waterway can be constructed using equation 2.1.1 where the loss of each pipe section is determined by 2.1.2 and Haaland's formula 2.1.3. The relative roughness of the pipes,  $\epsilon$ , is found

through iteration, as the simulated system must correspond to the rated values. By altering  $\epsilon$ , the simulations achieve the same rated pressure head and discharge as the actual system.

To simulate transient behaviour, the Method of Characteristics, as described in section 2.2, is implemented. By utilizing the parameters for each pipe section and the length increment of the system, the MOC constants, B and R is decided by formula 2.2.7 and 2.2.8. Thereafter, for all internal points, equation 2.2.3 and 2.2.4 is established to calculate the flow and pressure head. However, the behaviour of the flow in the system is determined by the boundary conditions.

The starting point of the pipe sections near the two reservoirs is set to be equal to the head of the magazine, in accordance with equation 2.2.12. If the end point is a junction, as for example between a stream intake and the main waterway, the boundary condition is set to formula 2.2.13. A stream intake is simulated as a surging device, thus the boundary condition of this pipe section is equation 2.2.16. The surface area and pipe length of the stream intakes have, as the other parameters, been found in technical drawings.

Also found in technical drawings, were the geometry of the two surge shafts in the system. They revealed that the surface area of the water will change with the height of the shaft. This has to be taken into account to have a reliable simulated system. Therefore, a check was implemented to make sure the correct surface area is used with the water level in the shaft.

Lastly, the transient behaviour of the flow in the draft tube is simulated by equation 2.2.17 and 2.2.18, where the parameters are also found in technical drawings. These equations are derived from the equation of motion and continuity for an expanding section, which is included in appendix D. The reason why the author decided to derive new equations for an expanding section is, that the formulas stated in [33] contained an error, which caused the simulations to appear faulty. The new set of equations seemed to better represent the behaviour of the flow in the draft tube and is thus implemented in the simulation model.

After the waterway with draft tube and surging devices is fully set up for steady-state and transient flow, the equations describing the turbine, generator, governor and grid are implemented.

### 3.2 Turbine, generator, governor and grid

As with the waterway, the rated values of the turbine and generator is found from technical documents. These values can be used to calculate the remaining rated parameters that are not found or specified, as for example the velocity vectors in section 2.3.1, the time constant  $T_w$  or the machine constants  $\xi$ ,  $\psi$  and  $\sigma$ .

The loss coefficients of equation 2.3.10 is determined by comparing the efficiency of the simulated system to the efficiency curve of the actual system. Loss measurements are also used to determine the coefficients.

In Thorbjørn Nielsen's thesis "Dynamic behaviour of governing turbines" [20], an equation for a PI frequency governor in the time domain is suggested based on the transfer function of a hydro power plant. This equation has been utilized before with seemingly good results, ([12] and [31]). Nevertheless, the author of this thesis wanted to develop a governing equation based on control theory and on documentation of the actual regulator at Songa hydro power plant. It was the belief of the author that this would make the governor easier to understand and therefore easier to change or expand if necessary. However, it was not possible to receive a full block diagram of the frequency regulator at Songa hydro power plant from Statkraft. Only a transfer function of the governor was acquired:

$$G(s) = K_p + \frac{K_p}{T_i} \frac{1}{s} + \frac{T_1 K_v s}{1 + T_1 s}$$

By using Laplace transformation, this transfer function correspond to the terms on the right hand side of equation 2.6.1, in the time domain. Therefore, a numerical model was developed based on this formula. The last term of the transfer function, as stated above, resemble the D-term from equation 2.6.2. A D-part in the time domain, equation 2.6.3, with  $K_P = K_v$  and  $T_1 = T_d = T_f$ , was therefore implemented in the frequency regulator.

The behaviour of the servo motor was simulated by setting a limit for the servo motor velocity. This limit is decided based on the closing time of the guide vanes, as described in technical documents. The servo motor velocity, thus, decides the opening of the guide vanes as they cannot open faster than the maximum velocity. [20]

$$\frac{d\kappa}{dt} = c_t \tag{3.2.1}$$

The equations describing the turbine behaviour, (2.3.9 and 2.3.10), generator and grid, (2.4.1, 2.4.2, 2.4.3 and 2.4.4), as well as the governing equations, (2.6.4 and 2.6.6), are set up using numerical methods. They produce eight unknowns, therefore a Newton solver is implemented to solve these equations simultaneously. The calculated head and flow over the turbine is inserted into the hydro power system by the MOC coupling equations, 2.3.23

## 4 Results and discussion

The qualification tests are performed on the simulation model with the same parameters as the actual hydro power plant and power system:

Parameter	Value
Proportional Gain, $K_p$ [-]	1.5
Integral Time, $T_i$ [s]	40
Droop, $b_p$ [%]	6
Derivative Time, $T_d$ [s]	4
Filter constant, $T_f$ [s]	4
FCR maximum load turbine, $P_{max}$ [MW]	136
FCR minimum load turbine, $P_{min}$ [MW]	60
Nominal grid frequency, $f_0$ [Hz]	50
System loading, $S_n$ [MW]	23 000
Inertia time constant of grid, $H_{grid}$ [s]	5.22
Load frequency dependence, $K_f$ [-]	0.005

*Table 2: Simulation parameters*

The tests are performed for both maximum and minimum load.



## 4.1 Maximum load

### 4.1.1 FCR-N step response

A frequency FCR-N step change, as described in the theory section, is applied to the system. The generator output response is plotted with the frequency:

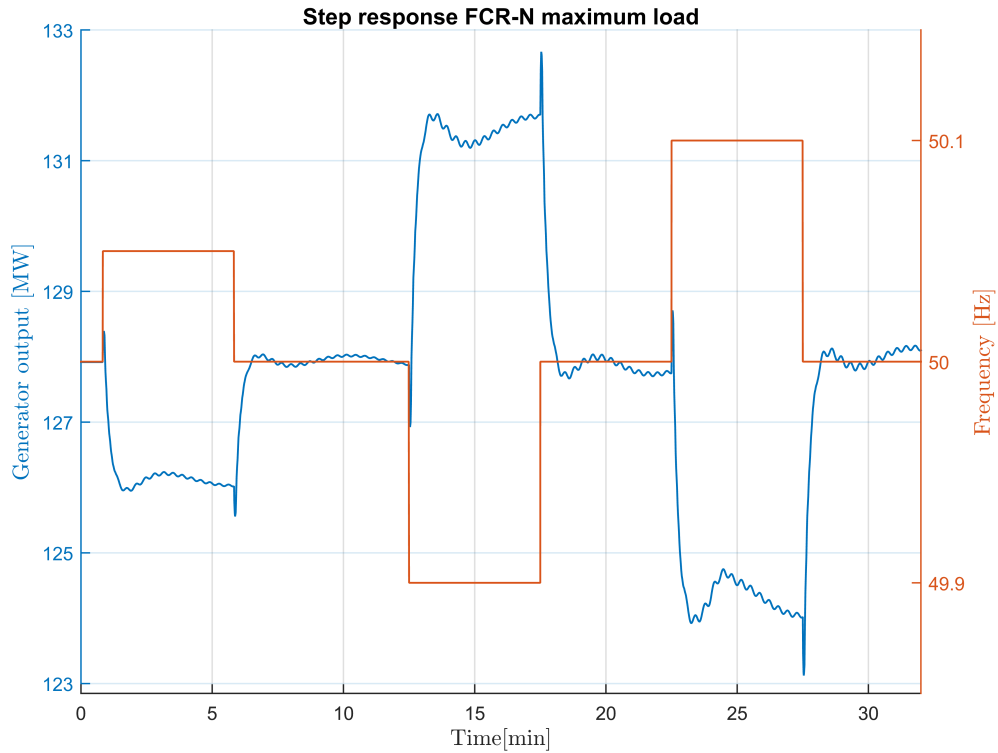


Figure 14: Generator output step response FCR-N at maximum load

As the power response is still oscillating towards a final steady-state value, the change in power is found by taking the mean value of the power response from stabilization time to the next frequency step is applied:

Frequency [Hz]	Step	Initiation time [min]	Stabilization time [min]	$\Delta P$ [MW]
49.9	$\Delta P_1$	12.5	3	3.7494
50	$\Delta P_2$	17.5	2.5	3.9151
50.1	$\Delta P_3$	22.5	3.5	3.671
50	$\Delta P_4$	27.5	2	4.0424

Table 3: Step response FCR-N maximum load

The average active response can then be calculated from equation 2.7.1:

$$\Delta P = \frac{3.7494 + 3.671}{2} = 3.7102MW$$

The backlash in the system is given by equation 2.7.2:

$$2D = \frac{|3.7494 - 3.9151| + |3.671 - 4.0424|}{2 \cdot 3.7102} = 0.072$$

Theoretically, there should be no backlash in a simulated system, as backlash is a mechanical feature and describes slowness in the system due to wear in rotary parts[3]. The calculated value of backlash is probably due to the fact that the power response has not stabilized properly before a change in frequency was applied. This causes a difference in response for the upwards and downwards step, which explains why the calculated value of  $2D$  is different from zero. The author has therefore decided to exclude the effect of backlash from the calculations, and the backlash scaling factor is therefore set to  $h_b = 1$ . From tables, [27], the value of  $h_b$  would have been 0.99, so the difference in result would be minimal.

Since the effect of backlash is not included, the capacity of FCR-N at maximum load is set to be equal to the average active power, in accordance with equation 2.7.3.

From the steady-state response, the normalization factor can be obtained from equation 2.7.10:

$$e_N = \frac{3.7102}{0.1} = 37.102MW/Hz$$

This value is used further to find the normalized gain from the sine sweep tests.

### 4.1.2 Sine sweep

A sinusoidal signal with an amplitude,  $A_f$ , of 0.1 Hz is superimposed on the frequency signal for ten different time periods.

T [s]	$\omega$ [rad/s]	$A_p$ [MW]	$\Delta t$ [s]	Gain [MW/Hz]	Norm Gain[pu]	Phase[°]
10	0.6283	1.7996	0.61	17.996	0.485	22
15	0.4189	2.0986	0.42	20.986	0.566	10
25	0.2513	2.3814	2.78	23.814	0.64	40
40	0.1571	2.4176	8.17	24.176	0.65	73.5
50	0.1257	2.5313	11.64	25.313	0.68	83.8
60	0.1047	2.6961	15.3	26.961	0.73	91.8
70	0.0898	2.8791	19.5	28.791	0.78	100.14
90	0.0698	3.1802	27.92	31.802	0.86	111.7
150	0.0419	3.9797	57.36	39.797	1.07	137.7
300	0.0209	3.8489	142.25	38.489	1.04	170.7

*Table 4: Sinus response maximum load*

According to the requirements, the response must be given time to stabilize before the parameters in table 4 can be registered. For time periods between 10-70 s, five stable sinusoidal responses are necessary and for time periods ranging from 90-300 s, three stable sinusoidal responses should be registered. [28]

The tabulated values in table 4 are:

- The power response amplitude,  $A_p$ , is found as the maximum height of the response minus the mean value.
- The time difference,  $\Delta t$ , between the frequency input and power output was registered as the time difference between the maximum values.
- The gain from each response is determined by equation 2.7.9 and dividing  $A_p$  with  $A_f$ .
- The normalized gain is calculated by equation 2.7.11, using the gain and normalization factor
- The phase is obtained from the time difference and period by equation 2.7.8.

A Bode diagram can then be constructed to illustrate the normalized gain and corresponding phase:

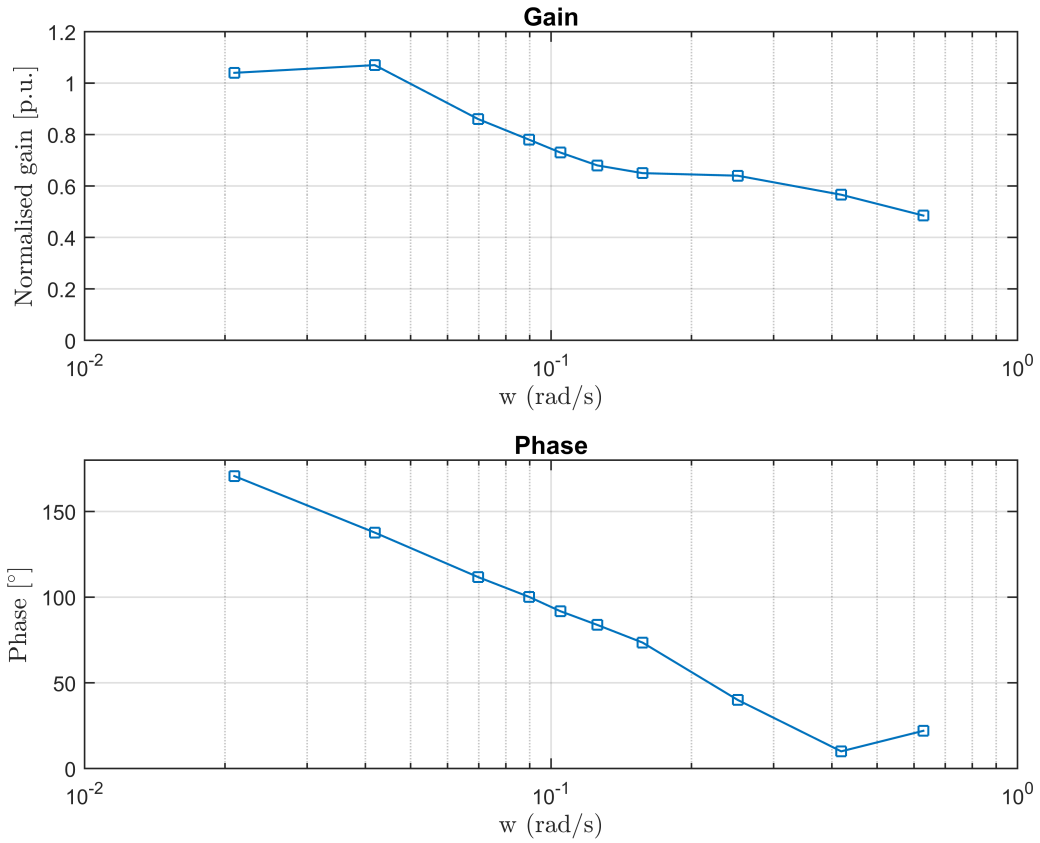
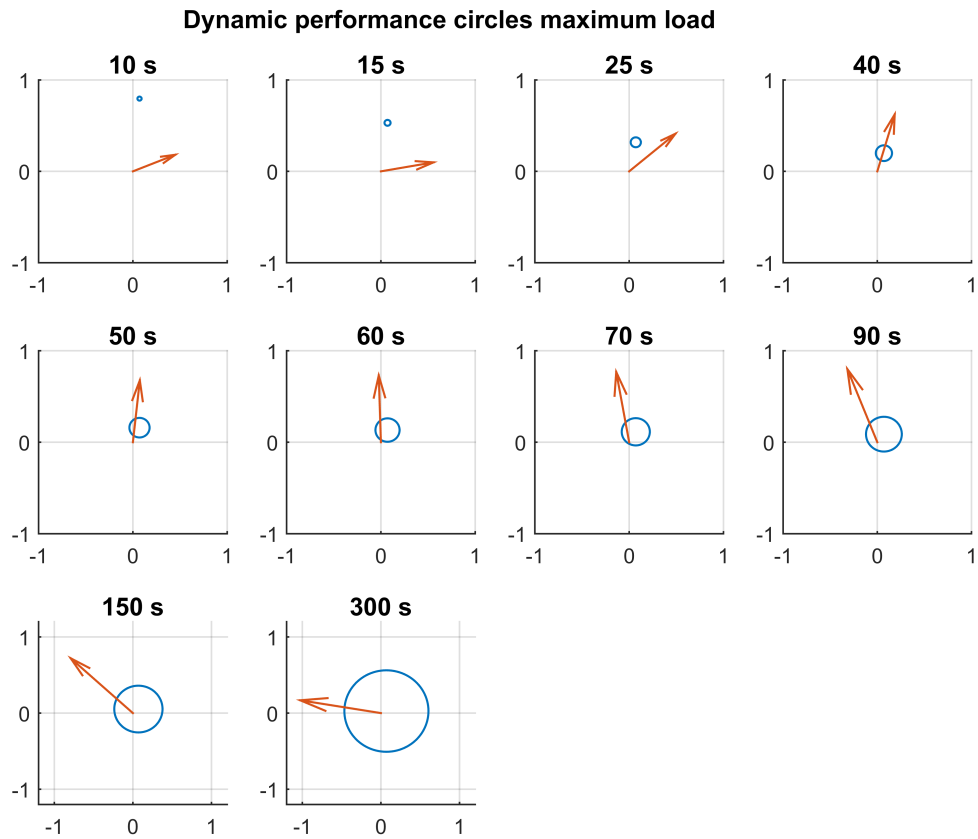


Figure 15: Bode plot maximum load

To test the dynamic performance of the unit, the normalized gain and phase are transformed by equation 2.7.12 and 2.7.13 to vectors in the complex plane. By plotting the vectors with the corresponding dynamic performance circle for specific time periods, one can see if the unit fulfills the criteria specified for FCR-N delivery.



*Figure 16: Dynamic performance circles at maximum load*

For a unit to comply with the requirements for dynamic performance, the vectors has to point outside the performance circles. As figure 16 shows, the criteria is fulfilled for all time periods.

To test the stability, the vectors are plotted with a set of stability performance circles:

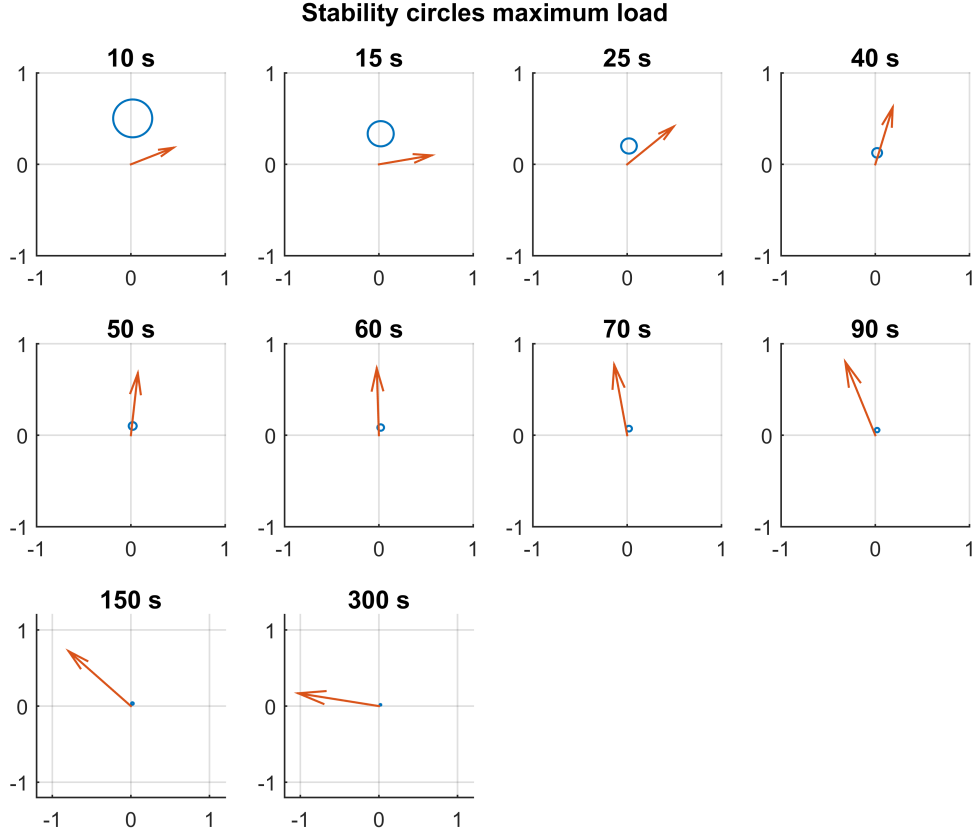


*Figure 17: Stability performance circles at maximum load*

As all FCR-Vectors point outside the corresponding circles, figure 17 show that the unit has sufficient stability margins. The stability circles do, however, only test the stability margins at discrete time periods. For a final stability verification, a Nyquist diagram showing the response for continuous time periods must be constructed.

The transfer function representing the grid in equation 2.7.14 is transformed to a vector in the complex plane by setting the Laplace variable  $s$  to  $j\omega$ , where  $j$  represents an imaginary number [15]:

$$G_{grid,FCR-N} = -\frac{600}{0.1} \frac{f_0}{S_n} \left( \frac{K_f f_0 - j2H_{grid}\omega}{(2H_{grid}\omega)^2 + (K_f f_0)^2} \right) \quad (4.1.1)$$

To plot a Nyquist diagram representing both the unit and grid, the vector  $G_{grid,FCR-N}$  is multiplied with the FCR-Vector corresponding to the specific time period and angular frequency:

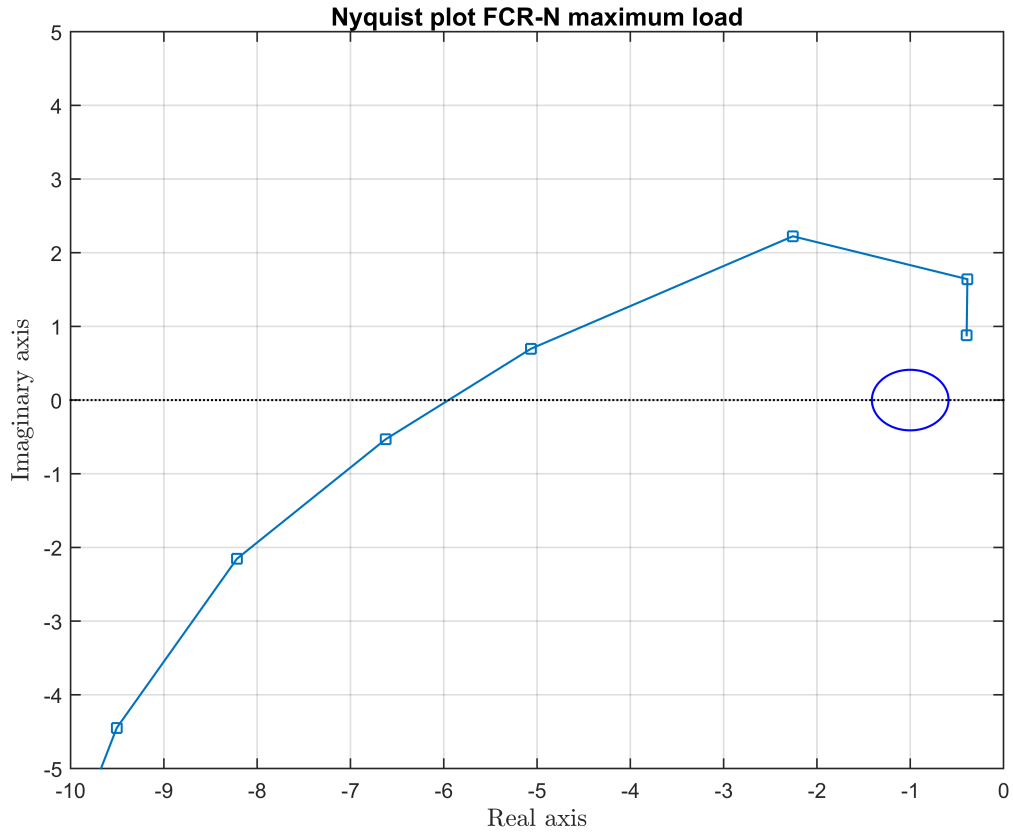


*Figure 18: Nyquist plot of FCR-N response at maximum load*

To fulfill the stability criteria, the Nyquist diagram has to pass the point  $(-1, j0)$  on the right hand side and bypass the stability margin circle. As can be seen in figure 18, the unit does not fulfill the stability requirement for FCR-N delivery as the Nyquist diagram crosses the imaginary axis far to the left of the stability requirement point and margin circle. Hence, the system is considered to be unstable.

### 4.1.3 FCR-D upwards regulation

For frequency disturbances between 49.9 to 49.5 Hz, the FCR-D upwards response is activated. To determine the FCR-D capacity of the unit, step and ramp response tests are applied to the system. The power response to a step response sequence is plotted against the frequency input:

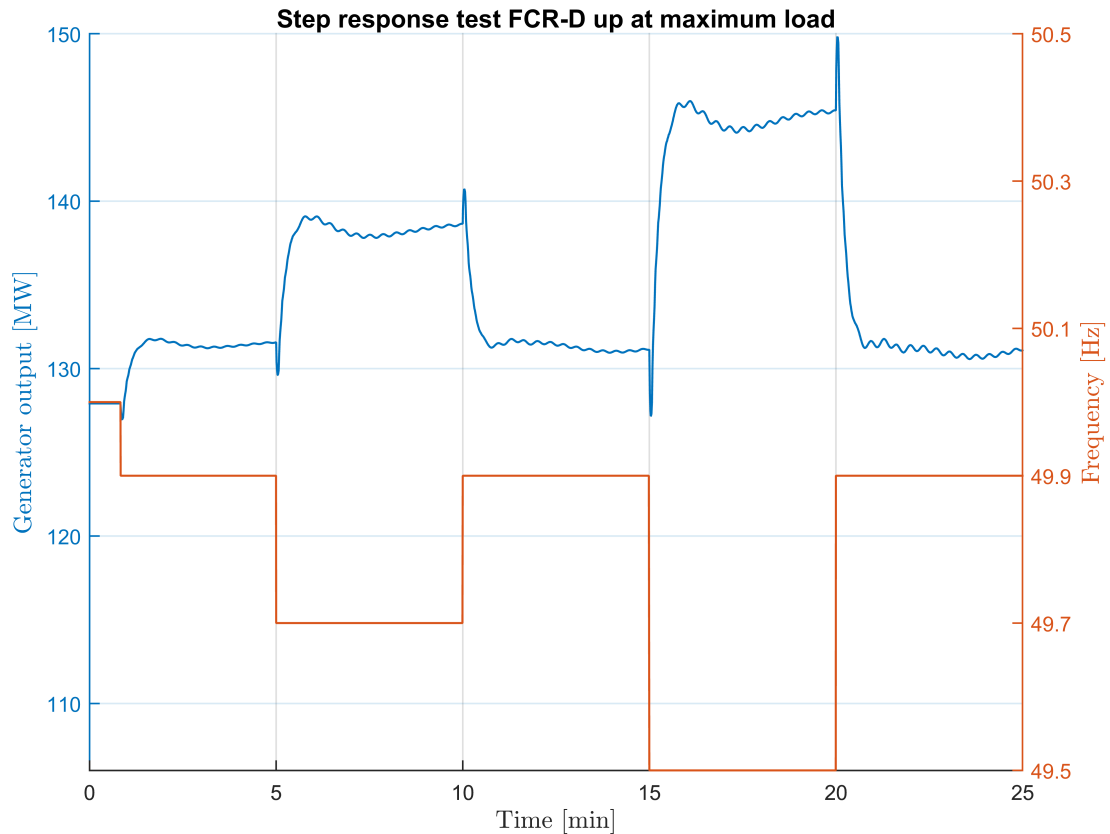


Figure 19: Generator output step response FCR-D up at maximum load

In the technical requirements, FCR-D upwards regulation is defined as positive from  $P_{current}$  to  $P_{start}$  [27]. Based on this definition, the power response to a change in frequency can be tabulated:

Step [Hz]	Initiation time [min]	Stabilization time [min]	$\Delta P$ [MW]
49.9	1	2.5	3.49
49.7	5	3	7.09
49.9	10.8	3	-7.43
49.5	15	3.5	14.2
49.9	20	3	-14.3

Table 5: Step response FCR-D upwards maximum load



From table 5, the steady-state FCR-D activation is obtained as the power response from a frequency step of 49.9-49.5 Hz:

$$\Delta P_{ss} = 14.2MW$$

The ramp response test is performed by applying a frequency input from 49.9 - 49.0 Hz with a slope of  $-0.3 \text{ Hz/s}$ :

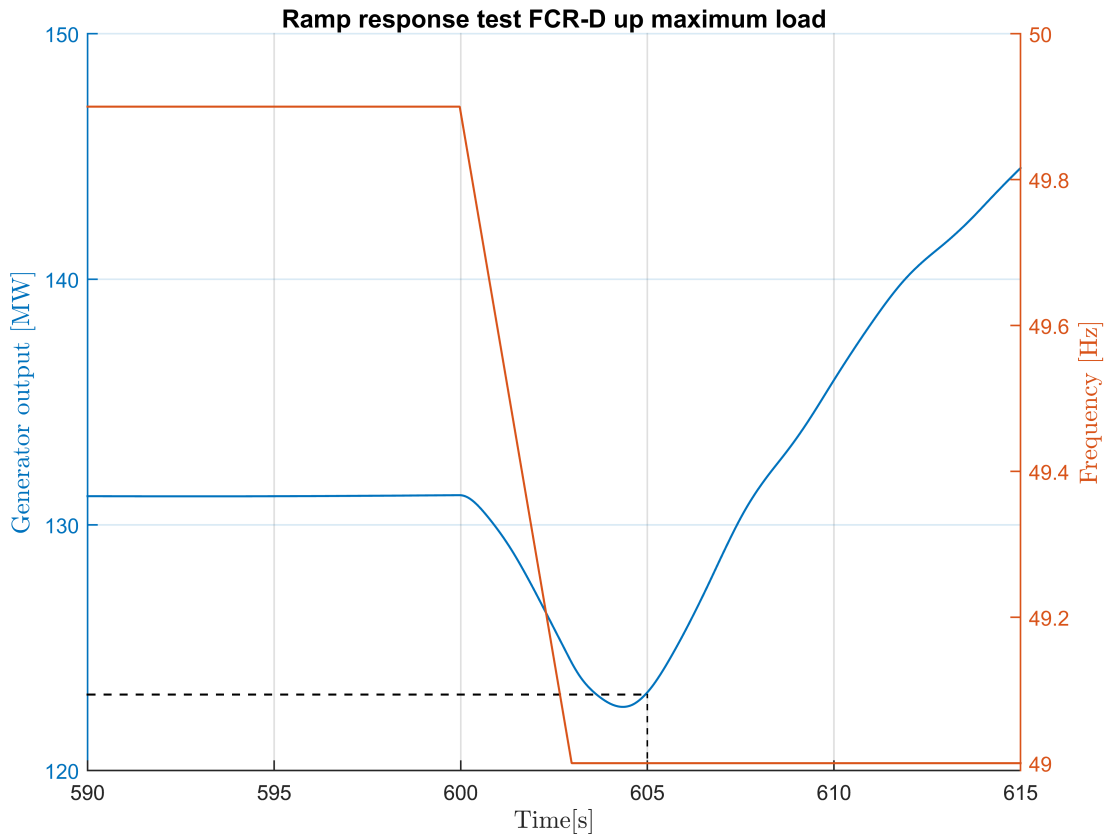


Figure 20: Generator output ramp response FCR-D up at maximum load

Since, only the response five seconds after the initiation of the ramp is of interest, the ramp response is only plotted at an interval of 25 seconds. The full ramp response can be seen in appendix C.

From figure 20, the activated power five seconds after the start of the ramp response is found to be:

$$\Delta P_{5sec} = -8.0292MW$$

By using an inbuilt MATLAB function that calculates the integral with the trapezoidal method, the activated energy five seconds after the initiation of the ramp is obtained as:

$$E_s = -24.025 MWs$$

The FCR-D upwards capacity can then be calculated by equation 2.7.5

$$C_{FCR-D} = \min(-8.63, 14.2, -13.35) = -13.35 MW$$

The capacity is also a measure of the FCR-D dynamic performance of the unit. No requirements for FCR-D delivery is described in the technical documents provided by the prequalification working group. However, in order to analyze the results, it is assumed that a negative capacity indicates a poor dynamic performance.

If the performance of the unit is measured five seconds after the start of the ramp, figure 20 illustrates that the power plant provides a negative power response. The plant would therefore cause a larger deviation from frequency within the first five seconds, as the power response is declining. This declining response is induced by a drop in pressure head over the turbine, as the load of the grid decreases rapidly. Given time, the governor will answer by opening the guide vanes to increase the flow, thus stabilizing the pressure head and raising the power, which will stabilize at around 160 MW according to figure 46. Nevertheless, the governor does not respond fast enough to reach the five second limit, resulting in a negative capacity and a poor dynamic performance.

Since the simulation is performed at the upper limit where FCR is to be provided, another limitation comes to mind. The unit cannot deliver more than the absolute maximum power, which is set to 140 MW for the generator at Songa. Both the step response test and the ramp response exceeds this limit. The results obtained from the simulation model would therefore differ from the actual system, as the real generator output would be restricted by the maximum value.

To check if the unit is capable of providing a stable FCR-D delivery, a Nyquist diagram representing the unit and power grid needs to be established. For FCR-D delivery, a grid transfer function is defined by equation 2.7.15, and transformed to a vector in the complex plane in the same manner as the FCR-N transfer function:

$$G_{grid,FCR-D} = -\frac{\Delta P_{ss}}{C_{FCR-D}} \frac{1450 MW}{0.4 Hz} \frac{f_0}{S_n} \left( \frac{K_f f_0 - j2H_{grid}\omega}{(2H_{grid}\omega)^2 + (K_f f_0)^2} \right) \quad (4.1.2)$$

As stated in the requirements [27], the same FCR-Vectors representing the FCR-N response can be utilized for FCR-D, if the governing parameters are the same. However, for FCR-D, only the time periods ranging from 10-50 s are utilized. To obtain the Nyquist diagram, the FCR-Vectors are multiplied with the grid transfer function using  $\Delta P_{ss}$  and  $C_{FCR-D}$  from the step and ramp response tests. Since, nothing else was specified, the absolute value of the capacity is applied, as the grid transfer function is defined to be negative. The Nyquist diagram is plotted for the different angular frequencies corresponding to time periods of 10-50 s:

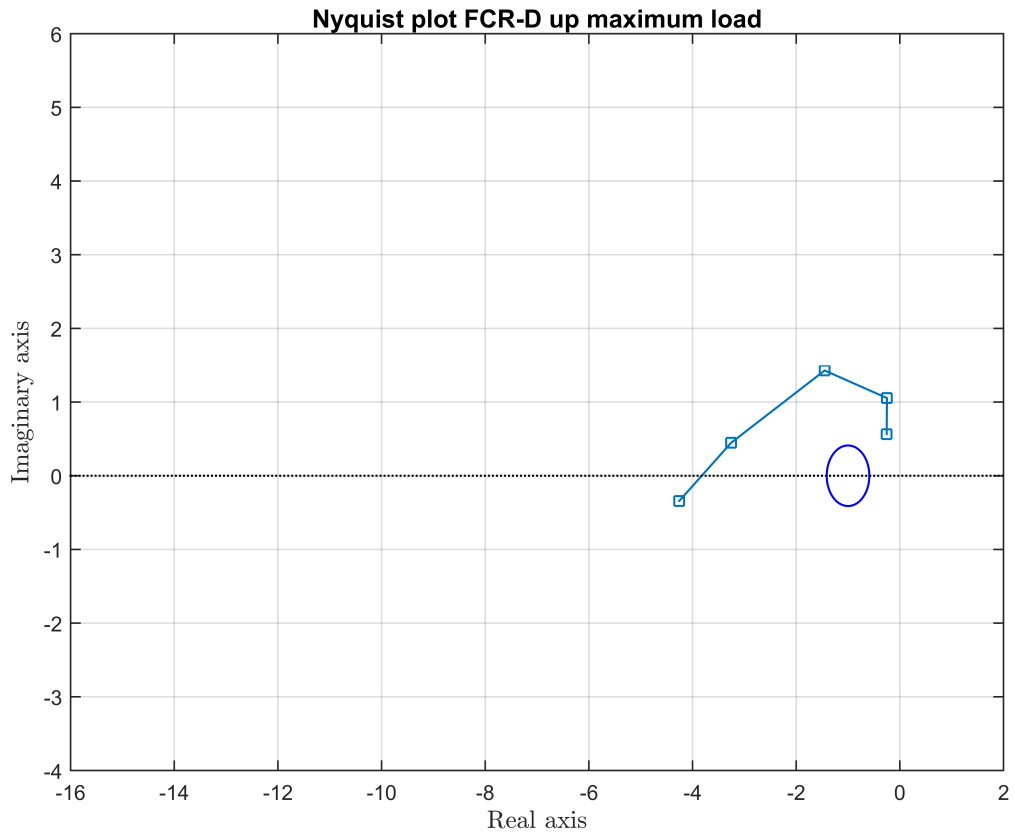


*Figure 21: Nyquist plot FCR-D upwards maximum load*

As the diagram passes the point  $(-1, j0)$  on the left hand side, the system is considered unstable for FCR-D upwards regulation at maximum load.

#### 4.1.4 FCR-D downwards regulation

As the frequency can deviate to less than the nominal frequency, it can also deviate above. FCR-D downwards regulation is activated for frequency disturbances between 50.1 Hz to 50.5 Hz. The response of the generator power output can be found by applying the following frequency step:

50.0 → 50.1 → 50.3 → 50.1 → 50.5

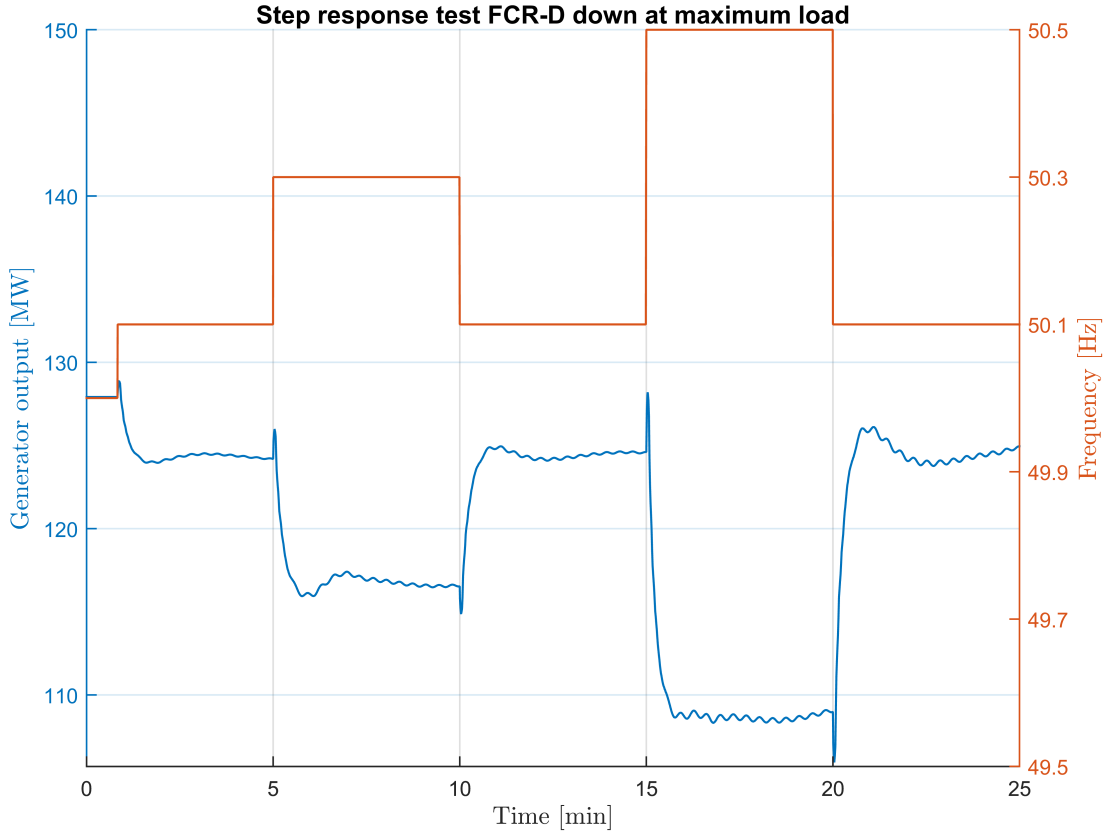


Figure 22: Generator output step response FCR-D down at maximum load

FCR-D downwards regulation is defined as positive from  $P_{start}$  to  $P_{current}$ , which is opposite of FCR-D upwards regulation [27]. Using this definition the power response to the applied frequency step response can be acquired as:

Step [Hz]	Initiation time [min]	Stabilization time [min]	$\Delta P$ [MW]
50.1	0.83	2.5	3.65
50.3	5	2.5	7.71
50.1	10	2.5	-8.02
50.5	15	2	15.75
50.1	20	2.5	-15.81

Table 6: Step response FCR-D downwards maximum load

From table 6, the value for the steady-state FCR-D activation is:

$$\Delta P_{ss} = 15.75 MW$$

There exist a discrepancy between the steady-state value of FCR-D upwards and downwards regulation. This difference is due to the variation of turbine efficiency with the variation of discharge, which will be explained in the next section.

To find the capacity of the FCR-D downwards regulation, a ramp response with a slope of + 0.3 Hz/s from 50.1 to 51.0 Hz is applied to the system:

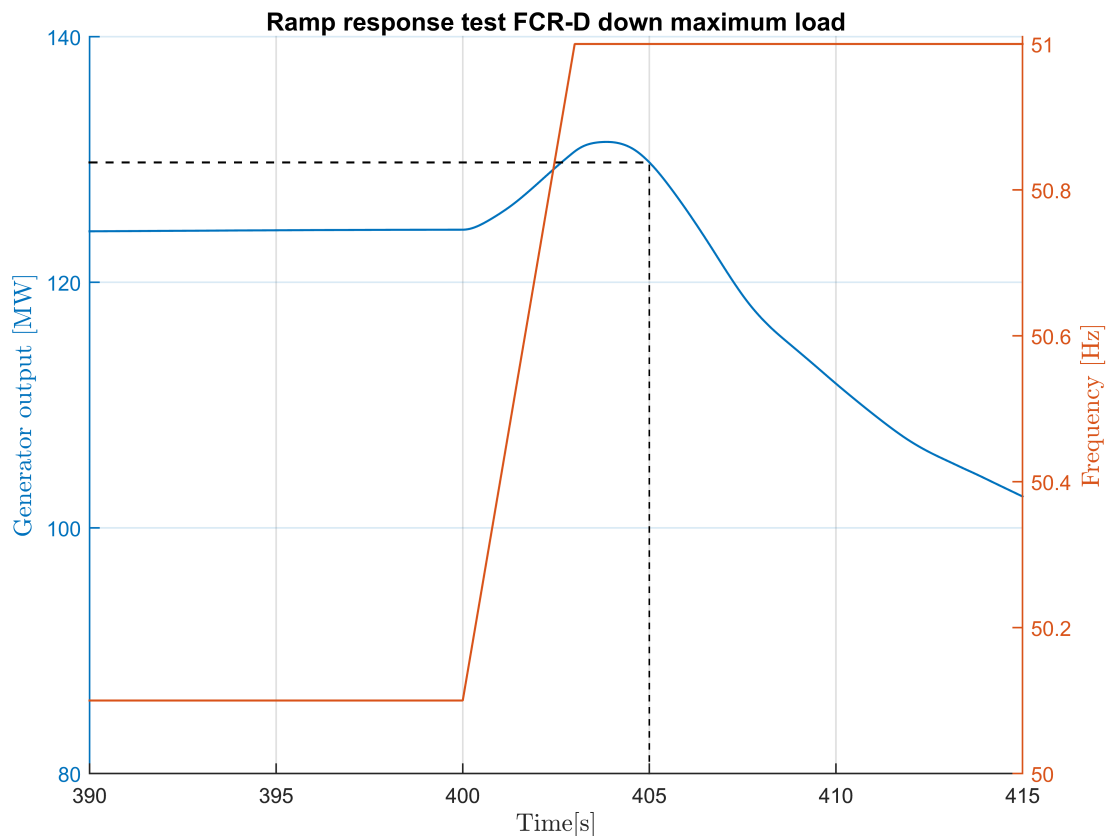


Figure 23: Generator output ramp response FCR-D down at maximum load

The activated power five seconds after the start of the ramp can be found in figure 23:

$$\Delta P_{5sec} = -5.74 MW$$

By integrating the area under the curve in the same manner as for FCR-D upwards regulation, the activated energy five seconds after the initiation of the ramp is:

$$E_s = -22.84 MW s$$

The FCR-D downwards capacity can then be calculated by equation 2.7.5

$$C_{FCR-D,down} = \min(-6.2, 15.75, -12.7) = -12.7MW$$

Based on the five second limit, the same conclusions that were drawn for the FCR-D upwards regulation can be stated for the downwards regulation. The governor does not respond fast enough to a deviation in frequency, meaning that the unit delivers a negative power response and energy within the first five seconds after the initiation of the ramp. This leads to a negative capacity and a poor FCR-D downwards dynamic performance of the unit.

A Nyquist diagram representing the grid by the transfer function,  $G_{grid,FCR-D}$ , and the unit for time periods ranging from 10-50s, is used to check the stability performance of the power plant. To obtain the plot, the absolute value of the capacity is utilized, as well as the steady-state active power:

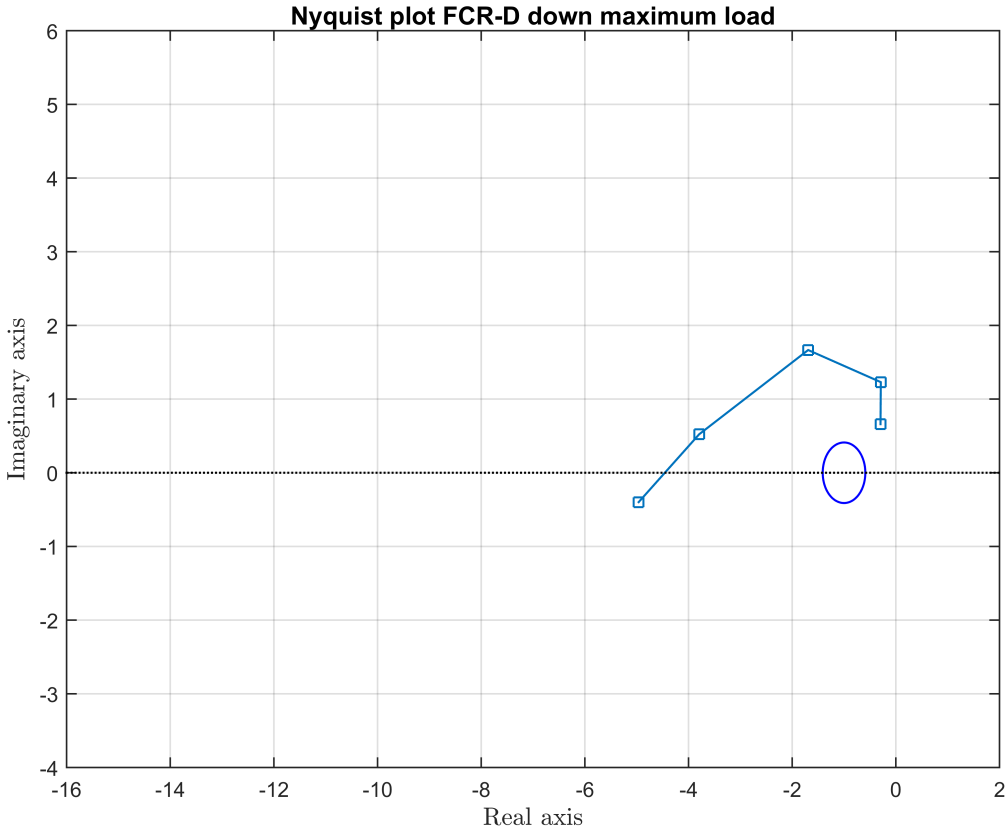


Figure 24: Nyquist plot FCR-D down maximum load

According to the Nyquist diagram, the unit is unstable for FCR-D downwards regulation.

## 4.2 Minimum load

Due to the non-linear relationship between power output and wicket gate opening, the simulations are also performed at minimum load where FCR is to be provided. The defined minimum load for Songa is at a turbine power of 60 MW.

### 4.2.1 FCR-N step response

The step response sequence is applied to the system in the same manner as for maximum load. This results in a power response which is plotted with the change in frequency:

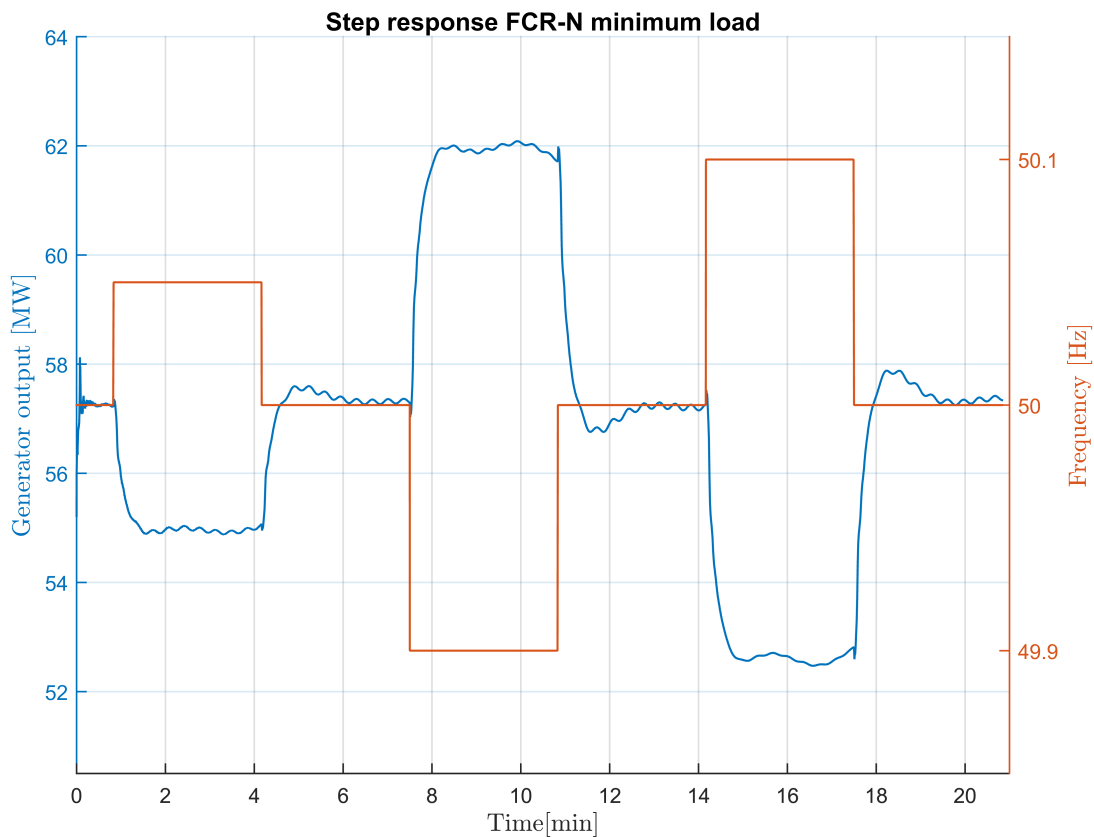


Figure 25: Generator output step response FCR-N at minimum load

Frequency [Hz]	Step	Initiation time [min]	Stabilization time [min]	$\Delta P$ [MW]
49.9	$\Delta P_1$	7.5 min	1.5 min	4.62
50.0	$\Delta P_2$	10.8 min	2 min	4.73
50.1	$\Delta P_3$	14.2 min	1.5 min	4.62
50.0	$\Delta P_4$	17.5 min	1.5 min	4.76

Table 7: Step response FCR-N minimum load

Using equation 2.7.1, the change in active power can be calculated as:

$$\Delta P = \frac{4.62 + 4.62}{2} = 4.62 MW$$

The obtained change in active power is shown to be higher for minimum load than the change in active power at maximum load. As the losses in the system are dependent on the flow rate, a lesser discharge would generate a lower head loss and friction, causing a larger value for the power response. The difference could also be explained by the shape of the efficiency curve. When the efficiency is plotted against the discharge for a Francis turbine, the curve is shaped like a parabola with the maximum point at the rated value. This means, that at lower flow rates, the slope of the curve will be steeper, and the difference in power output will thus be larger. Applying a frequency change will therefore cause a larger difference in power response, as the difference in efficiency is higher.

Another reason for the difference in active power change could be an overestimation of the efficiency. To model the parabola shape of the efficiency correctly, equation 2.3.22 is utilized. By adjusting the loss constants in the equation, the efficiency curve of the simulation model can be matched with the actual power plant. The tuning is performed in steady-state mode. When the frequency step is applied, the efficiency in the simulations increases to a value above the efficiency curve for the actual power plant. It seems that for values that are not rated, equation 2.3.22 overestimates the efficiency. This could be due to poor tuning of loss constants or that machine constants and initial values does not properly represent the system outside rated parameters. The increased efficiency leads to a larger difference between the power responses, hence the value of change in activated power is higher at minimum load. Discrepancies could therefore exist if the tests are performed at the actual hydro power plant. However, as the inaccuracy in efficiency is small and affects all simulations at minimum load, and the change in active power is used for normalization, the results presented here still provides a good image of the performance of the unit.

Equivalent to the FCR-N step response at maximum load, there should theoretically be no backlash in the system. Nevertheless, equation 2.7.2, is calculated to a value of:

$$2D = \frac{|4.62 - 4.73| + |4.62 - 4.76|}{2 \cdot 4.62} = 0.03$$

Utilizing the same argument as previously stated in section 4.1.1, the backlash scaling factor is set to  $h_b = 1$  at minimum load. Based on the calculated value of backlash,  $h_b$  should have been 0.997, so setting the value to one, does not lead to great differences. As the backlash is not included, the FCR-N capacity at minimum load is set equal to the active power response.

The normalization factor is:

$$e_N = \frac{4.62}{0.1} = 46.2 MW$$



### 4.2.2 Sine sweep

A sine sweep is performed on the simulation model for time periods ranging from 10-300 s. The tabulated values are found in the same manner as for maximum load:

T [s]	$\omega$ [rad/s]	Ap [MW]	$\Delta t$ [s]	Gain [MW/Hz]	Norm Gain[pu]	Phase[°]
10	0.6283	1.5477	0.5833	15.447	0.334	21
15	0.4189	1.8659	2.0278	18.659	0.4	48.67
25	0.2513	2.2929	5.86	22.929	0.496	84.4
40	0.1571	2.6859	11.58	26.859	0.581	104.25
50	0.1257	2.844	15.83	28.44	0.62	114
60	0.1047	3.1449	20.69	31.449	0.68	124.17
70	0.0898	3.4301	23.8056	34.301	0.74	122.43
90	0.0698	3.9860	32.94	39.860	0.86	131.8
150	0.0419	5.0675	66.17	50.675	1.1	158.8
300	0.0209	5.1018	133.56	51.018	1.104	160.3

Table 8: Sinus response minimum load

The Bode diagram is plotted based on the normalized gain and corresponding phase:

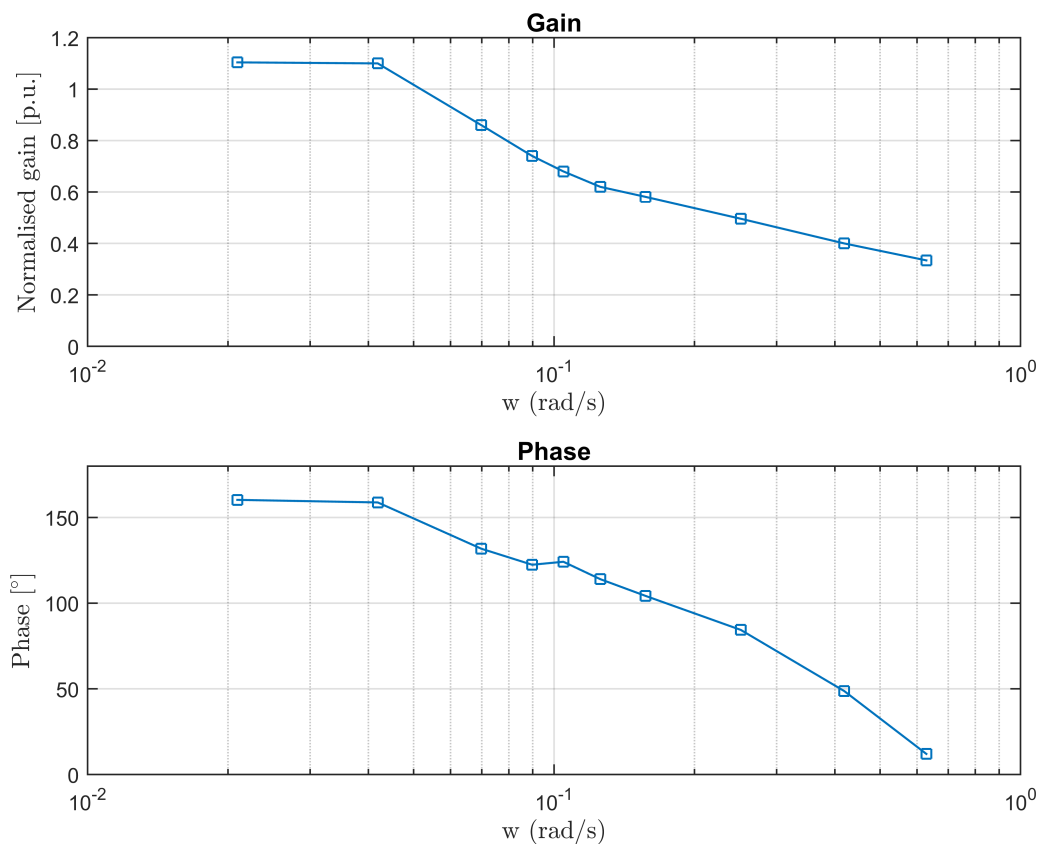
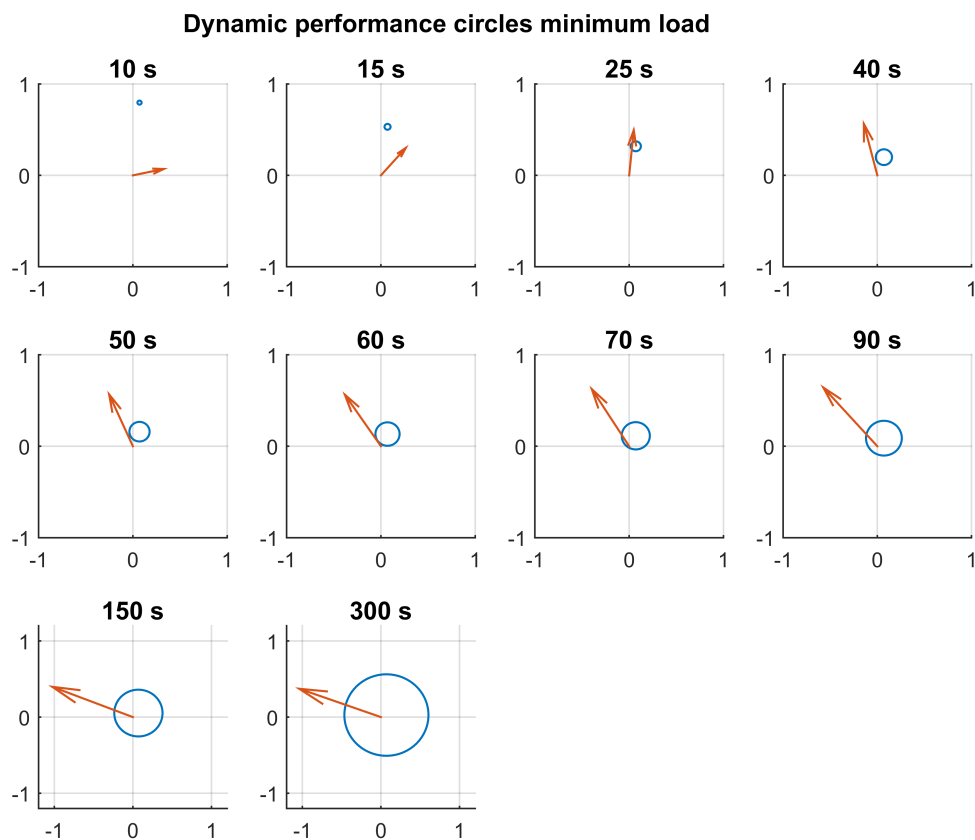


Figure 26: Bode plot minimum load

By transforming the normalized gain and phase to vectors in the complex plane, the dynamic performance of the unit can be established



*Figure 27: Dynamic Performance circles at minimum load*

The power plant can deliver a satisfying FCR-N dynamic performance at minimum load, as all vectors point outside the corresponding circles.

To test the stability, the vectors are plotted with a set of stability circles defined for each time period.

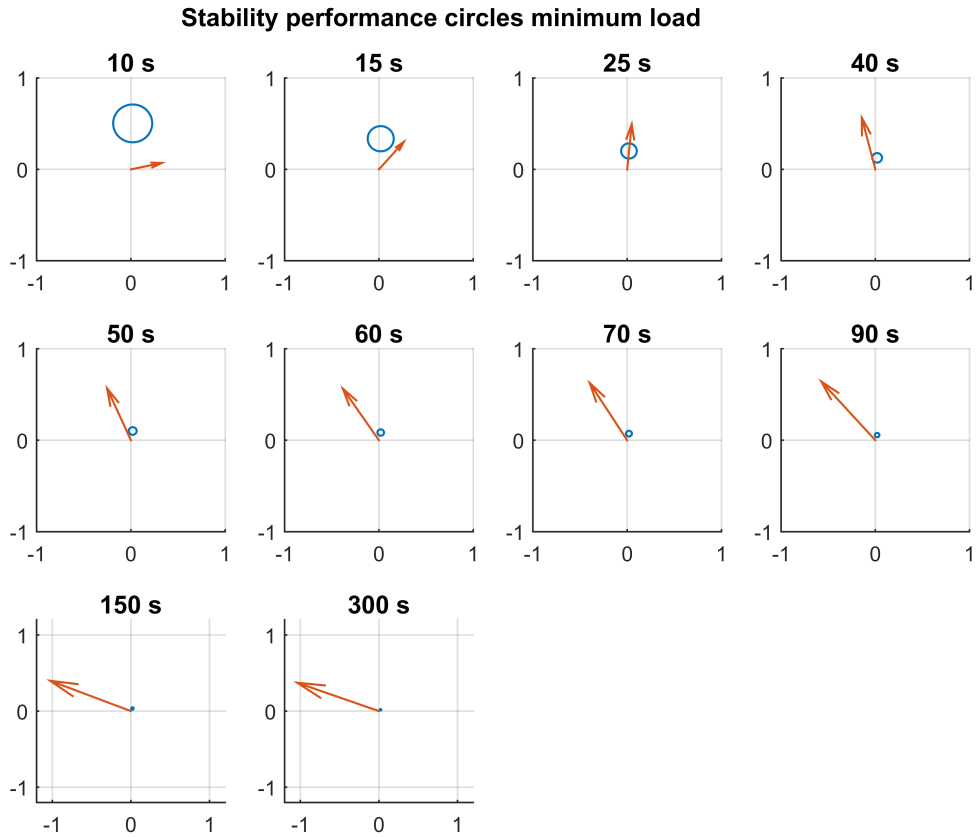


*Figure 28: Stability Performance circles at minimum load*

The requirement of stability is fulfilled for all time periods as the vectors point outside the stability performance circles. However, to check the absolute stability of the power plant at discrete time periods, the FCR-vectors are multiplied with the transformed grid transfer function,  $G_{grid,FCR-N}$ , to obtain a Nyquist diagram:

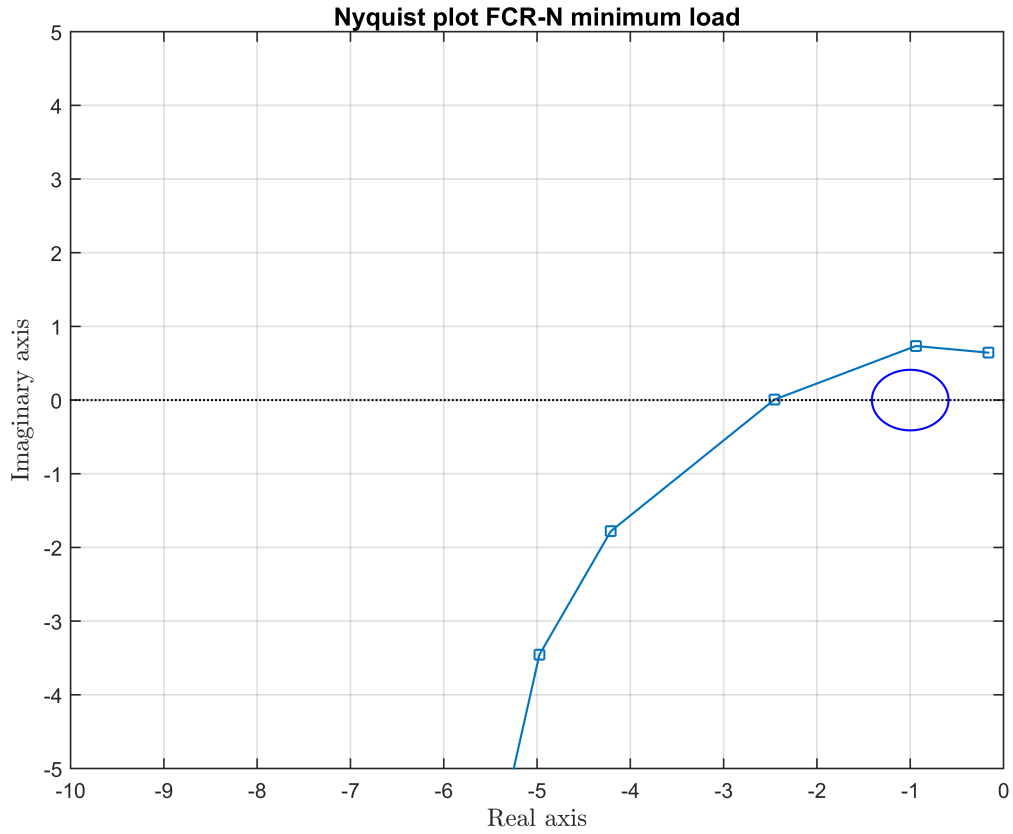


*Figure 29: Nyquist plot of FCR-N response at minimum load*

As the Nyquist curve passes the point  $(-1, j0)$  and stability margin circle on the left hand side, the overall stability requirement is not fulfilled by the power plant. The unit is therefore unfit for FCR-N delivery at minimum load.

### 4.2.3 FCR-D upwards regulation

To find the capacity and test the stability of the FCR-D upwards regulation at minimum load, the system is subjected to a step and ramp response sequence. The figure below illustrates the change in power response when a frequency step change is applied:

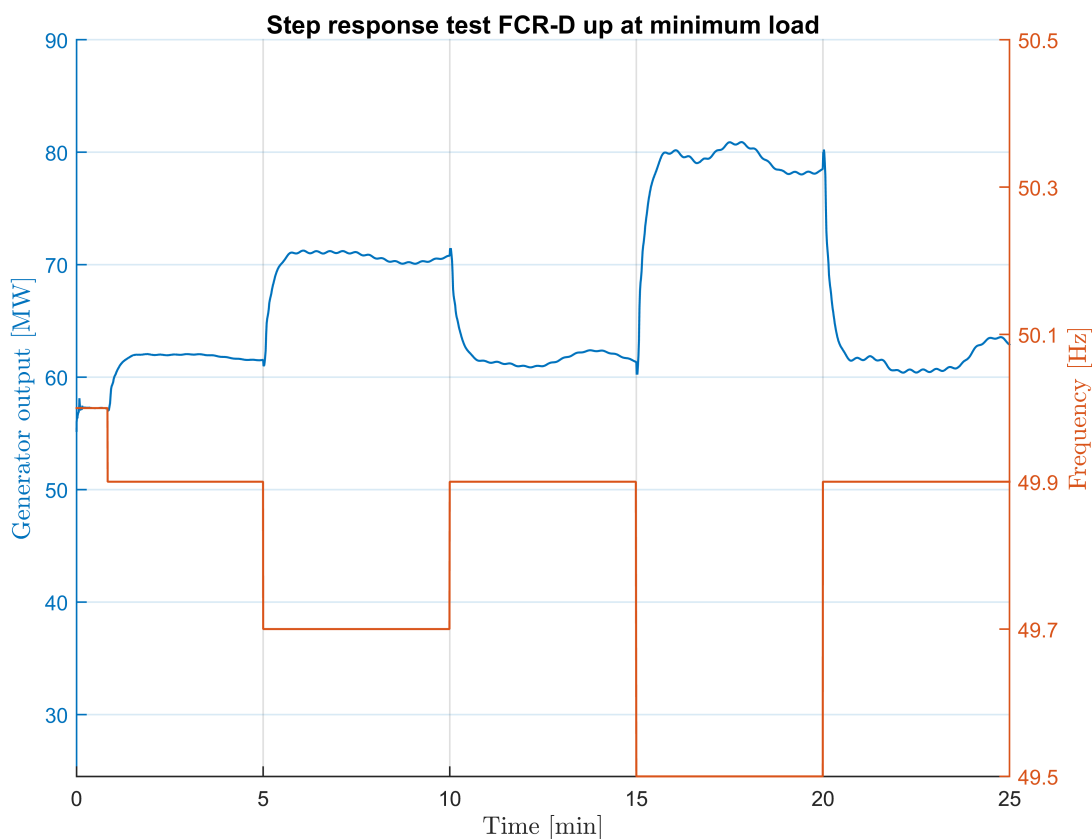


Figure 30: Generator output step response FCR-D up at minimum load

By taking the mean values from stabilization time to the application of a new frequency step, and utilizing the definition of positive direction for FCR-D upwards regulation, the difference in power can be tabulated as:

Step [Hz]	Initiation time [min]	Stabilization time [min]	$\Delta P$ [MW]
49.9	0.83	2.5	4.36
49.7	5	2.5	8.84
49.9	10	2.5	- 8.53
49.5	15	2.5	16.3
49.9	20	2.5	-14.95

Table 9: Step response FCR-D upwards minimum load

From table 9, the steady-state activation is:

$$\Delta P_{ss} = 16.3MW$$

A ramp response from 49.9 Hz to 49.0 Hz with a slope of -0.3 Hz/s is then applied to the system. The corresponding power response is:

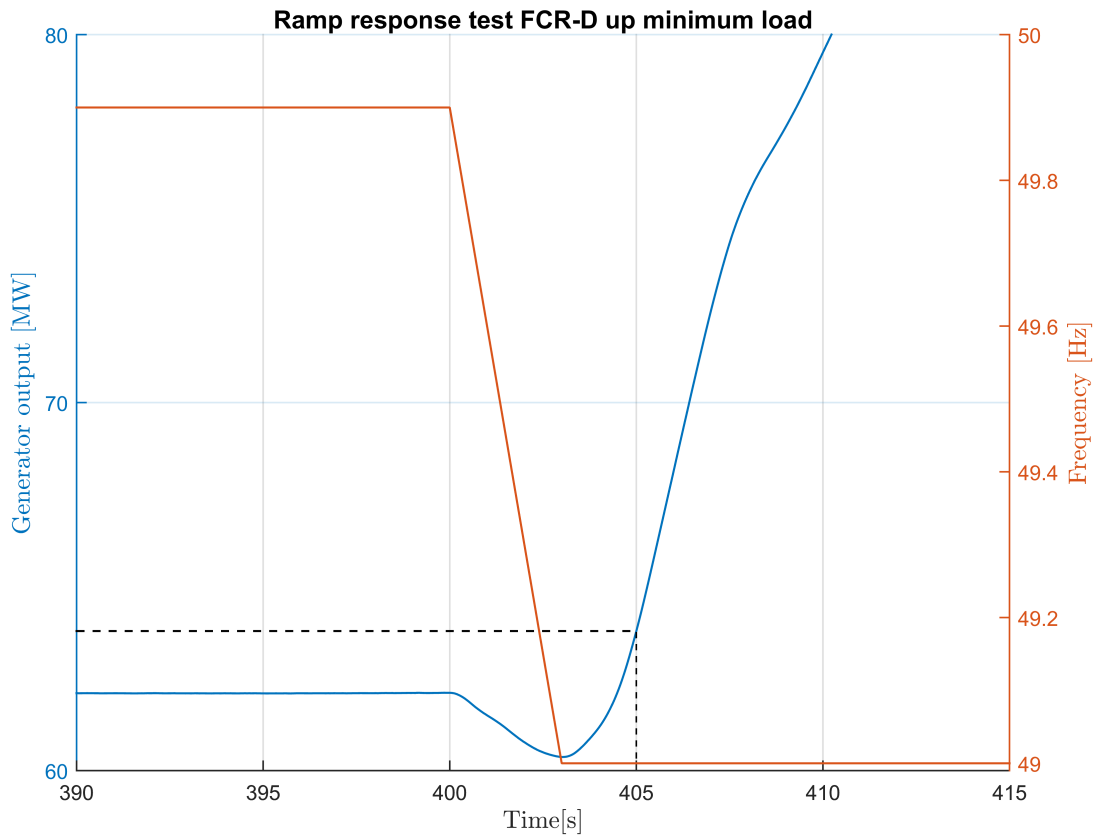


Figure 31: Generator output ramp response FCR-D down at minimum load

Utilizing the same definition for positive direction for FCR-D upwards, the activated power and energy five seconds after the initiation of the ramp is,

$$\Delta P_{5sec} = 1.8965MW$$

$$E_s = -3.0356MWs \quad ,$$

where  $E_s$  is found by integrating the area under the curve using the trapezoidal method.

At minimum load, the governor manages to deliver a positive power response five seconds after the start of the ramp. This stands in contrast to the response at maximum load, which was found to be negative. The reason for the difference can be explained by the efficiency curve and the self-governing parameter of the turbine. As previously mentioned, the efficiency curve is steeper at lower flow rates, causing a larger difference in power response. In addition, the overestimated efficiency could also influence the results.

The self-governing parameter of a Francis turbine,  $\sigma$ , is a constant defined by the geometry of the runner, the rated head and rotational speed, equation 2.3.17. Considering the equation for the turbine torque, 2.3.10, the self-governing parameter will affect the flow through the turbine, as the reaction of the rotational speed and wicket gate opening of the turbine will be roughly the same at minimum and maximum load. As  $\sigma$  is a constant it will have a larger impact at flow rates away from rated values, causing a larger increase in flow through the turbine. This again, causes a more rapid power response, and the value of the activated power within five seconds, is positive at minimum load.

After the step and ramp response tests are performed, the FCR-D upwards capacity at minimum load can be found by equation 2.7.5:

$$C_{FCR-D,up} = \min(2.04, 15.63, -1.67) = -1.67 MW$$

Due to the negative activated energy,  $E_s$ , the capacity of the FCR-D upwards regulation is shown to be negative. It can therefore be concluded that the FCR-D upwards dynamic performance is poor. The activated energy describes the overall power response of the unit within the five second limit. As the total response was negative, the governor is shown to be too slow to deliver a good performance five seconds after the initiation of the ramp, even though the activated power is positive within the limit.

To test the stability requirement, the Nyquist plot is obtained in the same manner as for maximum load, using the absolute value of the capacity:

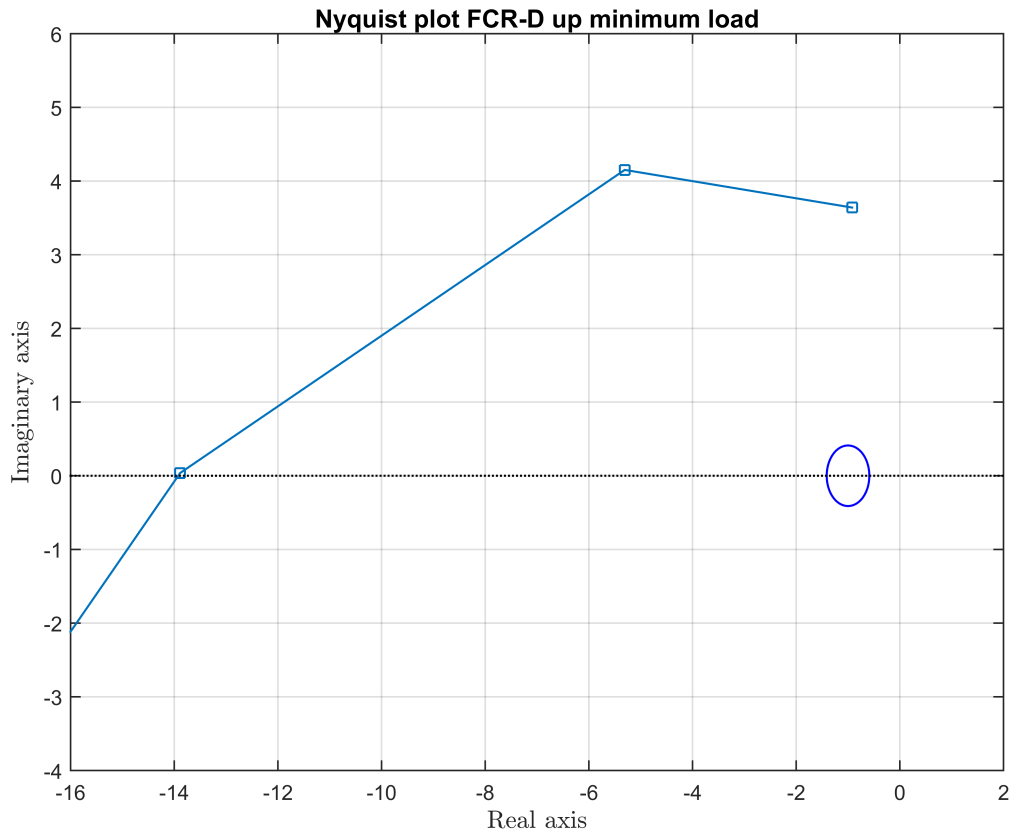


*Figure 32: Nyquist plot FCR-D upwards minimum load*

According to the demands set by the prequalification working group, the power plant cannot deliver FCR-D upwards regulation within the specified stability requirements.



#### 4.2.4 FCR-D downwards regulation

The FCR-D downwards capacity must also be established. A step response sequence is therefore applied to the system, and the corresponding power response is plotted along the frequency:

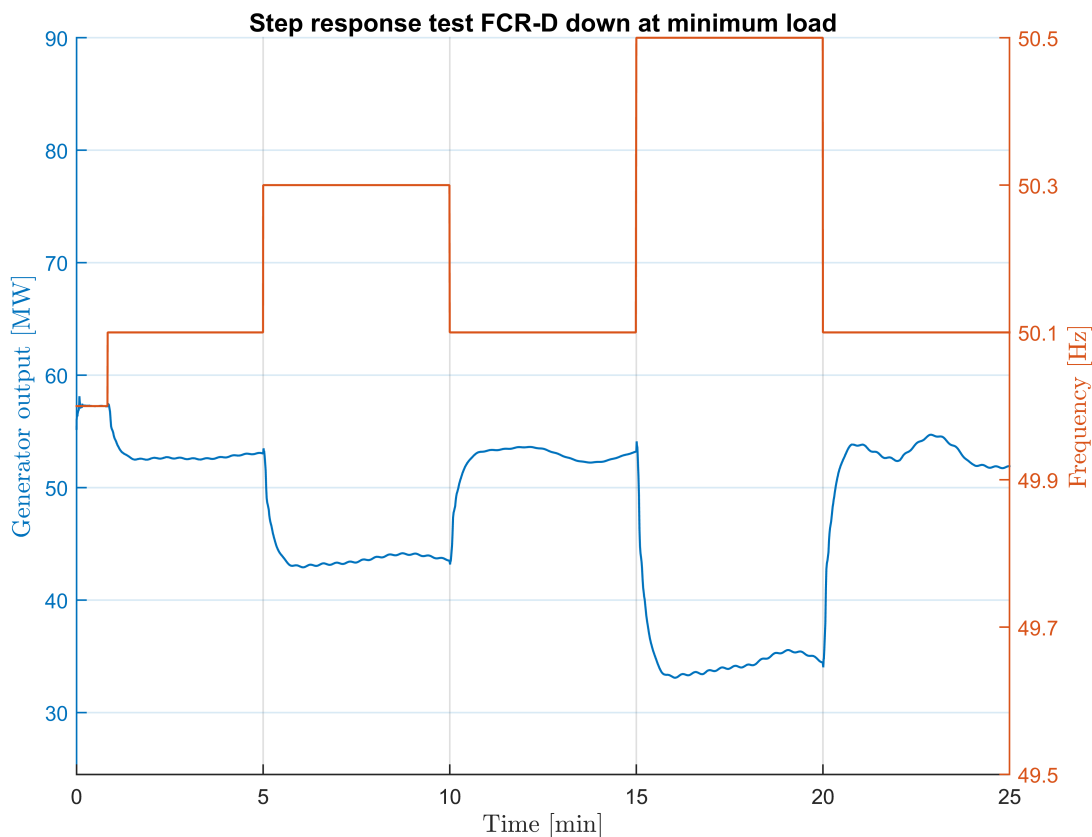


Figure 33: Generator output step response FCR-D down at minimum load

By using the same definition for positive direction as previously stated for FCR-D downwards regulation at maximum load, the power response can be tabulated by taking the mean value of power from the stabilization time to a new frequency step is applied:

Step[Hz]	Initiation time[min]	Stabilization time [min]	$\Delta P$ [MW]
50.1	0.83	2.5	4.3
50.3	5	2.5	9.1
50.1	10	2.5	-8.9
50.5	15	2	17.6
50.1	20	4	-16.7

Table 10: Step response FCR-D downwards minimum load

From table 10, the steady-state response for FCR-D downwards regulation at minimum load can be obtained:

$$\Delta P_{ss} = 17.6MW$$

In order to determine the active power and energy, a ramp response from 50.1 Hz to 51.0 Hz with a slope of 0.3 Hz/s is applied to the system:

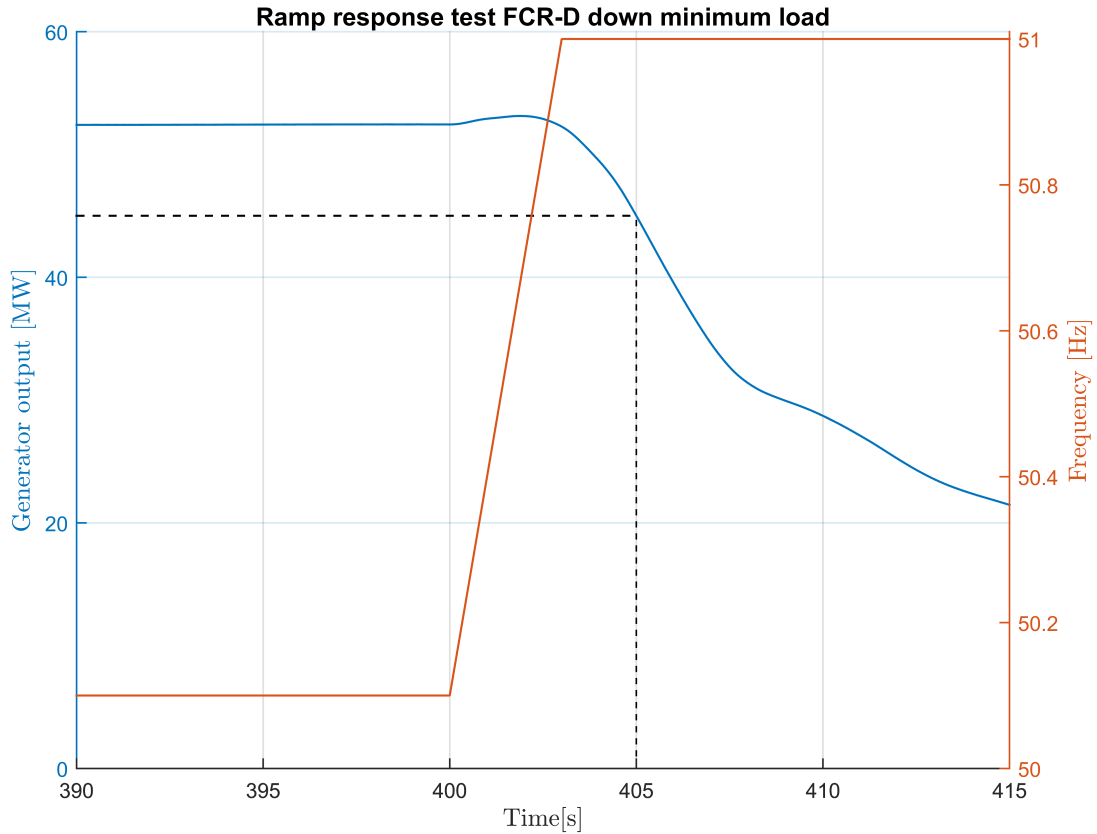


Figure 34: Generator output ramp response FCR-D down at minimum load

The active power and energy five seconds after the ramp is:

$$\Delta P_{5sec} = 7.65MW$$

$$E_s = 6.32MWs$$

Hence, the FCR-D upwards capacity can be calculated from equation 2.7.5

$$C_{FCR-D,down} = \min(8.23, 17.6, 3.51) = 3.51MW$$

The unit show a good dynamic performance for FCR-D upwards regulation at minimum load, as the governor manages to respond fast enough to provide a positive active power and energy.

The difference in result between FCR-D upwards and downwards regulation at minimum load is most likely due to the variation in efficiency with the discharge.

To plot a Nyquist diagram, the FCR-Vectors for time periods between 10-50 s was multiplied with the grid transfer function for FCR-D, equation 2.7.15:

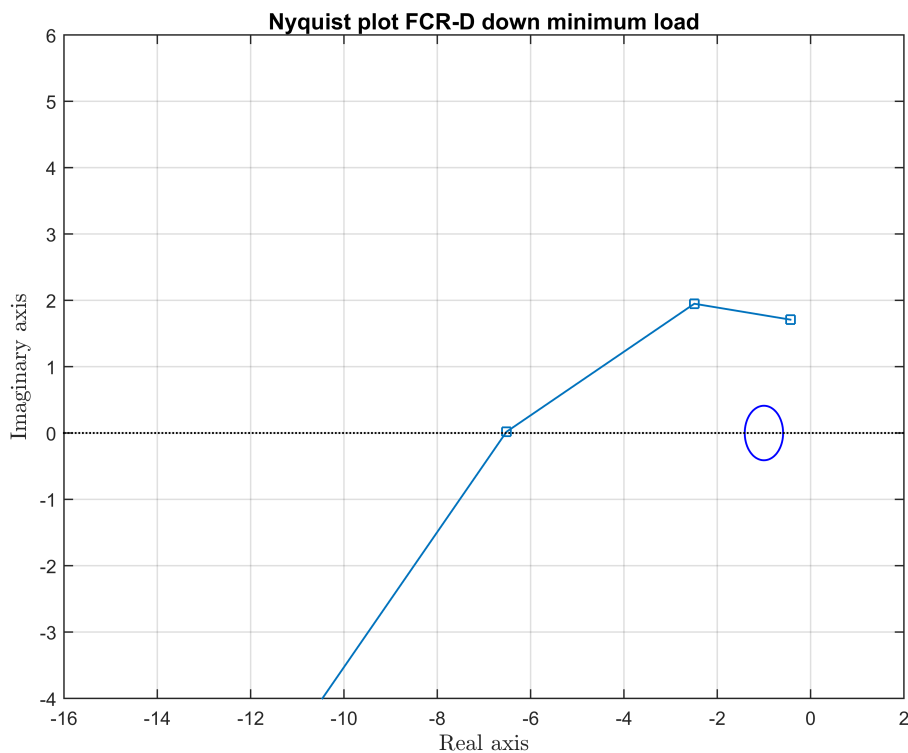


*Figure 35: Nyquist plot FCR-D down minimum load*

Again, the Nyquist diagram show that the unit cannot deliver a stable FCR-D downwards regulation at minimum load, as was the conclusion for maximum load.

The qualification tests revealed that the unit does not fulfill the stability requirements defined by the Nyquist diagram for neither FCR-N nor FCR-D. It would therefore be interesting to investigate other governor settings, to see if the stability criteria can be achieved for the hydro power unit.

### 4.3 Governor tuning

To tune the governor, a program developed by Vattenfall was provided by Statkraft. The program models the behaviour of a hydro power unit by the use of transfer functions representing the grid, governor, turbine and waterways.

In order to test the stability and performance of the power plant, parameters describing a normal and worst-case grid are defined by the user and implemented in the program. To obtain governor settings that correspond to the requirements stated in this thesis, the values are defined based on parameters given in the report "FCR specification - Methodology" [26]:

Parameter	Normal case grid	Worst case grid
Frequency dependent load [MW/Hz]	210	0
Kinetic energy [GWs]	190	0
Static Gain FCR-N [MW/Hz]	7530	7530

Table 11: Grid parameters

The behaviour of a hydro power unit is defined by the guide vane opening, servo time constant and delay, as well as backlash and regulator parameters. As the exact values at Songa were not possible to obtain, general values for a hydro power unit were utilized:

Parameter	Values
Mean guide vane opening [pu]	1
Guide vane servo time constant [s]	0.4
Guide vane backlash before feedback [pu]	0.0003
Guide vane backlash after feedback [pu]	0
Guide vane delay [s]	0.2
Incremental gain for guide vanes [pu/pu]	1
Water starting time [s]	0.94
$K_p$ [pu]	1.5
$K_i$ [pu/s]	0.038
droop	0.06
Phase margin [°]	25
Gain margin [ ]	2
Maximum sensitivity [pu/pu]	2.31
Static gain [%/Hz]	33

Table 12: Unit parameter utilized for governor tuning

Integral time is represented by the parameter  $K_i$ , which is defined as  $K_p/T_i$ . The static gain for the unit is found from the simulations by calculating the difference in guide vane opening and dividing with the change in frequency.

The program also defines a set of stability margins, such as phase and gain margin, as well as maximum sensitivity. However, in the technical documents, no stability margins

are defined, ([28] and [27]). It is therefore decided to implement the suggested values of the program, which roughly corresponds to the stability margins set in FIKS 2012 [30].

By running the program, the user is provided with a set of Bode and Nyquist diagrams, representing the power system and the hydro power unit with the current governor settings. The performance of the unit can therefore be tested by comparison with a bad and good plant, defined by Vattenfall. In addition, the program also provides a diagram presenting different governor settings, where a green colour means that the criteria for stability and performance is met:



Figure 36: Governor parameter set from Vattenfall Program

However, the results from the program should be used with care. The qualification tests and requirements presented in this thesis are based on reports dated March 2017. It is difficult to say exactly when the Vattenfall program was finalized, but the description is dated November 2015 [29]. The reason why the author suspects that the program is not updated with the final version, is that the Nyquist diagrams, provided by the program, show that the unit, with the current governor settings, is far within the limits of stability. This is in contrast to the results presented in the previous section. Further investigation of the program code revealed that the Vattenfall program utilizes a different transfer function to represent the power system than the one described in the technical documents [28], later stated in equation 4.4.1. This transfer function causes a lower amplification of the Nyquist response, and the plotted curve passes on the right hand side of the point  $(-1, j0)$ .

Another consideration is that the program uses a simple general model of a hydro power plant to describe the unit. For governor tuning, this model should be sufficient, but inaccuracies and differences between the simulated and actual plant will therefore exist. In addition, the program examines the performance based on a set of stability margins. As previously mentioned, no stability margins are defined in the technical documents for the qualification test [28]. As such, it is not known if the criteria defined by the program matches the ones defined in the technical documents, which may lead to differing conclusions.

However, the Vattenfall program does provide governor settings based on a representation of a hydro power unit and grid, as well as measuring the performance based on a set of stability margins. Therefore, the diagram provided is used as a suggestion for a change in governing parameters.

The results presented in the previous section showed that the unit did not fulfill the stability requirements of the Nyquist diagram. For this reason, it would be interesting to change the governing parameters with the aim of accomplishing the criteria. As the Vattenfall program is only valid for frequency deviations between  $\pm 0.1$  Hz, only the FCR-N step response and sine sweep are performed on the simulation model with the new regulator settings. In addition, the program only provides governor settings for PI-regulators, therefore the D-term is kept constant with the same parameters as the current regulator. The results from the FCR-N tests are used to construct a Nyquist diagram.

In order to use the diagram for governor settings, the values on the x- and y-axis has to be transformed to parameters that can be implemented in the simulation model for Songa. The proportional gain is acquired by following relation, where  $E_p$  is the droop of the governor:

$$K_p = \frac{y - value}{E_p} \quad (4.3.1)$$

In Sweden, the regulators of the hydro power plants are built differently than in Norway. Therefore, the value of  $T_i$  on the x-axis,  $T_{ix}$  in the relation below, cannot be directly utilized, but has to be transformed via  $K_i$ :

$$T_i = K_p E_p T_{ix} \quad (4.3.2)$$

Analyzing the Nyquist diagrams from the simulations, it seems that the normalized gain at low frequencies is too high to fulfill the requirements. To achieve a lower gain, the amplitude of the sinusoidal response needs to be reduced. This is accomplished by lowering the proportional gain of the controller. A low proportional gain will, on the other hand, result in a slower governing. To make up for this, the integral time can be decreased.

The results also showed that the governor responds quite slowly to changes in the system. This was evident for FCR-D delivery, where the governor was too slow, resulting in a negative capacity within the five second limit. By increasing the proportional gain, the governor will react faster to a deviation from set point. A faster regulator responds more quickly to changes in the system, and as such it could contribute to a more stable

governing. However, increasing  $K_p$  too much will lead to instability. Therefore, the integral time needs to be tuned to avoid large oscillations.

Based on the discussion above, two governor parameter set was found in figure 36. The lowest  $K_p$  that can be obtained from figure 36, which is lower than the current governor setting, is 0.83. Looking at the diagram for the governing parameters, utilizing this value for  $K_p$  will lead to a system with insufficient stability and performance, regardless of the value of  $T_i$ . However, as stated previously, the stability and performance criteria may be different in the program than in the requirements defined by the prequalification working group. For this reason, the author decided to test the performance of this governor setting on the simulation model. To ensure stability, the highest obtainable value of  $T_i$  from figure 36 was utilized. Hence, the value of the integral time was set to 5s.

A higher value of the proportional gain,  $K_p = 2.5$ , was also found in figure 36 with a corresponding integral time,  $T_i = 8.25s$ . These values fulfill the stability requirements set by the Vattenfall program, as figure 36 show a green colour for these parameters. In addition, the values coincide with a governor of medium quality, according to Statnett's "Function requirements in the power system" [30].

Lastly, a third governing parameter can be adjusted. To see if a change in FCR delivery could affect the stability, the droop of the governor was changed from 6% to 10%. The simulations were then performed with the original governor settings, but with a new value for the droop.

The different governor settings are summarized in the table below:

Set	$K_p$	$T_i$	droop
1	0.83	5 s	6 %
2	2.5	8.25 s	6 %
3	1.5	40 s	10 %

*Table 13: Governing parameters*

By implementing the different governor settings in the simulation model, and running the FCR-N step response sequence at minimum load, the performance of the different settings can be analyzed and compared with each other. In the figure below, the response is zoomed in on the power response for a frequency step of 50.0 Hz to 49.9 Hz, to clearly illustrate the differences. The step response for the original settings is also included as described in section 4.2.1. The full response can be seen in appendix C:

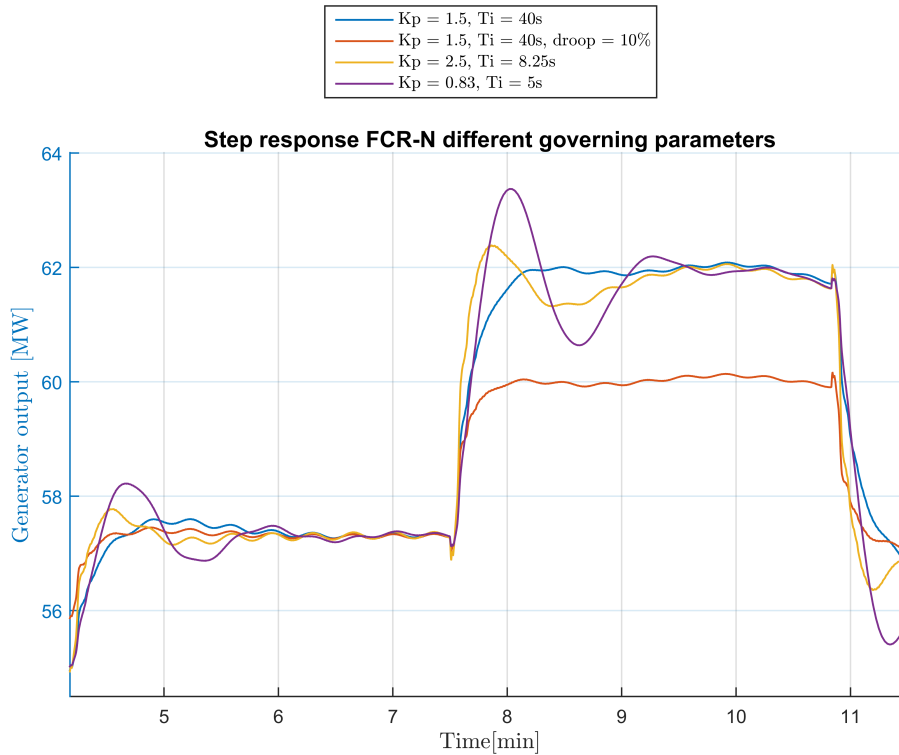


Figure 37: Step response different governing parameters

As figure 37 illustrates, the different settings leads to different power responses. By following the purple line, one can see that the lower value of  $K_p$  and  $T_i$  induces a large overshoot and an oscillating response. In addition, it seems that the initial power response is slower than the other regulator parameters. Hence, the lower  $K_p$  leads to a slower first response of the governor, but this is compensated for by the reduced  $T_i$ , which causes a faster governing towards the set point. However, the value of  $T_i$  is probably too low, causing an overshoot and oscillation towards the steady-state value.

The higher value of proportional gain induces a faster first response to the change in frequency. However, the increased value of  $K_p$  causes the system to overshoot. In addition, the integral time also contributes to overshoot and oscillations, and as such the value of  $T_i$  might be too low. In order to reduce these responses, the governor needs to be tuned either by reducing the proportional gain or increasing the integral time.

Looking at figure 37, it seems that the original governor settings manages to reach a steady-state value before the other settings. Theoretically, decreasing the value of the integral time would lead to a governor that manages to reach a steady-state value more quickly. However, in this case, an adjustment in  $K_p$  and  $T_i$  causes the regulator to overestimate the set point and the response must therefore be regulated towards a steady value, resulting in an oscillating response. As the oscillations are still occurring when the new frequency step response is applied, it may happen that the steady-state value is not achieved. Applying a longer time frame to the step response sequence, could reveal that one governor setting reaches a different steady-state value quicker than the others.



However, based on figure 37 above, it seems that the current settings advances towards a steady value more rapidly than the others.

As expected, changing the droop characteristic between power and frequency, changes the amount of FCR-N delivered by the unit. Hence, the red line in figure 37 reaches a lower set point than the other plots in the diagram. Other than that, the change in droop seems to have a negligible impact on the speed and behaviour of the regulator.

By applying a sine sweep to the simulations, the stability can be determined by a Nyquist plot. The diagram is obtained by finding the FCR-Vectors for each governor settings and multiplying with the FCR-N grid transfer function, as previously stated.

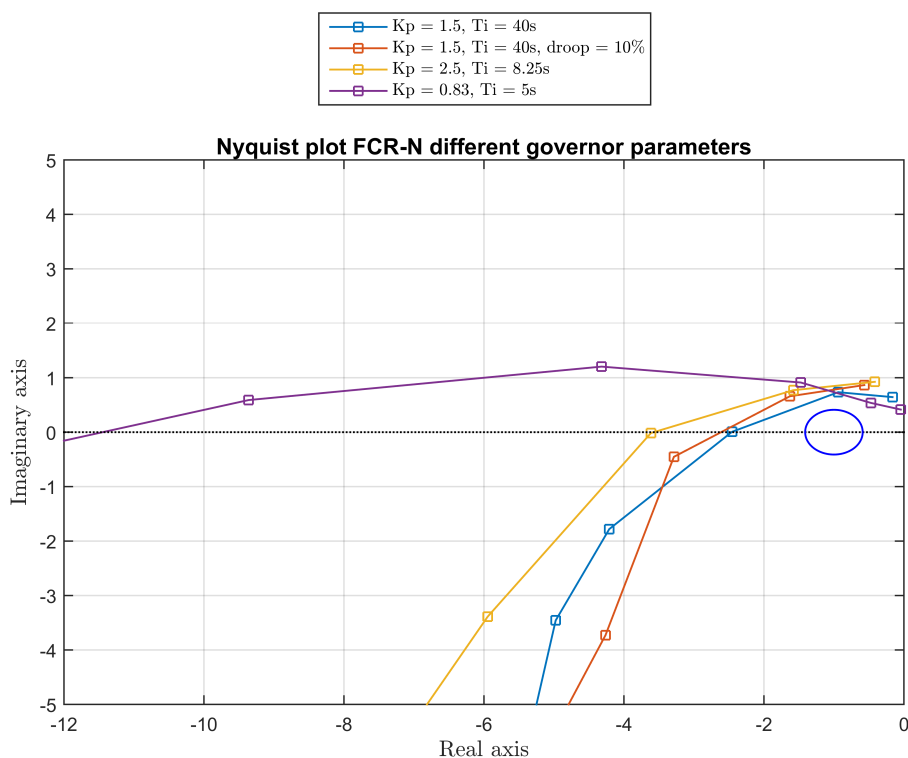


Figure 38: Nyquist plot for different governor parameters

As anticipated, looking at the purple line, the lower proportional gain leads to a reduced amplification of the sinus signal at lower frequencies. However, as the frequency increases the integral term starts to influence the regulation. According to [4], the integral term reacts quite slowly to a transient response, and as such, the integral part does not adjust the control variable of the governor fast enough, causing the system to overshoot. The low integral time therefore induces a larger amplification of the sinus response. This, in turn, leads to a higher normalized gain. The Nyquist diagram for the parameter settings of  $K_p = 0.83$  and  $T_i = 5s$ , therefore show a system that is more unstable than the other regulating parameters. This again corresponds to the Vattenfall program, which gave a red light for these settings, stating that the performance and stability was not good enough.

The yellow line illustrates a more stable response than the purple line. Still, the plot indicates that the response does not reach the Nyquist stability requirement and is thus unstable. The enhanced proportional gain and lower integral time leads to a higher amplification of the power output. As a consequence of this, the time difference changes and thus the phase changes in accordance with equation 2.7.8.

An adjustment in droop did not lead to a change in stability. As can be seen in figure 38, the red line crosses the imaginary axis at roughly the same place as the blue line. Hence, the stability of the two governing settings are equivalent.

Unfortunately, neither of the applied governor settings managed to fulfill the requirements defined by the Nyquist plot. The original regulator settings came closest, but the system is still shown to be unstable as the line crosses the imaginary axis on the left hand side of the point  $(-1, j0)$ . The Vattenfall program indicated that the governor settings with  $K_p = 2.5$  and  $T_i = 8.25$ , would provide sufficient stability margins. Nevertheless, figure 38 illustrate that the system is unstable. Therefore, a new and updated governing tool based on the criteria in [28] must be developed to aid in the tuning of hydro power plants participating in the FCR market.

Tuning a governor is not easy, and usually a lot of parameters are tested before the right match can be found. Further investigation of the requirements should, however, be performed to decipher how the governor should be tuned to deliver primary governing within sufficient stability.

## 4.4 Discussion on stability

From the qualification tests for FCR-N, stability circle plots and Nyquist diagrams were acquired at maximum and minimum load. For both simulations, the two stability plots came to contradictory conclusions, as the circle plot indicated stability and the Nyquist diagram did not.

According to the specifications, [26], the stability circles represent the difference between a normal and "worst-case" grid, as defined in table 11. Some stability margins are also illustrated by the circles, though they are not explicitly stated in the technical documents, [28]. The FCR-Vectors represent the response of the unit. As such, the circle plot illustrates the performance of the unit in correlation with the grid.

The Nyquist diagram is also an illustration of the power plant and grid, as the FCR-Vectors are multiplied with a mathematical expression for the power system. Hence, the conclusion from the two plots should not differ greatly.

In the previous section, it was stated that the Nyquist plot, provided by the Vattenfall program, indicated that the unit was stable for the current governor settings. The program uses a different mathematical expression for the grid:

$$G(s) = -\frac{1}{2H_{grid} + K_f f_0} \quad (4.4.1)$$

By transforming this function to a vector and multiplying with the FCR-Vectors obtained from the qualification tests, the following Nyquist diagram at minimum load is achieved:

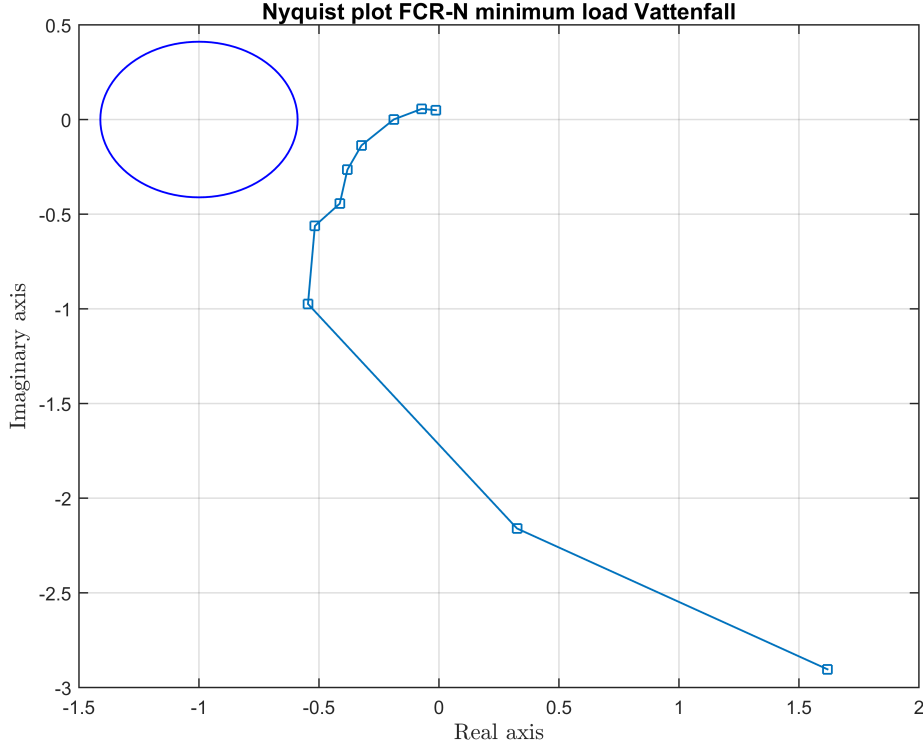


Figure 39: Nyquist plot with Vattenfall grid transfer function

Figure 39 indicates that the unit is stable for FCR-N regulation at minimum load.

The grid transfer function from the qualification tests is repeated below:

$$G(s)_{grid} = -\frac{600MW}{0.1Hz} \frac{f_0}{S_n} \frac{1}{2H_{grid}s + K_f f_0} \quad (2.7.14)$$

Looking at equation 2.7.14, the numerator of the formula is quite large. This has a considerable impact on the conclusion on stability, as the value of the numerator amplifies the distance from the origin of the response.

The first part of the numerator in equation 2.7.14,  $600MW/0.1Hz$ , refers to the total amount of FCR-N in the Nordic system, divided with the frequency change [26]. The parameters  $f_0$  and  $S_n$  are properties of the power system. It seems strange that the response of a single hydro power unit should be multiplied with the entire FCR-N capacity of the Nordic grid. The author tried to find a proper answer to why this is included in the mathematical expression. Several people were contacted, including Kjetil Uhlen, a professor at the Department of Electric Power Engineering at NTNU, who could not make sense of the first term in equation 2.7.14. He suggested that, if the capacity is included in the mathematical expression for the grid, the numerator should contain the static gain of the unit divided by the change in frequency.

For Songa, this implies that, based on theoretical values calculated from equation 2.5.1, the grid transfer function is:

$$G(s) = -\frac{4.3MW}{0.1Hz} \frac{f_0}{S_n} \frac{1}{2H_{grid} + K_f f_0} \quad (4.4.2)$$

By using this definition and multiplying with the FCR-Vectors from the simulations, the Nyquist diagram acquired is:

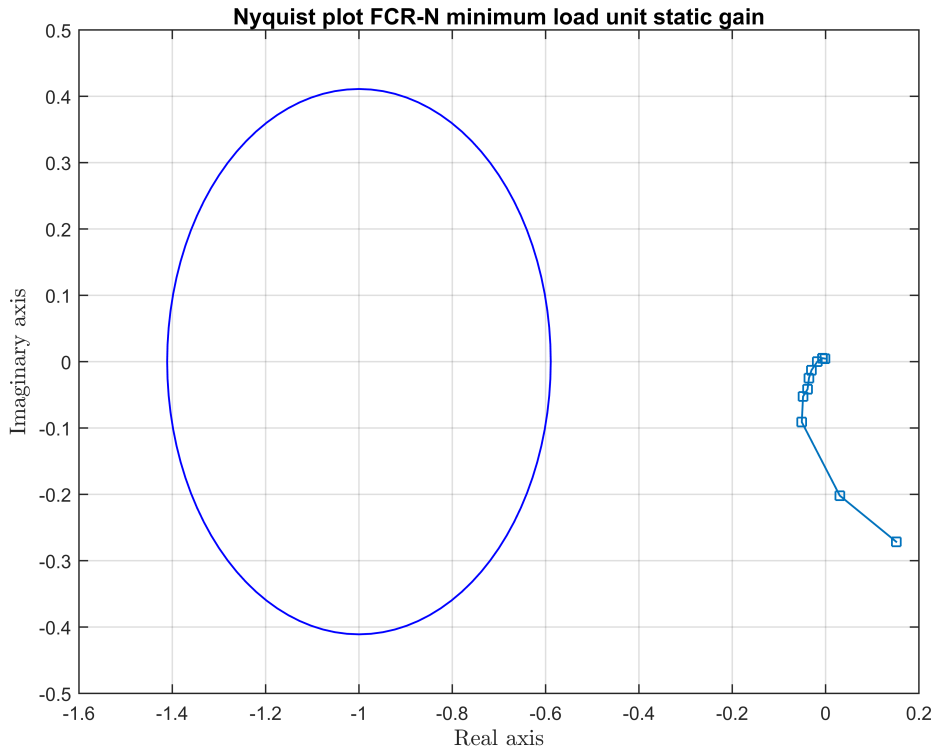


Figure 40: Nyquist plot with static gain grid transfer function

Using equation 4.4.2 to represent the grid will therefore lead to a Nyquist diagram illustrating that the unit is far within the limits of stability.

The documents provided by the prequalification working group, ([28] and [27]), offer no further explanation to the transfer function in equation 2.7.14. Reading the specification document [26], the model used to find the requirements consists of a representation of a FCR unit and a grid transfer function on the same form as equation 2.7.14, but without the FCR-N capacity. The model is therefore presented on non-normalized form, as the unit is  $Hz/MW$ . A Nyquist diagram can be obtained by this mathematical expression, but the function must be multiplied with the non-normalized form of the FCR-Vectors of the unit. These vectors are derived from the non-normalized gain of the sinusoidal response. Multiplying the two functions, an equivalent Nyquist diagram as in figure 40 is achieved. Hence, using the non-normalized form of the expressions gave the same result

as normalizing the grid transfer function by the static gain of the unit. It should be mentioned that the specification document is a draft, which means that changes could have been made after publication. For this reason, it is difficult to conclude on the matter.

Professors with expertise within the area cannot explain why the transfer function is defined the way it is in equation 2.7.14, and points to the formula utilized by the Vattenfall program as the right one, formula 4.4.1. Finding an explanation to the grid transfer function, as stated in the requirements, was not possible. This, unfortunately, makes it hard to explain why the stability circles and Nyquist plots from the simulations differ in conclusion. It seems strange that the same background theory for establishing performance and stability, should lead to such different results. The numerator of the grid transfer function has a great influence on the conclusion of stability. Based on the discussion above, it seems that the way of normalizing the expression, thus changing the numerator, has a great impact on the Nyquist response. Using the static gain of the unit as normalization parameter gave a stable Nyquist diagram, while using the FCR-N capacity of the Nordic grid provided unstable Nyquist plots. Further investigation should therefore be performed on the matter, to make sure the power system is correctly normalized.

The frequency containment reserve project is still a work in progress, meaning changes can be made after this thesis is published.

## 4.5 Discussion on simulation model

The simulation model has to the best ability attempted to mirror the behaviour of Songa hydro power plant. Parameters and constants for the plant has been found in technical documents and implemented in the model. A comparison of the performance between the two would therefore be of interest, to see if the simulation model manages to represent the actual power plant correctly.

Theoretically, the obtained steady-state value of FCR-N can be calculated from equation 2.5.1, by setting  $P_r$  equal to the generator reference value:

$$\Delta P_{FCR-N} = -\frac{0.1}{50} \cdot \frac{128}{-0.06} = 4.3MW$$

A value for the FCR-D regulation is obtained from the same equation by setting the frequency change to 0.4 Hz. The value of  $\Delta P_{FCR-D}$  is then 17.1MW. Compared to the values of active power from the simulations for maximum and minimum load, one can see that a discrepancy between theory and simulation exists. This can be explained by the loss and friction in the hydro power system, which is not accounted for in equation 2.5.1. In addition, the efficiency will change with the variation of discharge, affecting the power response. At minimum load, the steady-state values for FCR-N and FCR-D downwards regulation is given to be higher than the theoretical value. This could be due to the overestimated efficiency, as explained in section 4.2.1. Overall, the calculated theoretical value gives a rough estimate of how much primary governing the unit can deliver to the power system. Taking the loss, friction and efficiency into account, the values obtained from the simulations correspond well to theory.

In 2013, some measurements were performed at Songa hydro power plant and documented in [17]. Given the time frame, the measurements were performed before the qualification tests and requirements, as described in this thesis, was determined. A direct comparison with the simulation model is therefore difficult to perform, as there could be differences in method and presentation of results. However, an attempt has been made to utilize the report to check the performance of the simulation model compared to the actual power plant.

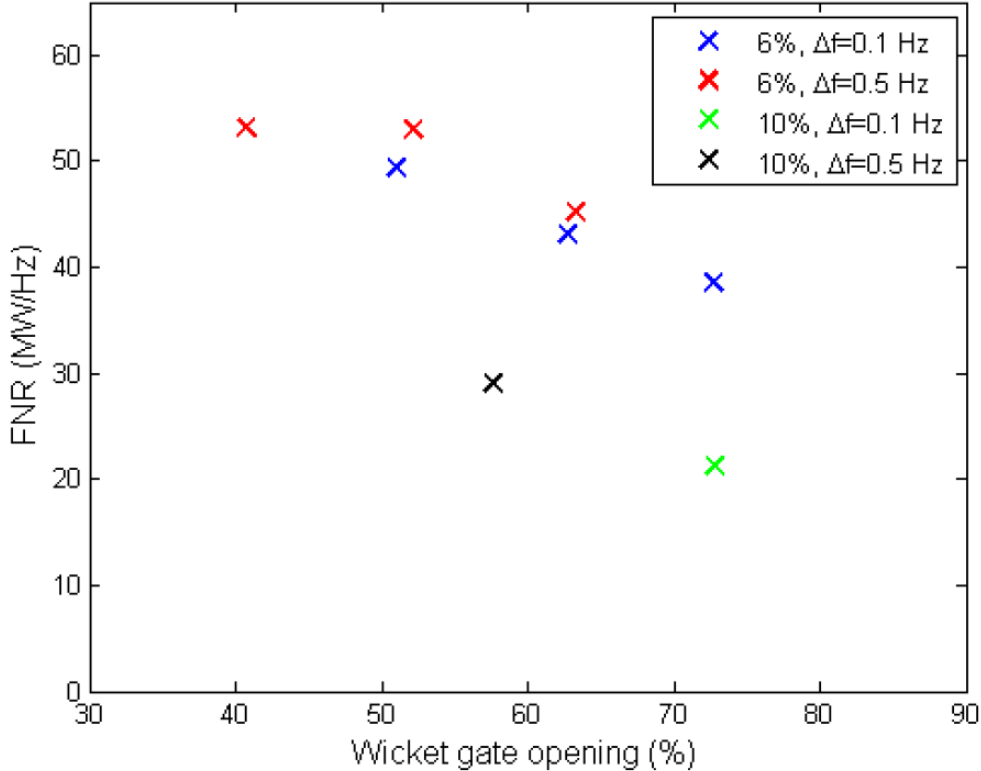


Figure 41: Amount of regulating power at Songa hydro power station [17]

FNR refers to the amount of regulating power measured by the active power at Songa hydro power plant. Following the blue crosses describing a frequency step of 0.1 Hz with a droop of 6%, one can see that the amount of regulating power decreases with increased wicket gate opening and delivered power. This corresponds to the findings presented in this thesis, as the FCR-N capacity at minimum load is higher than at maximum. The capacity presented in figure 41 is somewhat higher than the results presented in the previous sections, but this is due to the fact that the turbine power is measured and not the generator output. As with the simulation model, the variation of regulating power can be explained by the variation of turbine efficiency with discharge.

The report also provides a step response and Bode diagram. The Bode diagram is presented in the unit  $MW/Hz$ , hence a comparison must be made with the non-normalized gain from the simulations. Comparing these two plots, the gain obtained from the simulations is shown to be higher than the gain from the measurements performed at Songa. Unfortunately, the results are presented without a description of how the Bode diagram is acquired. Therefore, the difference could be due to a matter of definition, calculation or measurement method. As such, the results are not repeated in this thesis, as one can question whether a comparison is valid. However, a discussion on the difference in results is provided below.

Based on the step response provided in the report, it seems that the actual governor at Songa is slower than the regulator in the simulation model. This would explain the



differences in the Bode diagram, as a slower governor will cause a lower amplitude of the power response. The governor in the simulation model was built based on the transfer function provided by Statkraft, which is stated in section 3. A detailed block diagram of the regulator was not possible to obtain, as Statkraft did not have the documentation. The transfer function may therefore not tell the full story of the behaviour of the governor. Many governors have a filter term on both the integral and derivative term. A filtered integral term generates a reduced power response amplitude at lower frequencies. At higher frequencies, the filtered derivative term will lower the amplitude [4]. Correct implementation of these two elements is therefore of great importance of the gain in the Bode diagram.

Implementing a delay in the regulator, will cause a change in the time difference between the input and output sinusoidal response. In addition, a backlash will also lead to a delay in the system. Hence, the dissimilarity in phase between the Bode diagrams can be explained by these missing components in the simulated governor.

The servo motor is represented by setting a limit for the servo motor velocity based on the closing time of the guide vanes. This value should be a good representation, but the limit could be set too high, causing the simulated governor to respond faster than the actual system. A less responsive governor, causing a lower amplitude of the sinus response, could be explained by a slower servo motor than anticipated. Without a detailed block diagram it is difficult to explicitly explain the reasons for the discrepancy. The governor set up could be dissimilar and the governor parameters can be defined in a different way. In order to properly validate the model and find the reason for any discrepancies, documentation of the governor should be found and measurements with the aim of confirming the simulation model should be performed.

## 5 Conclusion

A set of qualification tests were performed on the simulation model of Songa hydro power plant. The FCR-N step response tests revealed that the unit can deliver an amount of  $3.7MW$  at maximum load and  $4.6MW$  at minimum load. A sine sweep at different time periods were then applied to the model to determine the dynamic performance and stability. At both minimum and maximum load, the dynamic performance of the unit was shown to be satisfactory. Interestingly, the stability circle plot and Nyquist diagram came to differing conclusions, as the circle plot indicated stability and the Nyquist diagram did not.

The FCR-D capacity and dynamic performance was determined by the use of a step and ramp response sequence. The steady-state FCR-D upwards delivery was  $14.2MW$  for maximum load and  $16.3MW$  for minimum load. For FCR-D downwards, the steady-state power response was  $15.75MW$  and  $17.6MW$ .

No requirements on the FCR-D dynamic performance is described in the technical documents. Regardless, in an attempt to conclude on the matter, it was assumed that a negative capacity indicated a poor dynamic performance. Hence, this was the conclusion for both FCR-D regulations at maximum load and for FCR-D upwards regulation at minimum load. Only FCR-D downwards regulation achieved a positive capacity and performance. Neither of the FCR-D responses managed to fulfill the stability criteria defined by the Nyquist diagram.

Different governor parameters were tested on the simulation model to see if they could fulfill the Nyquist stability criteria. The parameters were found by the use of a program developed by Vattenfall, which appeared to be flawed as it was not updated with the latest requirements, as described in this thesis. For this reason, even though the program indicated stability, the Nyquist diagram constructed by values found from the simulations illustrated that the unit was unstable for all tested regulator parameters. Hence, a new governor parameter set that would provide better stability for FCR-N regulation was not found. In addition, a change in droop was also tested on the system to see if the stability was affected. The Nyquist diagram indicated that a change in droop would provide roughly the same stability as the original governor settings.

A discussion on stability followed, as the author found it strange that the stability circle plot and Nyquist diagram resulted in such different outcomes. The conclusion on stability from the Nyquist diagram was shown to be largely dependent on the numerator of the grid transfer function, as this value increases the distance from the origin for the response. Further investigation revealed that different ways of normalizing the expression for the power system, leads to different Nyquist plots and conclusions.

An attempt to compare the simulation model with measurements performed at the actual power plant proved to be difficult, as there are likely differences in definition, calculation and measurement method. However, a discussion on possible discrepancies and causes followed. The FCR-N capacity from the simulations was shown to roughly correlate with the measurements from the actual power plant. In order to properly validate the model, new measurements with the aim of validation should be performed.

## 6 Further Work

A new governing tool based on the new set of requirements should be developed, to aid in the regulator tuning of units delivering FCR. The program should be able to provide Nyquist diagrams and circle plots based on a simple representation of a hydro power plant, so that the current performance of the unit can be analyzed. A bad and good plant can also be defined for comparison. The qualification tests should be performed at Songa hydro power plant to test the actual performance and validate the simulation model. If possible, a detailed block diagram of the governor with parameters should be obtained and compared to the simulated regulator. Provided that discrepancies are identified, the reason must be found, and the simulation model updated.

A new specification document needs to be developed by the prequalification working group, to properly explain the theory and assumptions behind the requirements. The defined grid transfer function and the normalization of this equation must be properly described. As the FCR-D dynamic performance criteria was not defined in the technical document, this requirement needs to be set in future documents. If there are any changes in qualification tests and criteria, new simulations must be performed on the simulation model.

## 7 References

- [1] Evert Agneholm. *Final report phase 2 - Measures to mitigate the frequency oscillations with a period of 60-90 seconds in the Nordic synchronous system*. Tech. rep. Gothia power, 2014.
- [2] Evert Agneholm. *Report - Measures to mitigate the frequency oscillations with a period of 60-90 seconds in the Nordic synchronous system*. Tech. rep. Gothia power, 2013.
- [3] Tony Atkins and Marcel Escudier. *Oxford dictionary of mechanical engineering*. Oxford university press, 2013.
- [4] Jens G. Balchen, Trond Andresen, and Bjarne A. Foss. *Reguleringsteknikk*. Institutt for teknisk kybernetikk NTNU, 2004.
- [5] Kåre Bjørvik and Per Hveem. *Reguleringsteknikk*. Kybernetes forlag, 2012.
- [6] Hermod Brekke. *Grunnkurs i hydrauliske strømningsmaskiner*. Vannkraftlaboratoriet NTNU, 2000.
- [7] Hermod Brekke. *Pumper og Turbiner*. Vannkraftlaboratoriet NTNU, 1999.
- [8] Yunus A. Cengel and John M. Cimbala. *Fluid Mechanics - Fundamentals and application*. McGraw-Hill, 2010.
- [9] Stephen J. Chapman. *Electric Machinery Fundamentals*. McGraw Hill, 2012.
- [10] S.E. Haaland. *Simple and Explicit Formulas for the Friction Factor in Turbulent Pipe Flow*. Tech. rep. NTNU, 1983.
- [11] Joel Hass, Maurice D. Weir, and George B. Thomas Jr. *Calculus 1*. Pearson Education Limited, 2009.
- [12] Even Lillefosse Haugen. *Verification of simulation program for high head hydro power plant with air cushion*. Tech. rep. NTNU, 2013.
- [13] Finn Aakre Haugen. *Reguleringsteknikk*. Fagbokforlaget, 2014.
- [14] Arne Kjølle. *Hydropower in Norway - Mechanical equipment*. Vannkraftlaboratoriet NTNU, 2001.
- [15] Erwin Kreyzig. *Advanced Engineering Mathematics*. Wiley, 2006.
- [16] M. Laasonen et al. *Test of the Frequency Control of Generation Units in the Nordic Power System*. Tech. rep. Entsoe, Unknown.
- [17] Monica Lexholm. *Report - Test performed at Songa power station*. Tech. rep. Gothia Power, 2013.
- [18] Jan Machowski, Janusz Bialek, and J.R. Bumby. *Power System Dynamics: Stability and control*. Wiley, 2008.
- [19] Torbjørn Nielsen. *Analytic model for dynamic simulations of Francis turbines - Implemented in MOC*. Tech. rep. NTNU, 1992.
- [20] Torbjørn Nielsen. *Dynamic behaviour of governing turbines sharing the same electrical grid*. Tech. rep. NTNU, 1996.
- [21] Torbjørn Nielsen. *Dynamic dimensioning of hydro power plants*. Vannkraftlaboratoriet NTNU, 2015.
- [22] Torbjørn Nielsen. *Main dimensions of Francis Turbines as a consequence of Euler turbine equation*. Tech. rep. NTNU, Unknown.
- [23] Torbjørn Nielsen. *Simulation model for Francis and Reversible Pump Turbines*. Tech. rep. NTNU, 2015.

- [24] FCP project Prequalification Working Group. *FCR-D test report*. Tech. rep. Entsoe, 2017.
- [25] FCP project Prequalification Working Group. *FCR-N test report*. Tech. rep. Entsoe, 2017.
- [26] FCP project Prequalification Working Group. *FRC specification - Methodology*. Tech. rep. Entsoe, 2015.
- [27] FCP project Prequalification Working Group. *Supporting Document on Technical Requirements for Frequency Containment Reserve Provision in the Nordic Synchronous Area*. Tech. rep. Entsoe, 2017.
- [28] FCP project Prequalification Working Group. *Technical Requirements for Frequency Containment Reserve Provision in the Nordic Synchronous Area*. Tech. rep. Entsoe, 2017.
- [29] Linn Saarinen and Erik Spiegelberg. *Instruction for the Vattenfall FCR model*. Tech. rep. Uppsala University and Vattenfall AB, 2015.
- [30] Statnett. *Funksjonskrav i kraftsystemet*. Tech. rep. Statnett, 2012.
- [31] Bjarne Vaage. *Simulation of hydraulic transients of operation at two hydro power plants*. Tech. rep. NTNU, 2016.
- [32] Frank M. White. *Fluid Mechanics Sixth edition*. McGraw-Hill, 2008.
- [33] E. Benjamin Wylie and Victor L. Streeter. *Fluid Transients*. FEB PRESS, 1983.

## Appendix A MATLAB script

```
clear all
clc

i = 1;

%-----Constants-----%
g = 9.81;
ro = 1000;
my = 1.788*10^-3;
%-----Data Songa
H0 = 956.5;
Hout = 683;
Qmax = 55;
Pturbmax = 144*10^6;
Pgenmax = 140*10^6;
nrturb = 0.952;
ngen = 0.988;
Hmax = Pturbmax/(ro*g*Qmax);
nref = 300;

%---Turbine and generator---%
omegaref = (nref*2*pi)/60;
Hr = 264;
Pr = 136*10^6;
Qr = Pr/(ro*g*Hr);
Eref = 17000;
fgrid = zeros(i,1);
omegagrid = zeros(i,1);
fgrid(i) = 50;
omegagrid(i) = 2*pi*fgrid(i);

%----Starting flow---%
%---Maximum---%
%Q0 = Qr;
%---Minimum--%
Q0 = 22.8;

%-----Turbine-----%
Ta = 6;
J = Ta*(Pr/(omegaref^2));
nhydr = 1;

%Turbine geometry
```

```

B_1 = 0.447;
D_1 = 3.3;
D_2 = 2.3;
cm2cm1 = 1.1;

%----Velocity triangle---
Hred = sqrt(2*g*Hr);
cm2 = (4*Qr)/(pi*(D_2^2));
cu2 = 0;
cm1 = Qr/(pi*D_1*B_1);
u2r = (pi*nref*D_2)/60;
beta2r = atan(cm2/u2r);
u1r = 0.5*omegaref*D_1;
cu1 = (g*Hr*nhydr)/u1r;
beta1r = atan(cm1/(u1r-cu1));
alpha1r = atan(cm1/cu1);
c1r = sqrt((cu1^2) + (cm1^2));

%----Self governing----%
s = (1/8)*D_1^2*(1-((D_2/D_1)^2));
sg = (s*omegaref)/(g*Hr);

%-----Machine constants---%
psi = (u2r^2)/(g*Hr);
ksi = (psi+1)*cos(alpha1r);

%----Rated values for generator and turbine--%
Ur = Eref;
Ttr = Pr/omegaref;
poles= 2*(omegagrid/omegaref);
Kmr = Ur/omegagrid(i);
Ir = Ttr/Kmr;
deltar = pi/4;

%-----Regulator---%
%Frequency regulator
%----Current setting---%
% Kp = 1.5;
% Ti = 40;
%---Vattenfall--%
Kp = 2.5;
Ti = 8.25;
% Kp = 0.83;
% Ti = 5;

```

```

Td = 4;
Tf = 4;
bt = 1/Kp;
bb = -0.06;
%bb = -0.1;
%Voltage regulator
Kpg = 14;
Tig = 1;
btg = 1/Kp;
bbg = 0.025;
K5 = 1/(btg*Ur);
K6 =1/(btg*Tig*Ur);
K7 = 1/(bbg*Ir);
%Servo motor time constant;
tclose = 27.5;
cmax = 1/tclose;

%-----Water Hammer test-----%
%Check for rectangular water hammer, set pipelements equal to each
%others area, eliminate the surge shafts and see if you get a rectangular
%water hammer
WHtest = false;
ST = 1;      %Exclude bekkeinntak if zero
BT = 1;      %Exclude Bitdalsvatn if zero
SST = 1;     %Exclude Surge shaft if zero
UCT = 1;     %Exclude UChamber if zero

%-----Find distribution of flow to junction-----%
pipeparameters = xlsread('Songa','B2:E16');
[A,D,dx,N,a,dt,L] = PipeParameter(pipeparameters);
%----Friction factor---%
%For raw blasted tunnel
eps1 = 0.783271237987559;
%For penstock, stainless steel
eps2 = 0.41;

fun = @(x) f(x,Q0,A,D,dx,N,eps1,g,ro,my,L);
x0 = [0 Q0];
Qs = fzero(fun,x0);
Qbit = Qs;
Qsonga = Q0-Qbit;

%----Collecting data---%
streamintake = xlsread('Bekkeinntak','B2:E9');
SSL = [3.5,6.7,68.5,73,5];

```



```

SA = [40,14,40,25];
SSAs = [40,204,40,430];
UCL = [6.8 8.9];
UA = [7.07,20];
UCAs = [7.07,362];
DTparameters = xlsread('DraftTube','B2:D22');

%-----Collecting data-----%
[R, B] = pipeelement(WHtest,Qsonga,Qbit,Q0,A,D,eps1,eps2,a,dx,g,ro,my);
[SR, SB, SN, Sdx, Sa, SAs] = ...
    bekkeinntak(dt,g,ro,my,eps1,Qsonga,Qbit,streamintake);
[SSAs, SSL, SSB, SSR, SSN] = surgeshaft(dt,g,ro,my,Q0,eps2,SSL,SA,SSAs);
[UCAs, UCL, UCB, UCR, UCN] = UChamber(dt,g,ro,my,Q0,eps2,UCL,UA,UCAs);
[DA, Da, Ddx, DN, DR, DB, DLDA] = DraftTubeParameters(dt,g,DTparameters);
%-----Calculation of steady state values-----%
%-----Songavatn - Trolldalen pipe element 1-----%
B1 = B(1);
R1 = R(1);
N1 = N(1);
L1 = L(1);
A1 = A(1);
H1 = zeros(i,N1);
Q1 = zeros(i,N1);
for j = 1:N1
    Q1(1,j) = Qsonga;
    H1(1,j) = H0 -((j-1)*R1*Q1(1,j)*Q1(1,j));
end
%-----Trolldalen pipe element 2-----%
B2 = SB(8);
R2 = SR(8);
N2 = SN(8);
A2 = 100000;
Q2 = zeros(i,N2);
H2 = H1(1,N1)*ones(i,N2);
%-----Songavatn/Trolldalen - Gammalstoyl pipe element 3-----%
B3 = B(3);
R3 = R(3);
N3 = N(3);
L3 = L(3);
A3 = A(3);
H3 = zeros(i,N3);
Q3= zeros(i,N3);
for j = 1:N3
    Q3(1,j)=Qsonga;
    H3(1,j) = H1(1,N1)-(j-1)*R3*Q3(1,j)*Q3(1,j);
end

```

```

%-----Stream intake 1 Gammalstøyl-----%
SB1 = SB(1);
SR1 = SR(1);
SN1 = SN(1);
SAs1 = SAs(1);
SH1 = H3(1,N3)*ones(i,SN1);
SQ1= zeros(i,SN1);
%-----Gammalstøyl - Reinkvam pipe element 4-----%
B4 = B(4);
R4 = R(4);
N4 = N(4);
L4 = L(4);
A4 = A(4);
H4 = zeros(i,N4);
Q4= zeros(i,N4);
for j = 1:N4
    Q4(1,j)=Qsonga;
    H4(1,j) = H3(1,N3)-(j-1)*R4*Q4(1,j)*Q4(1,j);
end
%-----Stream intake 2 Reinkvam-----%
SB2 = SB(2);
SR2 = SR(2);
SN2 = SN(2);
SAs2 = SAs(2);
SH2 = H4(1,N4)*ones(i,SN2);
SQ2= zeros(i,SN2);
%-----Reinkvam -Urdbø pipe element 5-----%
B5 = B(5);
R5 = R(5);
N5 = N(5);
L5 = L(5);
A5 = A(5);
H5 = zeros(i,N5);
Q5= zeros(i,N5);
for j = 1:N5
    Q5(1,j)=Qsonga;
    H5(1,j) = H4(1,N4)-(j-1)*R5*Q5(1,j)*Q5(1,j);
end
%-----Stream intake 3 Urdbø-----%
SB3 = SB(3);
SR3 = SR(3);
SN3 = SN(3);
SAs3 = SAs(3);
SH3 = H5(1,N5)*ones(i,SN3);
SQ3= zeros(i,SN3);
%-----Urdbø - Nipa pipe element 6-----%

```

```

B6 = B(6);
R6 = R(6);
N6 = N(6);
L6 = L(6);
A6 = A(6);
H6 = zeros(i,N6);
Q6= zeros(i,N6);
for j = 1:N6
    Q6(1,j)=Qsonga;
    H6(1,j) = H5(1,N5)-(j-1)*R6*Q6(1,j)*Q6(1,j);
end
%-----Stream intake 4 Nipa-----%
SB4 = SB(4);
SR4 = SR(4);
SN4 = SN(4);
SAs4 = SAs(4);
SH4 = H6(1,N6)*ones(i,SN4);
SQ4= zeros(i,SN4);
%-----Nipa - junction pipe element 7-----%
B7 = B(7);
R7 = R(7);
N7 = N(7);
L7 = L(7);
A7 = A(7);
H7 = zeros(i,N7);
Q7= zeros(i,N7);
for j = 1:N7
    Q7(1,j)=Qsonga;
    H7(1,j) = H6(1,N6)-(j-1)*R7*Q7(1,j)*Q7(1,j);
end
%-----Kvikkevatn - Bitdalen pipe element 11-----%
B11 = B(9);
R11 = R(9);
N11 = N(9);
L11 = L(9);
A11 = A(9);
H11 = zeros(i,N11);
Q11 = zeros(i,N11);
for j = 1:N11
    Q11(1,j)= Qbit;
    H11(1,j) = H0-((j-1)*R11*Q11(1,j)*Q11(1,j));
end

%-----Tunnel to Kvikkevatn pipe element 12-----%
B12 = B(8);
R12 = R(8);

```

```

N12 = N(8);
H12 = zeros(i,N12);
Q12 = zeros(i,N12);
for j = 1:N12
    Q12(1,j)=0;
    H12(1,j) = H11(1,N11)-(j-1)*R12*Q12(1,j)*Q12(1,j);
end
%-----Stream intake 7 Kvikkevatn-----%
SB7 = SB(7);
SR7 = SR(7);
SN7 = SN(7);
SAs7 = SAs(7);
SH7 = H12(1,N12)*ones(i,SN7);
SQ7= zeros(i,SN7);
%-----Vaa - Kvikkevatn pipe element 10-----%
B10 = B(10);
R10 = R(10);
N10 = N(10);
L10 = L(10);
A10 = A(10);
H10 = zeros(i,N10);
Q10 = zeros(i,N10);
for j = 1:N10
    Q10(1,j)=Qbit;
    H10(1,j) = H11(1,N11)-(j-1)*R10*Q10(1,j)*(Q10(1,j));
end

%-----Stream intake 6 Vaa-----%
SB6 = SB(6);
SR6 = SR(6);
SN6 = SN(6);
SAs6 = SAs(6);
SH6 = H10(1,N10)*ones(i,SN6);
SQ6= zeros(i,SN6);
%-----Farastad - Vaa pipe element 9-----%
B9 = B(11);
R9 = R(11);
N9 = N(11);
L9 = L(11);
A9 = A(11);
H9 = zeros(i,N9);
Q9= zeros(i,N9);
for j = 1:N9
    Q9(1,j)= Qbit;
    H9(1,j) = H10(1,N10)-(j-1)*R9*Q9(1,j)*(Q9(1,j));
end

```

```

%-----Stream intake 5 Farastad-----%
SB5 = SB(5);
SR5 = SR(5);
SN5 = SN(5);
SAs5 = SAs(5);
SH5 =H9(1,N9)*ones(i,SN5);
SQ5= zeros(i,SN5);
%-----Songavatn - Farastad pipe element 8-----%
B8 = B(12);
R8 = R(12);
N8 = N(12);
L8 = L(12);
A8 = A(12);
H8 = zeros(i,N8);
Q8= zeros(i,N8);
for j = 1:N8
    Q8(1,j)=Qbit;
    H8(1,j) = H9(1,N9)-(j-1)*R8*Q8(1,j)*(Q8(1,j));
end
%-----From cross Nipa to Surgeshaft pipe element 13-----%
B13 = B(13);
R13 = R(13);
N13 = N(13);
L13 = L(13);
H13 = zeros(i,N13);
Q13= zeros(i,N13);
A13 = A(13);
for j = 1:N13
    Q13(1,j)=Q0;
    H13(1,j) = H7(1,N7)-(j-1)*R13*Q13(1,j)*Q13(1,j);
end
%-----Upper Surge shaft-----%
SSH = H13(1,N13)*ones(i,SSN);
SSQ = zeros(i,SSN);
SSZ = zeros(i,1);
%-----Penstock pipe element 15-----%
B15 = B(14);
R15 = R(14);
N15 = N(14);
A15 = A(14);
L15 = L(14);
a15 = a(14);
H15 = zeros(i,N15);
Q15= zeros(i,N15);
for j = 1:N15

```

```

        Q15(1,j)=Q0;
        H15(1,j) = H13(1,N13)-(j-1)*R15*Q15(1,j)*Q15(1,j);
end

%-----U-channel pipe element 17-----%
B17 = B(15);
N17 = N(15);
A17 = A(15);
L17 = L(15);
H17 = zeros(i,N17);
Q17= zeros(i,N17);
R17 = R(15);
H17(i,N17) = Hout;
for j = N17:-1:1
    Q17(1,j)=Q0;
    H17(1,j) = H17(i,N17)+(N17-j)*R17*Q17(1,j)*abs(Q17(1,j));
end

%-----Lower surge shaft-----%
UCQ = zeros(i,UCN);
UCH = H17(1,1)*ones(i,UCN);
UCZ = zeros(i,1);
%-----Draft tube-----%
DH(1,DN) = H17(i,1);
DQ = Q0*ones(i,DN);
for j = DN:-1:1
    DH(1,j) = DH(1,DN)+(DN-j)*DR(j)*DQ(i,j)*abs(DQ(i,j));
end
Xd=zeros(i,DN);
Xa=zeros(i,DN);
Xb=zeros(i,DN);
Xc=zeros(i,DN);
Xe=zeros(i,DN);
Xf=zeros(i,DN);

%---Turbine and generator---%
%Generating matrices
Headturb = zeros(i,1);
power = zeros(i,1);
Tg = zeros(i,1);
omega = zeros(i,1);
kappa = zeros(i,1);
flow = zeros(i,1);
I = zeros(i,1);
U = zeros(i,1);
Km = zeros(i,1);

```

```

delta = zeros(i,1);
q = zeros(i,1);
c = zeros(i,1);
nt = zeros(i,1);
n = zeros(i,1);
ui = zeros(i,1);
ud = zeros(i,1);
power1 = zeros(i,1);
GenPower= zeros(i,1);
hdim = zeros(i,1);
Hturb = zeros(i,1);
e = zeros(i,1);

%---Loss and damping constants---%
if Q0 == Qr
Rm = 0.01;
else
Rm = 0.015;
end
md = 0.15;
Rf = 0.038;
Ra = 1;

%---Calculated values---%
%---Starting values---%
DeltaH = (H15(i,end)-DH(i,1));
Hturb(1) = DeltaH;
q(i) = Q15(i,end)/Qr;
h = DeltaH/Hr;
omegadim(i) = omegaref/omegaref;
omegat = omegadim(i)*omegaref;
kappa(i) = q;
flow(i) = q(i)*Qr;
alpha1 = asin(kappa(i)*sin(alpha1r));
qc = omegadim(i)*((1+cot(alpha1r)*tan(beta1r))/...
(1+cot(alpha1)*tan(beta1r)));
kappar = kappa(1);

%Torque equation
ms = ksi*(q(i)/kappa(i))*(cos(alpha1)+tan(alpha1r)*sin(alpha1));
nh = 1-(((Rf*q(i)^2)+(Ra*(q(i)-qc)^2))/h);
Tg(i) = Ttr*((q*nh*(ms-psi*omegadim(i)))-(Rm*omegadim(i)^2));
ntot(i) = (((q(i)*omegadim(i)*nh*(ms-psi*omegadim(i)))-...
(Rm*omegadim(i)^3))/(q(i)*h));

```

```

power(i) = ro*g*flow(i)*DeltaH;
power1(i) = ro*g*flow(i)*DeltaH;
GenPower(i) = power(i)*ntot(i)*ngen;
Tgenmax = Pgenmax/omegaref;

delta(i) = asin((Tg(i)/Tgenmax)*sin(deltar));

Km(i) = Kmr;
I(i) = Tg(i)/Kmr;
U(i) = Ur;

%-----Inflow time of masses---%
Tw = (Qr/(g*Hr))*((L15/A15)+sum(DLDA));

%-----Time step-----%
t = zeros(i,1);
i = 2;
t(i) = 0;
%-----Type of test-----%
tst =2;
%tst = 1: FCR-N step response
%tst = 2: Sine sweep
%tst = 3: FCR-D up step response
%tst = 4: FCR-D up ramp response
%tst = 5: FCR-D down step response
%tst = 6: FCR-D down ramp response

if tst == 1
tmax = 1250;
elseif tst == 2
Af = 0.1;
kl = 1;
T = [10 15 25 40 50 60 70 90 150 300];
w = (2*pi)./T;
tmax = 200;
elseif tst == 3
tmax = 1500;
elseif tst == 4
tmax = 600;
elseif tst == 5
tmax = 1500;
elseif tst == 6
tmax = 600;
elseif tst == 7
tmax = 100;
end

```



```

while t < tmax
%----Calculation of the inner points----%
for j = 2:N1-1
    CP = H1(i-1,j-1)+B1*Q1(i-1,j-1)-R1*Q1(i-1,j-1)*abs(Q1(i-1,j-1));
    CM = H1(i-1,j+1)-B1*Q1(i-1,j+1)+R1*Q1(i-1,j+1)*abs(Q1(i-1,j+1));
    H1(i,j) = 0.5*(CP+CM);
    Q1(i,j) = (H1(i,j)-CM)/B1;
end
for j = 2:N2-1
    CP = H2(i-1,j-1)+B2*Q2(i-1,j-1)-R2*Q2(i-1,j-1)*abs(Q2(i-1,j-1));
    CM = H2(i-1,j+1)-B2*Q2(i-1,j+1)+R2*Q2(i-1,j+1)*abs(Q2(i-1,j+1));
    H2(i,j) = 0.5*(CP+CM);
    Q2(i,j) = (H2(i,j)-CM)/B2;
end
for j = 2:N3-1
    CP = H3(i-1,j-1)+B3*Q3(i-1,j-1)-R3*Q3(i-1,j-1)*abs(Q3(i-1,j-1));
    CM = H3(i-1,j+1)-B3*Q3(i-1,j+1)+R3*Q3(i-1,j+1)*abs(Q3(i-1,j+1));
    H3(i,j) = 0.5*(CP+CM);
    Q3(i,j) = (H3(i,j)-CM)/B3;
end
for j = 2:SN1-1
    CP = SH1(i-1,j-1)+SB1*SQ1(i-1,j-1)-SR1*SQ1(i-1,j-1)*abs(SQ1(i-1,j-1));
    CM = SH1(i-1,j+1)-SB1*SQ1(i-1,j+1)+SR1*SQ1(i-1,j+1)*abs(SQ1(i-1,j+1));
    SH1(i,j) = 0.5*(CP+CM);
    SQ1(i,j) = (SH1(i,j)-CM)/SB1;
end
for j = 2:N4-1
    CP = H4(i-1,j-1)+B4*Q4(i-1,j-1)-R4*Q4(i-1,j-1)*abs(Q4(i-1,j-1));
    CM = H4(i-1,j+1)-B4*Q4(i-1,j+1)+R4*Q4(i-1,j+1)*abs(Q4(i-1,j+1));
    H4(i,j) = 0.5*(CP+CM);
    Q4(i,j) = (H4(i,j)-CM)/B4;
end
for j = 2:SN2-1
    CP = SH2(i-1,j-1)+SB2*SQ2(i-1,j-1)-SR2*SQ2(i-1,j-1)*abs(SQ2(i-1,j-1));
    CM = SH2(i-1,j+1)-SB2*SQ2(i-1,j+1)+SR2*SQ2(i-1,j+1)*abs(SQ2(i-1,j+1));
    SH2(i,j) = 0.5*(CP+CM);
    SQ2(i,j) = (SH2(i,j)-CM)/SB2;
end
for j = 2:N5-1
    CP = H5(i-1,j-1)+B5*Q5(i-1,j-1)-R5*Q5(i-1,j-1)*abs(Q5(i-1,j-1));
    CM = H5(i-1,j+1)-B5*Q5(i-1,j+1)+R5*Q5(i-1,j+1)*abs(Q5(i-1,j+1));
    H5(i,j) = 0.5*(CP+CM);
    Q5(i,j) = (H5(i,j)-CM)/B5;
end
for j = 2:SN3-1
    CP = SH3(i-1,j-1)+SB3*SQ3(i-1,j-1)-SR3*SQ3(i-1,j-1)*abs(SQ3(i-1,j-1));

```

```

    CM = SH3(i-1,j+1)-SB3*SQ3(i-1,j+1)+SR3*SQ3(i-1,j+1)*abs(SQ3(i-1,j+1));
    SH3(i,j) = 0.5*(CP+CM);
    SQ3(i,j) = (SH3(i,j)-CM)/SB3;
end
for j = 2:N6-1
    CP = H6(i-1,j-1)+B6*Q6(i-1,j-1)-R6*Q6(i-1,j-1)*abs(Q6(i-1,j-1));
    CM = H6(i-1,j+1)-B6*Q6(i-1,j+1)+R6*Q6(i-1,j+1)*abs(Q6(i-1,j+1));
    H6(i,j) = 0.5*(CP+CM);
    Q6(i,j) = (H6(i,j)-CM)/B6;
end
for j = 2:SN4-1
    CP = SH4(i-1,j-1)+SB4*SQ4(i-1,j-1)-SR4*SQ4(i-1,j-1)*abs(SQ4(i-1,j-1));
    CM = SH4(i-1,j+1)-SB4*SQ4(i-1,j+1)+SR4*SQ4(i-1,j+1)*abs(SQ4(i-1,j+1));
    SH4(i,j) = 0.5*(CP+CM);
    SQ4(i,j) = (SH4(i,j)-CM)/SB4;
end
for j = 2:N7-1
    CP = H7(i-1,j-1)+B7*Q7(i-1,j-1)-R7*Q7(i-1,j-1)*abs(Q7(i-1,j-1));
    CM = H7(i-1,j+1)-B7*Q7(i-1,j+1)+R7*Q7(i-1,j+1)*abs(Q7(i-1,j+1));
    H7(i,j) = 0.5*(CP+CM);
    Q7(i,j) = (H7(i,j)-CM)/B7;
end
for j = 2:N8-1
    CP = H8(i-1,j-1)+B8*Q8(i-1,j-1)-R8*Q8(i-1,j-1)*abs(Q8(i-1,j-1));
    CM = H8(i-1,j+1)-B8*Q8(i-1,j+1)+R8*Q8(i-1,j+1)*abs(Q8(i-1,j+1));
    H8(i,j) = 0.5*(CP+CM);
    Q8(i,j) = (H8(i,j)-CM)/B8;
end
for j = 2:SN5-1
    CP = SH5(i-1,j-1)+SB5*SQ5(i-1,j-1)-SR5*SQ5(i-1,j-1)*abs(SQ5(i-1,j-1));
    CM = SH5(i-1,j+1)-SB5*SQ5(i-1,j+1)+SR5*SQ5(i-1,j+1)*abs(SQ5(i-1,j+1));
    SH5(i,j) = 0.5*(CP+CM);
    SQ5(i,j) = (SH5(i,j)-CM)/SB5;
end
for j = 2:N9-1
    CP = H9(i-1,j-1)+B9*Q9(i-1,j-1)-R9*Q9(i-1,j-1)*abs(Q9(i-1,j-1));
    CM = H9(i-1,j+1)-B9*Q9(i-1,j+1)+R9*Q9(i-1,j+1)*abs(Q9(i-1,j+1));
    H9(i,j) = 0.5*(CP+CM);
    Q9(i,j) = (H9(i,j)-CM)/B9;
end
for j = 2:SN6-1
    CP = SH6(i-1,j-1)+SB6*SQ6(i-1,j-1)-SR6*SQ6(i-1,j-1)*abs(SQ6(i-1,j-1));
    CM = SH6(i-1,j+1)-SB6*SQ6(i-1,j+1)+SR6*SQ6(i-1,j+1)*abs(SQ6(i-1,j+1));
    SH6(i,j) = 0.5*(CP+CM);
    SQ6(i,j) = (SH6(i,j)-CM)/SB6;
end

```

```

for j = 2:N10-1
    CP = H10(i-1,j-1)+B10*Q10(i-1,j-1)-R10*Q10(i-1,j-1)*abs(Q10(i-1,j-1));
    CM = H10(i-1,j+1)-B10*Q10(i-1,j+1)+R10*Q10(i-1,j+1)*abs(Q10(i-1,j+1));
    H10(i,j) = 0.5*(CP+CM);
    Q10(i,j) = (H10(i,j)-CM)/B10;
end
for j = 2:N11-1
    CP = H11(i-1,j-1)+B11*Q11(i-1,j-1)-R11*Q11(i-1,j-1)*abs(Q11(i-1,j-1));
    CM = H11(i-1,j+1)-B11*Q11(i-1,j+1)+R11*Q11(i-1,j+1)*abs(Q11(i-1,j+1));
    H11(i,j) = 0.5*(CP+CM);
    Q11(i,j) = (H11(i,j)-CM)/B11;
end
for j = 2:N12-1
    CP = H12(i-1,j-1)+B12*Q12(i-1,j-1)-R12*Q12(i-1,j-1)*abs(Q12(i-1,j-1));
    CM = H12(i-1,j+1)-B12*Q12(i-1,j+1)+R12*Q12(i-1,j+1)*abs(Q12(i-1,j+1));
    H12(i,j) = 0.5*(CP+CM);
    Q12(i,j) = (H12(i,j)-CM)/B12;
end
for j = 2:SN7-1
    CP = SH7(i-1,j-1)+SB7*SQ7(i-1,j-1)-SR7*SQ7(i-1,j-1)*abs(SQ7(i-1,j-1));
    CM = SH7(i-1,j+1)-SB7*SQ7(i-1,j+1)+SR7*SQ7(i-1,j+1)*abs(SQ7(i-1,j+1));
    SH7(i,j) = 0.5*(CP+CM);
    SQ7(i,j) = (SH7(i,j)-CM)/SB7;
end
for j = 2:N13-1
    CP = H13(i-1,j-1)+B13*Q13(i-1,j-1)-R13*Q13(i-1,j-1)*abs(Q13(i-1,j-1));
    CM = H13(i-1,j+1)-B13*Q13(i-1,j+1)+R13*Q13(i-1,j+1)*abs(Q13(i-1,j+1));
    H13(i,j) = 0.5*(CP+CM);
    Q13(i,j) = (H13(i,j)-CM)/B13;
end
for j = 2:N15-1
    CP = H15(i-1,j-1)+B15*Q15(i-1,j-1)-R15*Q15(i-1,j-1)*abs(Q15(i-1,j-1));
    CM = H15(i-1,j+1)-B15*Q15(i-1,j+1)+R15*Q15(i-1,j+1)*abs(Q15(i-1,j+1));
    H15(i,j) = 0.5*(CP+CM);
    Q15(i,j) = (H15(i,j)-CM)/B15;
end
for j = 2:N17-1
    CP = H17(i-1,j-1)+B17*Q17(i-1,j-1)-R17*Q17(i-1,j-1)*abs(Q17(i-1,j-1));
    CM = H17(i-1,j+1)-B17*Q17(i-1,j+1)+R17*Q17(i-1,j+1)*abs(Q17(i-1,j+1));
    H17(i,j) = 0.5*(CP+CM);
    Q17(i,j) = (H17(i,j)-CM)/B17;
end
%Upper Surge shaft
for j = 2:SSN-1
    CP = SSH(i-1,j-1)+SSB(1)*SSQ(i-1,j-1)-...
        SSR(1)*SSQ(i-1,j-1)*abs(SSQ(i-1,j-1));

```

```

    CM = SSH(i-1,j+1)-SSB(1)*SSQ(i-1,j+1)+...
        SSR(1)*SSQ(i-1,j+1)*abs(SSQ(i-1,j+1));
    SSH(i,j) = 0.5*(CP+CM);
    SSQ(i,j) = (SSH(i,j)-CM)/SSB(1);
end
%Lower surge shaft
for j = 2:UCN-1
    CP = UCH(i-1,j-1)+UCB(1)*UCQ(i-1,j-1)-...
        UCR(1)*UCQ(i-1,j-1)*abs(UCQ(i-1,j-1));
    CM = UCH(i-1,j+1)-UCB(1)*UCQ(i-1,j+1)+...
        UCR(1)*UCQ(i-1,j+1)*abs(UCQ(i-1,j+1));
    UCH(i,j) = 0.5*(CP+CM);
    UCQ(i,j) = (UCH(i,j)-CM)/UCB(1);
end

%-----Boundary conditions Songavatn-----%
%-----Boundary conditions reservoir-----%
H1(i,1) = H0;
Q1(i,1) = (H1(i,1)-H1(i-1,2)+B1*Q1(i-1,2)-...
    (R1*Q1(i-1,2)*abs(Q1(i-1,2))))/B1;
H2(i,N2) = H2(i-1,N2)+((dt/A2)*Q2(i-1,N2));
Q2(i,N2) = (H2(i-1,N2-1)+B2*Q2(i-1,N2-1)-...
    (R2*Q2(i-1,N2-1)*abs(Q2(i-1,N2-1)))-H2(i,N2))/B2;

%----- Boundary conditions branch Songavatn/Troll/Gammal-----%
CP1 = H1(i-1,N1-1)+(B1*Q1(i-1,N1-1))-(R1*Q1(i-1,N1-1)*abs(Q1(i-1,N1-1)));
CM2 = H2(i-1,1+1)-(B2*Q2(i-1,1+1))+(R2*Q2(i-1,1+1)*abs(Q2(i-1,1+1)));
CM3 = H3(i-1,1+1)-(B3*Q3(i-1,1+1))+(R3*Q3(i-1,1+1)*abs(Q3(i-1,1+1)));

HP_NEW = ((CP1/B1)+((ST*CM2)/B2)+(CM3/B3))/((1/B1)+((ST*1)/B2)+(1/B3));
Q1(i,N1) = (-HP_NEW/B1)+(CP1/B1);
Q2(i,1) = (HP_NEW/B2)-(CM2/B2);
Q3(i,1) = (HP_NEW/B3)-(CM3/B3);
H1(i,N1) = HP_NEW;
H2(i,1) = HP_NEW;
H3(i,1) = HP_NEW;

%-----BC for branch Gammal/bekkeinntak/Reinkvam-----%
CP3 = H3(i-1,N3-1)+(B3*Q3(i-1,N3-1))-(R3*Q3(i-1,N3-1)*abs(Q3(i-1,N3-1)));
CMS1 = SH1(i-1,2)-SB1*SQ1(i-1,2)+(SR1*SQ1(i-1,2)*abs(SQ1(i-1,2)));
CM4 = H4(i-1,2)-B4*Q4(i-1,2)+(R4*Q4(i-1,2)*abs(Q4(i-1,2)));

HP_NEW2 = ((CP3/B3)+((ST*CMS1)/SB1)+(CM4/B4))/((1/B3)+((ST*1)/SB1)+(1/B4));
Q3(i,N3) = (-HP_NEW2/B3)+(CP3/B3);
SQ1(i,1) = (HP_NEW2/SB1)-(CMS1/SB1);

```

```

Q4(i,1) = (HP_NEW2/B4)-(CM4/B4);
H3(i,N3) = HP_NEW2;
H4(i,1) = HP_NEW2;
SH1(i,1) = HP_NEW2;

%-----Boundary condition Bekkeinntak/surge shaft Gammalstoylen--%
SH1(i,SN1) = SH1(i-1,SN1) +((dt/SAs1)*SQ1(i-1,SN1));
SQ1(i,SN1) = (SH1(i-1,SN1-1)+SB1*SQ1(i-1,SN1-1)-...
(SR1*SQ1(i-1,SN1-1)*abs(SQ1(i-1,SN1-1)))-SH1(i,SN1))/SB1;

%-----Boundary condition junction Reinkvam-----%
CP4 = H4(i-1,N4-1)+B4*Q4(i-1,N4-1)-(R4*Q4(i-1,N4-1)*abs(Q4(i-1,N4-1)));
CMS2 = SH2(i-1,1+1)-SB2*SQ2(i-1,1+1)+(SR2*SQ2(i-1,1+1)*abs(SQ2(i-1,1+1)));
CM5 = H5(i-1,1+1)-B5*Q5(i-1,1+1)+(R5*Q5(i-1,1+1)*abs(Q5(i-1,1+1)));

HP_NEW3 = ((CP4/B4)+((ST*CMS2)/SB2)+(CM5/B5))/((1/B4)+((ST*1)/SB2)+(1/B5));
Q4(i,N4) = (-HP_NEW3/B4)+(CP4/B4);
SQ2(i,1) = (HP_NEW3/SB2)-(CMS2/SB2);
Q5(i,1) = (HP_NEW3/B5)-(CM5/B5);
H4(i,N4) = HP_NEW3;
SH2(i,1) = HP_NEW3;
H5(i,1) = HP_NEW3;

%-----Boundary condition Bekkeinntak/surge shaft 2 Reinkvam--%
SH2(i,SN2) = SH2(i-1,SN2) +((dt/SAs2)*SQ2(i-1,SN2));
SQ2(i,SN2) = (SH2(i-1,SN2-1)+SB2*SQ2(i-1,SN2-1)-...
(SR2*SQ2(i-1,SN2-1)*abs(SQ2(i-1,SN2-1)))-SH2(i,SN2))/SB2;

%-----Boundary condition junction Urdbø-----%
CP5 = H5(i-1,N5-1)+B5*Q5(i-1,N5-1)-(R5*Q5(i-1,N5-1)*abs(Q5(i-1,N5-1)));
CMS3 = SH3(i-1,1+1)-SB3*SQ3(i-1,1+1)+(SR3*SQ3(i-1,1+1)*abs(SQ3(i-1,1+1)));
CM6 = H6(i-1,1+1)-B6*Q6(i-1,1+1)+(R6*Q6(i-1,1+1)*abs(Q6(i-1,1+1)));

HP_NEW4 = ((CP5/B5)+((ST*CMS3)/SB3)+(CM6/B6))/((1/B5)+((ST*1)/SB3)+(1/B6));
Q5(i,N5) = (-HP_NEW4/B5)+(CP5/B5);
SQ3(i,1) = (HP_NEW4/SB3)-(CMS3/SB3);
Q6(i,1) = (HP_NEW4/B6)-(CM6/B6);
H5(i,N5) = HP_NEW4;
SH3(i,1) = HP_NEW4;
H6(i,1) = HP_NEW4;

%-----Boundary condition Bekkeinntak/surge shaft 3 Urdbø-----%
SH3(i,SN3) = SH3(i-1,SN3) +((dt/SAs3)*SQ3(i-1,SN3));
SQ3(i,SN3) = (SH3(i-1,SN3-1)+SB3*SQ3(i-1,SN3-1)-...
(SR3*SQ3(i-1,SN3-1)*abs(SQ3(i-1,SN3-1)))-SH3(i,SN3))/SB3;

```

```

%-----Boundary condition junction Nipa-----%
CP6 = H6(i-1,N6-1)+B6*Q6(i-1,N6-1)-(R6*Q6(i-1,N6-1)*abs(Q6(i-1,N6-1)));
CMS4 = SH4(i-1,1+1)-SB4*SQ4(i-1,1+1)+(SR4*SQ4(i-1,1+1)*abs(SQ4(i-1,1+1)));
CM7 = H7(i-1,1+1)-B7*Q7(i-1,1+1)+(R7*Q7(i-1,1+1)*abs(Q7(i-1,1+1)));

HP_NEW5 = ((CP6/B6)+((ST*CMS4)/SB4)+(CM7/B7))/((1/B6)+((ST*1)/SB4)+(1/B7));
Q6(i,N6) = (-HP_NEW5/B6)+(CP6/B6);
SQ4(i,1) = (HP_NEW5/SB4)-(CMS4/SB4);
Q7(i,1) = (HP_NEW5/B7)-(CM7/B7);
H6(i,N6) = HP_NEW5;
SH4(i,1) = HP_NEW5;
H7(i,1) = HP_NEW5;

%-----Boundary condition Bekkeinntak/surge shaft 4 Nipa----%
SH4(i,SN4) = SH4(i-1,SN4) +((dt/SAs4)*SQ4(i-1,SN4));
SQ4(i,SN4) = (SH4(i-1,SN4-1)+SB4*SQ4(i-1,SN4-1)-...
(SR4*SQ4(i-1,SN4-1)*abs(SQ4(i-1,SN4-1)))-SH4(i,SN4))/SB4;

%-----Boundary conditions Bitdalsvatnet-----%
%-----Boundary conditions reservoir Bitdalsvatn-----%
H11(i,1) = H0;
Q11(i,1) = (H11(i,1)-H11(i-1,2)+B11*Q11(i-1,2)-...
(R11*Q11(i-1,2)*abs(Q11(i-1,2))))/B11;

%-----Boundary condition junction Kvikkevatn-----%
CP11 = H11(i-1,N11-1)+B11*Q11(i-1,N11-1)-...
(R11*Q11(i-1,N11-1)*abs(Q11(i-1,N11-1)));
CM12 = H12(i-1,1+1)-B12*Q12(i-1,1+1)+(R12*Q12(i-1,1+1)*abs(Q12(i-1,1+1)));
CM10 = H10(i-1,1+1)-B10*Q10(i-1,1+1)+(R10*Q10(i-1,1+1)*abs(Q10(i-1,1+1)));

HP_NEW9 = ((CP11/B11)+((ST*CM12)/B12)+(CM10/B10))/...
((1/B11)+((ST*1)/B12)+(1/B10));
Q11(i,N11) = -(HP_NEW9/B11)+(CP11/B11);
Q12(i,1) = (HP_NEW9/B12)-(CM12/B12);
Q10(i,1) = (HP_NEW9/B10)-(CM10/B10);
H11(i,N11) = HP_NEW9;
H12(i,1) = HP_NEW9;
H10(i,1) = HP_NEW9;

%-----Boundary conditions Kvikkevatn-----%
CP12 = H12(i-1,N12-1)+(B12*Q12(i-1,N12-1))-...
(R12*Q12(i-1,N12-1)*abs(Q12(i-1,N12-1)));
CMS7 = SH7(i-1,1+1)-(SB7*SQ7(i-1,1+1))+...
(SR7*SQ7(i-1,1+1)*abs(SQ7(i-1,1+1)));
Q12(i,N12) = (CP12-CMS7)/(B12+SB7);
SQ7(i,1) = Q12(i,N12);

```

```

H12(i,N12) = CP12-(B12*Q12(i,N12));
SH7(i,1) = H12(i,N12);

%-----Boundary condition Bekkeinntak/surge shaft 7 Kvikkevatn-----%
SH7(i,SN7) = SH7(i-1,SN7) +((dt/SAs7)*SQ7(i-1,SN7));
SQ7(i,SN7) = (SH7(i-1,SN7-1)+SB7*SQ7(i-1,SN7-1)-...
    (SR7*SQ7(i-1,SN7-1)*abs(SQ7(i-1,SN7-1)))-SH7(i,SN7))/SB7;

%-----Boundary condition junction Vaa------%
CP10 = H10(i-1,N10-1)+(B10*Q10(i-1,N10-1))-...
    (R10*Q10(i-1,N10-1)*abs(Q10(i-1,N10-1)));
CMS6 = SH6(i-1,1+1)-SB6*SQ6(i-1,1+1)+(SR6*SQ6(i-1,1+1)*abs(SQ6(i-1,1+1)));
CM9 = H9(i-1,1+1)-B9*Q9(i-1,1+1)+(R9*Q9(i-1,1+1)*abs(Q9(i-1,1+1)));

HP_NEW8 = ((CP10/B10)+((ST*CMS6)/SB6)+(CM9/B9))/...
    ((1/B10)+((ST*1)/SB6)+(1/B9));

Q10(i,N10) = -(HP_NEW8/B10)+(CP10/B10);
SQ6(i,1) = (HP_NEW8/SB6)-(CMS6/SB6);
Q9(i,1) = (HP_NEW8/B9)-(CM9/B9);
H10(i,N10) = HP_NEW8;
SH6(i,1) = HP_NEW8;
H9(i,1) = HP_NEW8;

%-----Boundary condition Bekkeinntak/surge shaft 6 Vaa-----%
SH6(i,SN6) = SH6(i-1,SN6) +((dt/SAs6)*SQ6(i-1,SN6));
SQ6(i,SN6) = (SH6(i-1,SN6-1)+SB6*SQ6(i-1,SN6-1)-...
    (SR6*SQ6(i-1,SN6-1)*abs(SQ6(i-1,SN6-1)))-SH6(i,SN6))/SB6;

%-----Boundary condition junction Farastad------%
CP9 = H9(i-1,N9-1)+B9*Q9(i-1,N9-1)-(R9*Q9(i-1,N9-1)*abs(Q9(i-1,N9-1)));
CMS5 = SH5(i-1,1+1)-SB5*SQ5(i-1,1+1)+(SR5*SQ5(i-1,1+1)*abs(SQ5(i-1,1+1)));
CM8 = H8(i-1,1+1)-B8*Q8(i-1,1+1)+(R8*Q8(i-1,1+1)*abs(Q8(i-1,1+1)));

HP_NEW7 = ((CP9/B9)+((ST*CMS5)/SB5)+(CM8/B8))/((1/B9)+((ST*1)/SB5)+(1/B8));
Q9(i,N9) = -(HP_NEW7/B9)+(CP9/B9);
SQ5(i,1) = (HP_NEW7/SB5)-(CMS5/SB5);
Q8(i,1) = (HP_NEW7/B8)-(CM8/B8);
H9(i,N9) = HP_NEW7;
SH5(i,1) = HP_NEW7;
H8(i,1) = HP_NEW7;

%-----Boundary condition Bekkeinntak/surge shaft 5 Farastad-----%
SH5(i,SN5) = SH5(i-1,SN5) +((dt/SAs5)*SQ5(i-1,SN5));
SQ5(i,SN5) = (SH5(i-1,SN5-1)+SB5*SQ5(i-1,SN5-1)-...

```

(SR5\*SQ5(i-1,SN5-1)\*abs(SQ5(i-1,SN5-1)))-SH5(i,SN5))/SB5;

%-----Boundary condition JUNCTION-----%

CP7 = H7(i-1,N7-1)+B7\*Q7(i-1,N7-1)-(R7\*Q7(i-1,N7-1)\*abs(Q7(i-1,N7-1)));

CP8 = H8(i-1,N8-1)+B8\*Q8(i-1,N8-1)-(R8\*Q8(i-1,N8-1)\*abs(Q8(i-1,N8-1)));

CM13 = H13(i-1,1+1)-B13\*Q13(i-1,1+1)+(R13\*Q13(i-1,1+1)\*abs(Q13(i-1,1+1)));

HP\_NEW6 = ((CP7/B7)+((BT\*CP8)/B8)+(CM13/B13))/((1/B7)+(BT/B8)+(1/B13));

Q7(i,N7) = (-HP\_NEW6/B7)+(CP7/B7);

Q8(i,N8) = (-HP\_NEW6/B8)+(CP8/B8);

Q13(i,1) = (HP\_NEW6/B13)-(CM13/B13);

H7(i,N7) = HP\_NEW6;

H8(i,N8) = HP\_NEW6;

H13(i,1) = HP\_NEW6;

% %-----Junction Surge shaft-----%

CP13 = H13(i-1,N13-1)+B13\*Q13(i-1,N13-1)-...

(R13\*Q13(i-1,N13-1)\*abs(Q13(i-1,N13-1)));

CMSS = SSH(i-1,1+1)-SSB(1)\*SSQ(i-1,1+1)+...

(SSR(1)\*SSQ(i-1,1+1)\*abs(SSQ(i-1,1+1)));

CM15 = H15(i-1,1+1)-B15\*Q15(i-1,1+1)+(R15\*Q15(i-1,1+1)\*abs(Q15(i-1,1+1)));

HP\_NEW10 = ((CP13/B13)+((SST\*CMSS)/SSB(1))+(CM15/B15))/...

((1/B13)+(SST/SSB(1))+(1/B15));

Q13(i,N13) = -(HP\_NEW10/B13)+(CP13/B13);

SSQ(i,1) = (HP\_NEW10/SSB(1))-(CMSS/SSB(1));

Q15(i,1) = (HP\_NEW10/B15)-(CM15/B15);

H13(i,N13) = HP\_NEW10;

SSH(i,1) = HP\_NEW10;

H15(i,1) = HP\_NEW10;

%-----Upper Surge shaft-----%

SSZ(i,1) = H0-HP\_NEW10;

if (SSZ(i,1) > 0 && SSZ(i,1) < SSL(1)) || (SSZ(i,1) > SSL(2)...

&& SSZ(i,1) < SSL(3)) || SSZ(i,1) == 0

SSH(i,SSN) = SSH(i-1,SSN) +((dt/SSAs(1))\*SSQ(i-1,SSN));

SSQ(i,SSN) = (SSH(i-1,SSN-1)+SSB(1)\*SSQ(i-1,SSN-1)-...

(SSR(1)\*SSQ(i-1,SSN-1)\*abs(SSQ(i-1,SSN-1)))-SSH(i,SSN))/SSB(1);

elseif SSZ(i,1) > SSL(1) && SSZ(i,1) < SSL(2)

SSH(i,SSN) = SSH(i-1,SSN) +((dt/SSAs(2))\*SSQ(i-1,SSN));

SSQ(i,SSN) = (SSH(i-1,SSN-1)+SSB(2)\*SSQ(i-1,SSN-1)-...

(SSR(2)\*SSQ(i-1,SSN-1)\*abs(SSQ(i-1,SSN-1)))-SSH(i,SSN))/SSB(2);

elseif SSZ(i,1) > SSL(2) && SSZ(i,1) < SSL(3)

SSH(i,SSN) = SSH(i-1,SSN) +((dt/SSAs(3))\*SSQ(i-1,SSN));

SSQ(i,SSN) = (SSH(i-1,SSN-1)+SSB(3)\*SSQ(i-1,SSN-1)-...

(SSR(3)\*SSQ(i-1,SSN-1)\*abs(SSQ(i-1,SSN-1)))-SSH(i,SSN))/SSB(3);



```

elseif SSZ(i,1) > SSL(4)
    SSH(i,SSN) = SSH(i-1,SSN) +((dt/SSAs(4))*SSQ(i-1,SSN));
    SSQ(i,SSN) = (SSH(i-1,SSN-1)+SSB(4)*SSQ(i-1,SSN-1)-...
        (SSR(4)*SSQ(i-1,SSN-1)*abs(SSQ(i-1,SSN-1)))-SSH(i,SSN))/SSB(4);
elseif SSZ(i,1) < 0
    SSH(i,SSN) = SSH(i-1,SSN) +((dt/SSAs(1))*SSQ(i-1,SSN));
    SSQ(i,SSN) = (SSH(i-1,SSN-1)+SSB(1)*SSQ(i-1,SSN-1)-...
        (SSR(1)*SSQ(i-1,SSN-1)*abs(SSQ(i-1,SSN-1)))-SSH(i,SSN))/SSB(1);
end

%-----Boundary conditions lower reservoir-----%
%-----Reservoir U-tunnel-----%
H17(i,N17) = Hout;
Q17(i,N17) = (H17(i-1,N17-1)+B17*Q17(i-1,N17-1)-...
    R17*Q17(i-1,N17-1)*abs(Q17(i-1,N17-1))-H17(i,N17))/B17;

% % %----- Junction Draft tube/U-chamber/U-tunnel-----%
CM17 = H17(i-1,1+1)-B17*Q17(i-1,1+1)+(R17*Q17(i-1,1+1)*abs(Q17(i-1,1+1)));
CMUC = UCH(i-1,1+1)-UCB(1)*UCQ(i-1,1+1)+...
    (UCR(1)*UCQ(i-1,1+1)*abs(UCQ(i-1,1+1)));
CPDT = DH(i-1,DN-1)+DB(end-1)*DQ(i-1,DN-1)-...
    (DR(end-1)*DQ(i-1,DN-1)*abs(DQ(i-1,DN-1)));

HP_NEW11 = ((CPDT/DB(end-1))+((UCT*CMUC)/UCB(1))+(CM17/B17))/...
    ((1/DB(end-1))+UCT/UCB(1))+(1/B17));
DQ(i,DN) = -(HP_NEW11/DB(end-1))+CPDT/DB(end-1));
UCQ(i,1) = (HP_NEW11/UCB(1))-(CMUC/UCB(1));
Q17(i,1) = (HP_NEW11/B17)-(CM17/B17);
DH(i,DN) = HP_NEW11;
UCH(i,1) = HP_NEW11;
H17(i,1) = HP_NEW11;

% %-----Lower surge shaft-----%
UCZ(i,1) = HP_NEW11-Hout;
if UCZ(i,1) > 0 && UCZ(i,1) < UCL(1) || UCZ(i,1) == 0
    UCH(i,UCN) = UCH(i-1,UCN) + ((dt/UCAs(1))*UCQ(i-1,UCN));
    UCQ(i,UCN) = (UCH(i-1,UCN-1)+UCB(1)*UCQ(i-1,UCN-1)-...
        (UCR(1)*UCQ(i-1,UCN-1)*abs(UCQ(i-1,UCN-1)))-UCH(i,UCN))/UCB(1);
elseif UCZ(i,1) > UCL(1) && UCZ(i,1) < UCL(2)
    UCH(i,UCN) = UCH(i-1,UCN) + ((dt/UCAs(2))*UCQ(i-1,UCN));
    UCQ(i,UCN) = (UCH(i-1,UCN-1)+UCB(2)*UCQ(i-1,UCN-1)-...
        (UCR(2)*UCQ(i-1,UCN-1)*abs(UCQ(i-1,UCN-1)))-UCH(i,UCN))/UCB(2);
elseif UCZ(i,1) < 0
    UCH(i,UCN) = UCH(i-1,UCN) + ((dt/UCAs(1))*UCQ(i-1,UCN));
    UCQ(i,UCN) = (UCH(i-1,UCN-1)+UCB(1)*UCQ(i-1,UCN-1)-...
        (UCR(1)*UCQ(i-1,UCN-1)*abs(UCQ(i-1,UCN-1)))-UCH(i,UCN))/UCB(1);

```

```

elseif UCZ(i,1) > UCL(2)
    UCH(i,UCN) = UCH(i-1,UCN) + ((dt/UCAs(1))*UCQ(i-1,UCN));
    UCQ(i,UCN) = (UCH(i-1,UCN-1)+UCB(1)*UCQ(i-1,UCN-1)-...
        (UCR(1)*UCQ(i-1,UCN-1)*abs(UCQ(i-1,UCN-1)))-UCH(i,UCN))/UCB(1);
end
%-----Draft tube-----%
for k = 2:DN-1
    Xd = (1/DA(k))+(1/(2*DA(k+1)))+(1/(2*DA(k-1)));
    Xa = (g/Da)*(DH(i-1,k-1)-DH(i-1,k+1));
    Xb = (0.5*DQ(i-1,k+1))*((1/DA(k))+(1/DA(k+1)));
    Xc = (0.5*DQ(i-1,k-1))*((1/DA(k))+(1/DA(k-1)));
    DQ(i,k) = ((Xa+Xb+Xc)/Xd);

    Xf = (DQ(i,k)+DQ(i-1,k-1))*0.5*((1/DA(k))-(1/DA(k-1)));
    Xe = (DQ(i,k)/DA(k))-(DQ(i-1,k-1)/DA(k-1));
    DH(i,k) = DH(i-1,k-1)-((Da/g)*(Xe-Xf));
end

%-----Turbine and generator---%
BH = B15+DB(2);
CPH = H15(i-1,N15-1)+B15*Q15(i-1,N15-1)-...
    (R15*Q15(i-1,N15-1)*abs(Q15(i-1,N15-1)));
CMH = DH(i-1,2)-DB(2)*DQ(i-1,1+1)+(DR(2)*DQ(i-1,1+1)*abs(DQ(i-1,1+1)));
HC = CPH-CMH;

%-----Previous values---%
omegaprev = omegadim(i-1);
deltaprev = delta(i-1);
kappaprev = kappa(i-1);
Uprev = U(i-1);
Kmprev = Km(i-1);
qprev = q(i-1);
Tgprev = Tg(i-1);
Iprev = I(i-1);
cprev = c(i-1);
eprev = e(i-1);
uiprev = ui(i-1);
udprev = ud(i-1);

%----Frequency tests----%
if tst == 1
if t(i) < 50
    fgrid(i) = 50;
    omegagrid(i) = 2*pi*fgrid(i);

```

```

    i1 = i;
elseif t(i) > 50 && t(i) < 250
    fgrid(i) = 50.05;
    omegagrid(i) = 2*pi*fgrid(i);
    i2 = i;
elseif t(i) > 250 && t(i) < 450
    fgrid(i) = 50;
    omegagrid(i) = 2*pi*fgrid(i);
    i3 = i;
elseif t(i) > 450 && t(i) < 650
    fgrid(i) = 49.9;
    omegagrid(i) = 2*pi*fgrid(i);
    i4 = i;
elseif t(i) > 650 && t(i) < 850
    fgrid(i) = 50;
    omegagrid(i) = 2*pi*fgrid(i);
    i5 = i;
elseif t(i) > 850 && t(i) < 1050
    fgrid(i) = 50.1;
    omegagrid(i) = 2*pi*fgrid(i);
    i6 = i;
elseif t(i) > 1050 && t(i) < tmax
    fgrid(i) = 50;
    omegagrid(i) = 2*pi*fgrid(i);
    i7 = i;
end
elseif tst == 2
    if t(i) < 50
        fgrid(i) = 50;
    else
        fgrid(i) = fgrid(1) + Af*sin(w(kl)*t(i));
    end
    omegagrid(i) = 2*pi*fgrid(i);
elseif tst == 3
    if t(i) < 50
        fgrid(i) = 50;
        omegagrid(i) = 2*pi*fgrid(i);
        i1 = i;
    elseif t(i) > 50 && t(i) < 300
        fgrid(i) = 49.9;
        omegagrid(i) = 2*pi*fgrid(i);
        i2 = i;
    elseif t(i) > 300 && t(i) < 600
        fgrid(i) = 49.7;
        omegagrid(i) = 2*pi*fgrid(i);
        i3 = i;

```

```

elseif t(i) > 600 && t(i) < 900
  fgrid(i) = 49.9;
  omegagrid(i) = 2*pi*fgrid(i);
  i4 = i;
elseif t(i) > 900 && t(i) < 1200
  fgrid(i) = 49.5;
  omegagrid(i) = 2*pi*fgrid(i);
  i5 = i;
elseif t(i) > 1200
  fgrid(i) = 49.9;
  omegagrid(i) = 2*pi*fgrid(i);
  i6 = i;
end
elseif tst == 4
  if t(i) < 50
    fgrid(i) = 50;
    omegagrid(i) = 2*pi*fgrid(i);
    i1 = i;
  elseif t(i) > 50 && t(i) < 200
    fgrid(i) = 49.8;
    omegagrid(i) = 2*pi*fgrid(i);
    i2 = i;
  elseif t(i) > 200 && t(i) < 400
    fgrid(i) = 49.9;
    omegagrid(i) = 2*pi*fgrid(i);
    i3 = i;
  elseif t(i) > 400
    fgrid(i) = fgrid(i-1)-(0.3*dt);
    if fgrid(i) < 49.0
      fgrid(i) = 49.0;
    end
    omegagrid(i) = 2*pi*fgrid(i);
    i4 = i;
  end
elseif tst == 5
  if t(i) < 50
    fgrid(i) = 50;
    omegagrid(i) = 2*pi*fgrid(i);
    i1 = i;
  elseif t(i) > 50 && t(i) < 300
    fgrid(i) = 50.1;
    omegagrid(i) = 2*pi*fgrid(i);
    i2 = i;
  elseif t(i) > 300 && t(i) < 600
    fgrid(i) = 50.3;
    omegagrid(i) = 2*pi*fgrid(i);

```

```

i3 = i;
elseif t(i) > 600 && t(i) < 900
fgrid(i) = 50.1;
omegagrid(i) = 2*pi*fgrid(i);
i4 = i;
elseif t(i) > 900 && t(i) < 1200
fgrid(i) = 50.5;
omegagrid(i) = 2*pi*fgrid(i);
i5 = i;
elseif t(i) > 1200
fgrid(i) = 50.1;
omegagrid(i) = 2*pi*fgrid(i);
i6 = i;
end
elseif tst == 6
if t(i) < 50
fgrid(i) = 50;
omegagrid(i) = 2*pi*fgrid(i);
i1 = i;
elseif t(i) > 50 && t(i) < 200
fgrid(i) = 50.2;
omegagrid(i) = 2*pi*fgrid(i);
i2 = i;
elseif t(i) > 200 && t(i) < 400
fgrid(i) = 50.1;
omegagrid(i) = 2*pi*fgrid(i);
i3 = i;
elseif t(i) > 400
fgrid(i) = fgrid(i-1)+0.3*dt;
if fgrid(i) > 51.0
fgrid(i) = 51.0;
end
omegagrid(i) = 2*pi*fgrid(i);
i4 = i;
end
end

syms Tgx kappax qdimx omegadimx deltax cx Ux Ix Kmx
alpha1 = asin(kappax*sin(alpha1r));
ms = ksi*(qdimx/kappax)*(cos(alpha1)+tan(alpha1r)*sin(alpha1));
qc = omegadimx*((1+cot(alpha1r)*tan(beta1r))/(1+cot(alpha1)*tan(beta1r)));
h = (HC-(BH*Qr*qdimx))/Hr;
nh = 1-(((Rf*qdimx^2)+(Ra*(qdimx-qc)^2))/h);

enow = ((omegaref-omegadimx*omegaref)/omegaref)-(bb*(kappar-kappax));
%Turbine

```

```

EQ1 = (qdimx*nh*(ms-psi*omegadimx))-((Tgx/Ttr))-...
      ((Ta/dt)*(omegadimx-omegaprev))-Rm*omegadimx^2....
      -((md/dt)*(deltax-deltaprev));
EQ2 = (HC-(BH*Qr*qdimx))-(Hr*((qdimx/kappax)^2)-...
      (sg*((omegadimx^2)-1))))-(Tw*(qdimx-qprev)/dt);
%Generator
EQ3 = ((poles/2)*(omegadimx*omegaref))-omegagrid(i)-...
      ((deltax-deltaprev)/dt);
EQ4 = (Kmx*omegagrid(i))-Ux;
EQ5 = (Kmx*Ix)-Tgx;
EQ6 = ((sin(deltax)/sin(deltar)))-(Tgx/Tgenmax);
%Governing
%Voltage governing
EQ9 = (-K5*((Ux-Uprev)/dt))+K6*((Ur-Ux)+(K7*(Ix-Ir)))-((Kmx-Kmprev)/dt);
%Frequency governing
EQ8 = ((1/bt)*enow)+(uiprev+0.5*(enow+eprev)*dt*(1/(bt*Ti)))+...
      (((Tf*udprev)+((Td/bt)*(enow-eprev)))/(dt+Tf))-(kappax-kappaprev)/dt;
%NewtonSolver
nsol = newton_n_dim(0.1,...
      [Tgprev,kappaprev,qprev,omegaprev,deltaprev,Uprev,Iprev,Kmprev],...
      [Tgx,kappax,qdimx,omegadimx,deltax,Ux,Ix,Kmx],...
      [EQ1;EQ2;EQ3;EQ4;EQ5;EQ6;EQ9;EQ8]);

Tg(i) = double(nsol(1));
kappa(i) = double(nsol(2));
q(i) = double(nsol(3));
omegadim(i) = double(nsol(4));
delta(i) = double(nsol(5));
U(i) = double(nsol(6));
I(i) = double(nsol(7));
Km(i) = double(nsol(8));

e(i) = ((omegaref-omegadim(i)*omegaref)/omegaref)-(bb*(kappar-kappa(i)));
ui(i) = ui(i-1)+(0.5*(e(i)+e(i-1))*dt*(1/(bt*Ti)));
ud(i) = (Tf*ud(i-1)+(Td/bt)*(e(i)-e(i-1)))/(dt+Tf);

Hturb(i)= Hr*((q(i)/kappa(i))^2+sg*(omegadim(i)^2-1));
flow(i) = Qr*q(i);
power1(i) = ro*g*Hturb(i)*flow(i);
%Servo motor
c(i) = (kappa(i)-kappa(i-1))/dt;
if c(i) > cmax
    c(i) = cmax;
    kappa(i) = kappa(i-1)+(dt*c(i));
elseif c(i) < -cmax
    c(i) = -cmax;

```

```

    kappa(i) = kappa(i-1)+(dt*c(i));
end

alpha1 = asin(kappa(i)*sin(alpha1r));
ms = ksi*(q(i)/kappa(i))*(cos(alpha1)+tan(alpha1r)*sin(alpha1));
qc = omegadim(i)*((1+cot(alpha1r)*tan(beta1r))/...
    (1+cot(alpha1)*tan(beta1r)));
DeltaH = HC-(BH*Qr*q(i));
h = DeltaH/Hr;
nhyd = 1-(((Rf*q(i)^2)+Ra*(q(i)-qc)^2)/h);

power(i) = ro*g*flow(i)*DeltaH;
ntot(i) = (((q(i)*omegadim(i)*nhyd*(ms-psi*omegadim(i)))-...
    (Rm*omegadim(i)^3))/(q(i)*h));
GenPower(i) = power(i)*ntot(i)*ngen;
%----- BC at turbine-----%

Q15(i,N15) = flow(i);
DQ(i,1) = flow(i);
H15(i,N15) = H15(i-1,N15-1)+B15*Q15(i-1,N15-1)-...
    R15*Q15(i-1,N15-1)*abs(Q15(i-1,N15-1))-B15*Q15(i,N15);
DH(i,1) = DH(i-1,1+1)-DB(2)*DQ(i-1,1+1)+...
    (DR(2)*DQ(i-1,1+1)*DQ(i-1,1+1))+DB(2)*DQ(i,1);

%-----Increase time step-----%
i = i+1;
t(i) = t(i-1)+dt;

end

if tst == 2
Ap = mean(GenPower)-max(GenPower);
NonGain = Ap/Af;
tau1 = find(GenPower == max(GenPower));
tau2 = find(fgrid == max(fgrid));
Deltat = min(abs(t(tau1)-t(tau2)));
Phase = (360/T(kl))*Deltat;
elseif tst == 4 || tst == 6
tau1 = find(t > t(i3)+5);
i5sek = min(tau1)-1;
tau2 = find(fgrid == max(fgrid));
    if tst == 6
        tau2 = find(fgrid == min(fgrid));
    end
istop = min(tau2)-1;
DeltaP5s = mean(GenPower(i3-2000:i3))-GenPower(i5sek);

```

```
Es = trapz(t(i3:i5sek),mean(GenPower(i3-2000:i3))-GenPower(i3:i5sek));  
end
```



## Appendix B Parameters Songa

Pipe distance	Length [m]	Area [m <sup>2</sup> ]	Diameter [m]
Songavatnet-Trolldalen	1761	20	4
Trolldalen-Gammalstøyl	1311	42	8
Gammalstøyl-Reinkvam	942	42	8
Reinkvam - Urdbø	3547	42	8
Urdbø - Nipa	1453	42	8
Nipa- Junction	850	43	8
Junction - Farastad	390	10	3
Farastad - Vå	6557	10	3
Vå - Kvikkevatn	100	9.6	3
Kvikkevatn - Bitdalsvatnet	3755	11	3
Junction - Surge shaft	39	43	8
Surge shaft - Turbine	327	7.5	3.1
U-chamber - Totak	462	40	7.1

Table 14: Full waterway parameters

Parameter	Value
Turbine rated power[MW]	136
Rated pressure head [m]	264
Rated discharge [m <sup>3</sup> /s]	52
Rated rotational speed[rpm]	300
Rated generator voltage[V]	17000
$T_a$ [s]	6
Upper reservoir level [m]	956.5
Lower reservoir level [m]	683
Proportional Gain voltage regulator, $K_{pg}$	14
Integral Time voltage regulator [s], $T_{ig}$	1
Drop voltage regulator [%], $b_{pg}$	2.5

Table 15: Rated values turbine and generator

# Appendix C Figures and values

## C.1 Full FCR-N Nyquist response

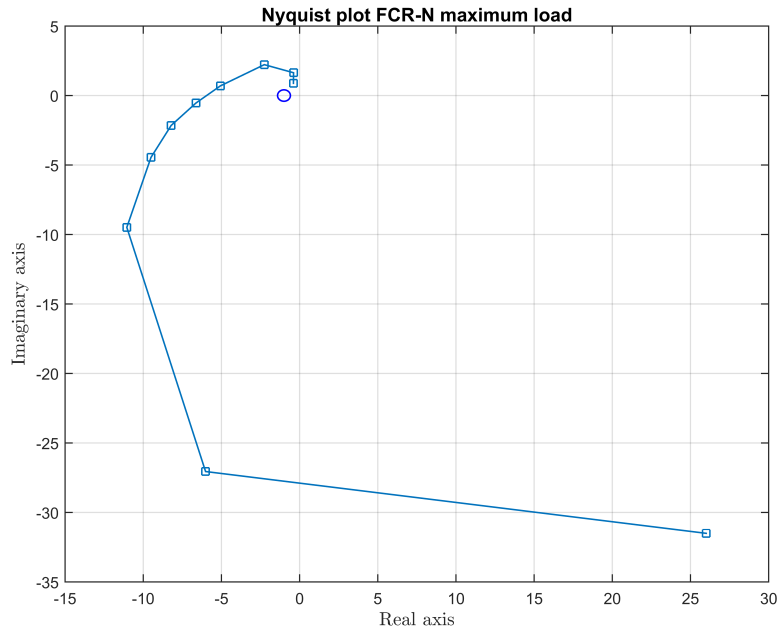


Figure 42: Full FCR-N Nyquist response maximum load

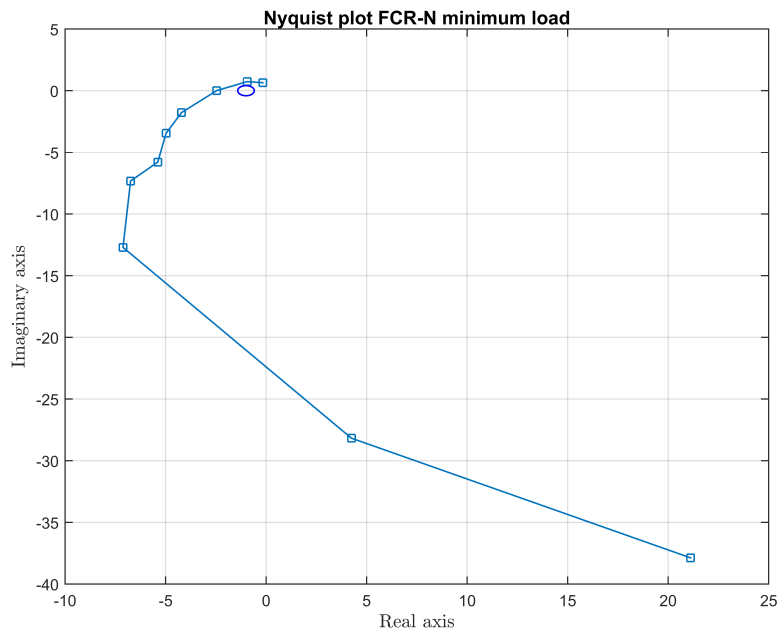


Figure 43: Full FCR-N Nyquist response minimum load

## C.2 Full ramp response

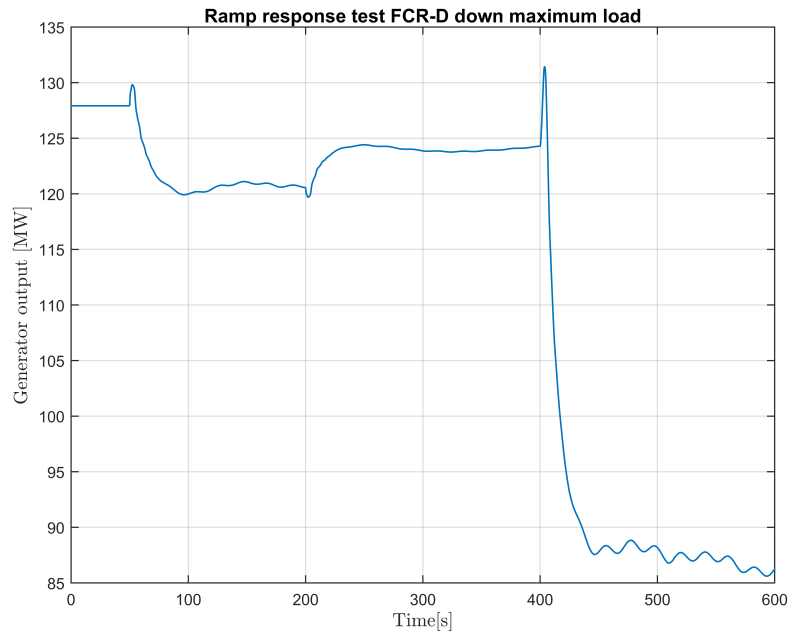


Figure 44: Full ramp response FCR-D downwards at maximum load

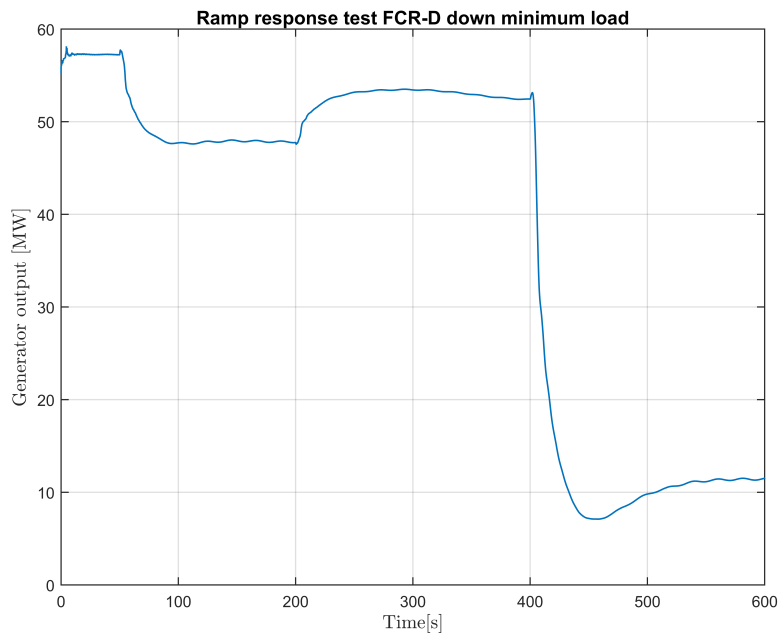


Figure 45: Full ramp response FCR-D downwards at minimum load

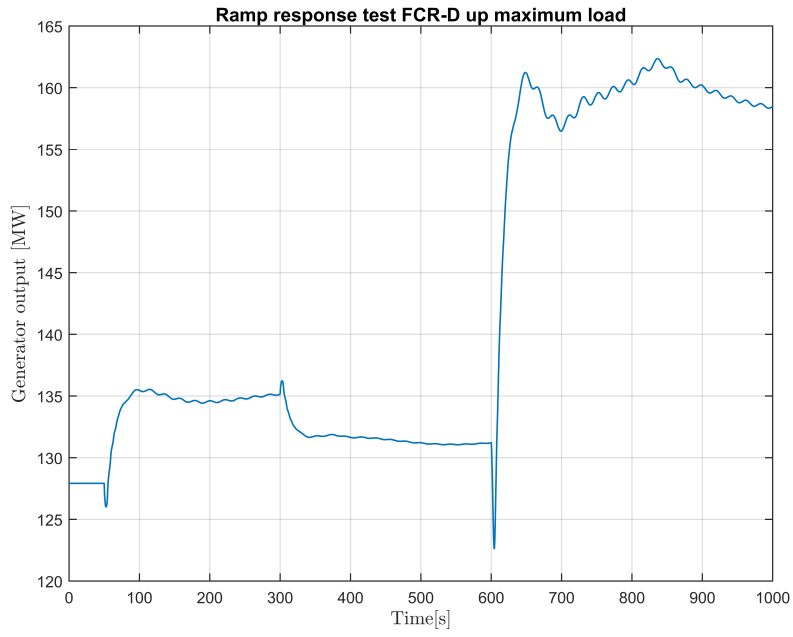


Figure 46: Full ramp response FCR-D upwards at maximum load

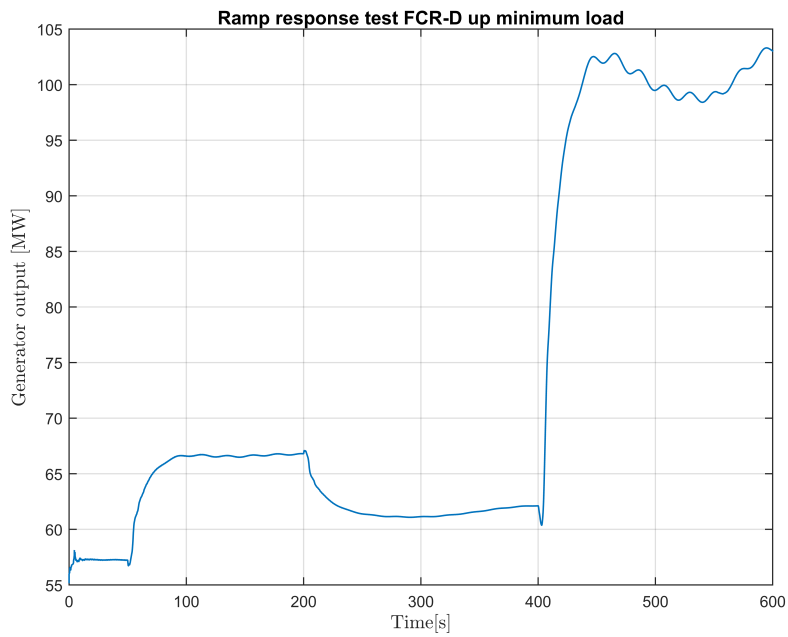


Figure 47: Full ramp response FCR-D upwards at minimum load

### C.3 Governor tuning

Full step response of the governing parameters:

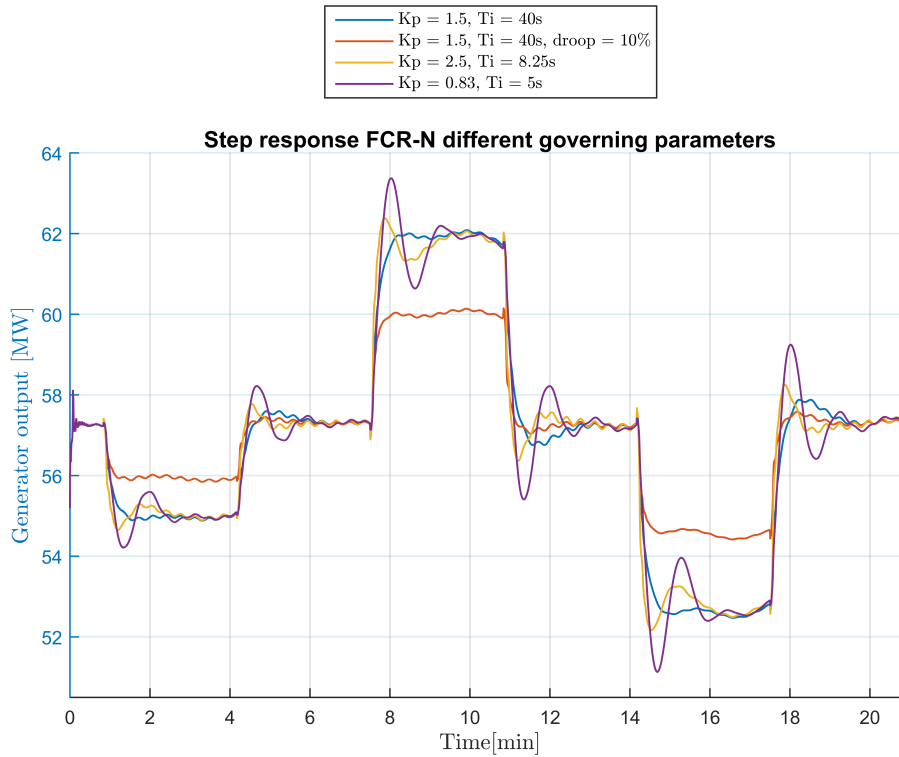


Figure 48: Full step response FCR-N different governing parameters

Values obtained from sine sweep, utilized to construct a Nyquist diagram

For simulation with  $K_p = 0.83$  and  $T_i = 5$

$$\Delta P = \frac{4.559 + 4.5556}{2} = 4.557 MW$$

$$e_N = 45.6 MW$$

T [s]	$\omega$ [rad/s]	$A_p$ [MW]	$\Delta t$ [s]	Gain [MW/Hz]	Norm Gain[pu]	Phase[°]
10	0.6283	0.966	0.111	9.66	0.21	4
15	0.4189	1.1013	1.58	11.013	0.24	38
25	0.2513	1.58	3.6	15.8	0.35	52.8
40	0.1571	2.58	7.3	25.8	0.57	65.75
50	0.1257	4.37	10.5	43.7	0.96	75.6
60	0.1047	6.9894	13.8	69.894	1.53	82.83
70	0.0898	8.96	21.4	89.6	1.96	110.3
90	0.0698	7.998	37.2	79.98	1.75	148.8
150	0.0419	5.7429	70.94	57.429	1.26	170.3
300	0.0209	4.83	143.7	48.3	1.06	172.4

For simulation with  $K_p = 2.5$  and  $T_i = 8.25s$

$$\Delta P = \frac{4.5494 + 4.5465}{2} = 4.55MW$$

$$e_N = 45.5MW$$

T [s]	$\omega$ [rad/s]	Ap [MW]	$\Delta t$ [s]	Gain [MW/Hz]	Norm Gain[pu]	Phase[°]
10	0.6283	2.3164	0.61	23.164	0.51	22
15	0.4189	2.6983	2.5278	26.983	0.59	60.7
25	0.2513	3.3086	5.9	33.086	0.73	84.8
40	0.1571	4.0778	12.3	40.778	0.896	111
50	0.1257	4.9203	16.8	49.203	1.08	120.8
60	0.1047	5.5544	22	55.544	1.22	132
70	0.0898	5.799	28.06	57.99	1.27	144.3
90	0.0698	5.7108	39.7	57.108	1.26	158.8
150	0.0419	4.9825	68	49.825	1.1	163.2
300	0.0209	4.7166	145.9	47.166	1.04	175.1

For simulation with lower droop, 10 %

$$\Delta P = \frac{2.7353 + 2.7288}{2} = 2.723MW$$

$$e_N = 27.23MW$$

T [s]	$\omega$ [rad/s]	Ap [MW]	$\Delta t$ [s]	Gain [MW/Hz]	Norm Gain[pu]	Phase[°]
10	0.6283	1.4284	0.86	14.284	0.52	31
15	0.4189	1.5968	2.69	15.968	0.59	64.7
25	0.2513	1.8290	6.42	18.29	0.67	92.4
40	0.1571	1.9498	13.61	19.498	0.72	122.5
50	0.1257	2.1066	17.7	21.066	0.77	127.2
60	0.1047	2.2676	22.36	22.676	0.83	134.2
70	0.0898	2.3953	26.6	23.953	0.88	136.7
90	0.0698	2.6623	36.6	26.623	0.98	146.3
150	0.0419	3.0661	69.72	30.661	1.13	167.3
300	0.0209	2.9466	134.5	29.466	1.08	161.4

## Appendix D Expanding section

For an expanding section the continuity equation can be written as:

$$\frac{g}{a^2} \left( V \frac{dH}{dx} + \frac{dH}{dt} \right) + \frac{dV}{dx} + \frac{2\beta V}{D} + \frac{q}{A} = 0 \quad (\text{D.0.1})$$

The equation of momentum can be written as:

$$g \frac{dH}{dx} + V \frac{dV}{dx} + \frac{dV}{dt} + \frac{fV|V|}{2D} + \frac{Vq}{A}(\psi - 1) = 0 \quad (\text{D.0.2})$$

The reduced equation using the method of characteristics becomes:

$$\frac{dH}{dt} \pm \frac{a}{g} \frac{dV}{dt} + \frac{a^2}{g} \left[ \frac{2\beta V}{D} + \frac{q}{A} \right] \pm \frac{a}{g} \left[ \frac{fV|V|}{2D} + \frac{Vq(\psi - 1)}{gA} \right] \quad (\text{D.0.3})$$

$$\frac{dx}{dt} = \pm a \quad (\text{D.0.4})$$

Where  $q$  is the outflow of the pipe per unit length,  $\beta$  is the rate of expansion of the original diameter and  $\psi$  represents the axial momentum leaving the segment of fluid in the tube [33]. If  $\psi = 1$ , the fluid leaving reduces its axial momentum and if  $\psi = 0$  the axial momentum of the fluid leaving is entirely reduced within the segment. The other terms are as described earlier in thesis.

Due to  $a^2$ , the first bracketed term will be large compared to the other bracketed terms. Therefore, to simplify, these terms are excluded from the equation. In addition we assume that no flow escapes the pipe and  $q$  is therefore zero. The characteristic equation is then reduced to:

$$\frac{dH}{dt} \pm \frac{a}{g} \frac{dV}{dt} + \frac{a^2}{g} \left[ \frac{2\beta V}{D} \right] = 0 \quad (\text{D.0.5})$$

$$\frac{dx}{dt} = \pm a \quad (\text{D.0.6})$$

For integration along the C+ characteristic:  $\frac{dx}{dt} = +a$

Inserting this into the equation and setting  $V = Q/A$ :

$$\frac{dH}{dt} + \frac{a}{gA} \frac{dQ}{dt} + \frac{a}{g} \frac{dx}{dt} \left[ \frac{2\beta Q}{DA} \right] = 0 \quad (\text{D.0.7})$$

$$a = + \frac{dx}{dt} \quad (\text{D.0.8})$$

Rewriting into the known format of point A and B as introduced earlier and setting the area  $A = \frac{\pi D^2}{4}$

$$H_P - H_A + \frac{a}{g} \left( \frac{Q_P}{A_P} + \frac{Q_A}{A_A} \right) + \frac{4 \cdot 2\beta Q}{\pi D^3} dx = 0 \quad (\text{D.0.9})$$

The expanding diameter is described as

$$D = D_0 + \beta x \quad (\text{D.0.10})$$

Inserting this into the expression:

$$H_P - H_A + \frac{a}{g} \left( \frac{Q_P}{A_P} - \frac{Q_A}{A_A} \right) + \frac{8\beta a}{\pi g} \int_{x_A}^{x_P} \frac{Q dx}{(D_0 + \beta x)^3} \quad (\text{D.0.11})$$

The integral term needs to be resolved in order to solve the problem numerically. This is not straightforward as the variation of Q is unknown. The book "Fluid transients" by Wylie and Streeter [33] suggests that the integral is approximated by the use of the Trapezoidal rule[11] and set:

$$Q = \frac{\Delta x}{2} (Q_P + Q_A) \quad (\text{D.0.12})$$

Which leads to a  $C^+$  characteristics as described in the book[33] :

$$H_P - H_A + \frac{a}{g} \left[ \frac{Q_P}{A_P} - \frac{Q_A}{A_A} - \frac{\Delta x}{2} (Q_P + Q_A) \left( \frac{1}{A_P} - \frac{1}{A_A} \right) \right] = 0 \quad (\text{D.0.13})$$

However, after implementing this equation into the code and found that it was not working as desired, the equation was further investigated. One found that the units did not correspond. On the right hand side the units should obviously be zero as there are no terms present. On the left hand side there was an extra unit of [m]. As [m] cannot equal 0, it was decided to look at the integral again as it was most likely there the error occurred.

The author suggests that the flow is approximated by using an average value and setting:

$$Q = \frac{1}{2} (Q_P + Q_A) \quad (\text{D.0.14})$$

This expression can now be set outside the integral as it is not dependent on x, and the integral can therefore be solved as follows:



$$\int_{x_A}^{x_P} (D_0 + \beta x)^{-3} dx \quad (\text{D.0.15})$$

$$u = D_0 + \beta x \quad (\text{D.0.16})$$

$$\frac{du}{dx} = \beta \quad (\text{D.0.17})$$

$$\int_{x_A}^{x_P} u^{-3} \frac{du}{\beta} = \quad (\text{D.0.18})$$

$$-\frac{1}{2}u^{-2} = -\frac{1}{2}(D_0 + \beta x)^{-2} = -\frac{1}{2}D^{-2} \quad (\text{D.0.19})$$

$$\int_{x_A}^{x_P} u^{-3} \frac{du}{\beta} = \frac{1}{\beta} \left[ -\frac{1}{2}D^{-2} \right]_{x_A}^{x_P} = \quad (\text{D.0.20})$$

$$\frac{1}{\beta} \left[ -\frac{1}{2D_P^2} + \frac{1}{2D_A^2} \right] \quad (\text{D.0.21})$$

$$A = \frac{1}{4}\pi D^2 \quad (\text{D.0.22})$$

The integral can now be written as:

$$\frac{a}{g} \frac{8\beta}{\pi} \int_{x_A}^{x_P} \frac{Q dx}{(D_0 + \beta x)^3} = \frac{a}{g} \frac{8\beta}{\pi} (Q_A + Q_P) \frac{1}{2} \left( -\frac{1}{2D_P^2} + \frac{1}{2D_A^2} \right) \frac{1}{\beta} \quad (\text{D.0.23})$$

$$= \frac{a}{g} \frac{1}{2} (Q_A + Q_P) \left( -\frac{1}{A_P} + \frac{1}{A_A} \right) \quad (\text{D.0.24})$$

$$= -\frac{a}{g} \frac{1}{2} (Q_A + Q_P) \left( \frac{1}{A_P} - \frac{1}{A_A} \right) \quad (\text{D.0.25})$$

Inserting this into the final equation we get the  $C^+$ -characteristic equation:

$$H_P - H_A + \frac{a}{g} \left[ \frac{Q_P}{A_P} - \frac{Q_A}{A_A} - \frac{1}{2} (Q_P + Q_A) \left( \frac{1}{A_P} - \frac{1}{A_A} \right) \right] = 0 \quad (\text{D.0.26})$$

In order to solve the equation we need to find the corresponding  $C^-$  equation where

$$\frac{dx}{dt} = -a \quad (\text{D.0.27})$$

Inserting this into the ordinary differential equation and multiply with  $dt$ :

$$\frac{dH}{dt} - \frac{a}{g} \frac{dQ}{dAdt} - \frac{a}{g} \frac{dx}{dt} \left[ \frac{2\beta Q}{AD} \right] = 0 \quad (\text{D.0.28})$$

$$dH - \frac{a}{g} \frac{dQ}{dA} - \frac{a}{g} dx \left[ \frac{8\beta Q}{\pi D^3} \right] = 0 \quad (\text{D.0.29})$$

The  $C^-$  equation is defined from P to B:

$$H_P - H_B - \frac{a}{g} \left( \frac{Q_P}{A_P} - \frac{Q_B}{A_B} \right) - \frac{a8\beta}{g\pi} \int_{x_B}^{x_P} \frac{Qdx}{(D_0 + \beta x)^3} \quad (\text{D.0.30})$$

By using the same approximation as earlier, the integral can be solved in a similar manner

$$\frac{a8\beta}{g\pi} \frac{1}{2} (Q_B + Q_P) \int_{x_P}^{x_B} (D_0 + \beta x)^{-3} \quad (\text{D.0.31})$$

$$u = D_0 + \beta x \quad (\text{D.0.32})$$

$$\frac{du}{dx} = \beta \quad (\text{D.0.33})$$

$$\frac{1}{\beta} \int u^{-3} du = -\frac{1}{2\beta} [u^{-2}] = \quad (\text{D.0.34})$$

$$-\frac{1}{2\beta} [(D_0 + \beta x)^{-2}]_{x_B}^{x_P} = \quad (\text{D.0.35})$$

$$-\frac{1}{2\beta} [(D_0 + \beta x_P)^{-2} - (D_0 + \beta x_B)^{-2}] = \quad (\text{D.0.36})$$

$$-\frac{1}{2\beta} \left[ \frac{1}{D_P^2} - \frac{1}{D_B^2} \right] = \quad (\text{D.0.37})$$

$$-\frac{1}{2\beta} \left[ \frac{\pi}{4A_P} - \frac{\pi}{4A_B} \right] \quad (\text{D.0.38})$$

The integral term can be resolved:

$$-\frac{a8\beta}{g\pi} \int_{x_B}^{x_P} \frac{Qdx}{(D_0 + \beta x)^3} = -\frac{a8\beta}{g\pi} \frac{1}{2} (Q_P + Q_B) \left( -\frac{1}{2\beta} \left[ \frac{\pi}{4A_P} - \frac{\pi}{4A_B} \right] \right) \quad (\text{D.0.39})$$

$$= +\frac{a}{g} \frac{1}{2} (Q_P + Q_B) \left( \frac{1}{A_P} - \frac{1}{A_B} \right) \quad (\text{D.0.40})$$

The final format of the  $C^-$  characteristic is then:

$$H_P - H_B - \frac{a}{g} \left[ \left( \frac{Q_P}{A_P} - \frac{Q_B}{A_B} \right) - \frac{1}{2} (Q_P + Q_B) \left( \frac{1}{A_P} - \frac{1}{A_B} \right) \right] = 0 \quad (\text{D.0.41})$$

Hence, there are two equations and two unknowns,  $H_P$  and  $Q_P$ . The last equation solved for  $H_P$  is:

$$H_P = H_B + \frac{a}{g} \left[ \left( \frac{Q_P}{A_P} - \frac{Q_B}{A_B} \right) - \frac{1}{2} (Q_P + Q_B) \left( \frac{1}{A_P} - \frac{1}{A_B} \right) \right] \quad (\text{D.0.42})$$

Inserted into the  $C^+$  characteristic, an expression for  $Q_P$  can be found.

$$\begin{aligned} H_B + \frac{a}{g} \left[ \frac{Q_P}{A_P} - \frac{Q_B}{A_B} - \frac{1}{2} (Q_P + Q_B) \left( \frac{1}{A_P} - \frac{1}{A_B} \right) \right] \\ - H_A + \frac{a}{g} \left[ \frac{Q_P}{A_P} - \frac{Q_A}{A_A} - \frac{1}{2} (Q_P + Q_A) \left( \frac{1}{A_P} - \frac{1}{A_A} \right) \right] = 0 \end{aligned} \quad (\text{D.0.43})$$

Rearranging:

$$\begin{aligned} \frac{g}{a} (H_B - H_A) + \frac{2Q_P}{A_P} - \frac{Q_B}{A_B} - \frac{Q_A}{A_A} - \frac{1}{2} \frac{Q_P}{A_P} + \frac{1}{2} \frac{Q_P}{A_B} - \frac{1}{2} \frac{Q_B}{A_P} + \frac{1}{2} \frac{Q_B}{A_B} \\ - \frac{1}{2} \frac{Q_P}{A_P} + \frac{1}{2} \frac{Q_P}{A_A} - \frac{1}{2} \frac{Q_A}{A_P} + \frac{1}{2} \frac{Q_A}{A_A} = 0 \end{aligned} \quad (\text{D.0.44})$$

Sorting and moving terms except for  $Q_P$  over to the right hand side:

$$\begin{aligned} Q_P \left( \frac{1}{A_P} + \frac{1}{2A_B} + \frac{1}{2A_A} \right) \\ = \frac{g}{a} (H_A - H_B) + Q_B \left( \frac{1}{2A_P} + \frac{1}{2A_B} \right) + Q_A \left( \frac{1}{2A_P} + \frac{1}{2A_A} \right) \end{aligned} \quad (\text{D.0.45})$$

In order to make the equation a bit easier to read and handle in the code, it is split up into four:

$$X_d = \frac{1}{A_P} + \frac{1}{2A_B} + \frac{1}{2A_A} \quad (\text{D.0.46})$$

$$X_a = \frac{g}{a} (H_A - H_B) \quad (\text{D.0.47})$$

$$X_b = \frac{1}{2} Q_B \left( \frac{1}{A_P} + \frac{1}{A_B} \right) \quad (\text{D.0.48})$$

$$X_c = \frac{1}{2} Q_A \left( \frac{1}{A_P} + \frac{1}{A_A} \right) \quad (\text{D.0.49})$$

Which leads to:

$$Q_P = \frac{X_a + X_b + X_c}{X_d} \quad (\text{D.0.50})$$

The unknown  $Q_P$  can now be found.  $H_P$  can then be calculated by using one of the equations that was described earlier

$$H_P = H_A - \frac{a}{g} \left[ \frac{Q_P}{A_P} - \frac{Q_A}{A_A} - \frac{1}{2} (Q_P + Q_A) \left( \frac{1}{A_P} - \frac{1}{A_A} \right) \right] \quad (\text{D.0.51})$$

The equation can also here be split up to get a better overview:

$$X_f = \frac{1}{2} (Q_P + Q_A) \left( \frac{1}{A_P} - \frac{1}{A_A} \right) \quad (\text{D.0.52})$$

$$X_e = \frac{Q_P}{A_P} - \frac{Q_A}{A_A} \quad (\text{D.0.53})$$

As follows, the equation for  $H_P$  is:

$$H_P = H_A - \frac{a}{g} [X_e - X_f] \quad (\text{D.0.54})$$

# Appendix E Paper presented at CRHT-VII

Please do not alter/edit or  
add anything to this  
information

*Proceedings of the International Symposium on Current Research in Hydraulic Turbines*

**CRHT – VII**

*April 04, 2016, Turbine Testing Lab, Kathmandu University, Dhulikhel, Nepal*

**Paper no. \_ \_ \_**

## **Simulation and analysis of FCR operation of a Francis turbine**

**Anna Holm Aftret<sup>1\*</sup>**

<sup>1</sup>*Department of Energy and Process Engineering, NTNU University, Alfred Getz vei 4 Trondheim, Norway*

*\* Corresponding author (annahoaf@stud.ntnu.no)*

---

### **Abstract**

The Nordic grid has in the later years experienced several frequency fluctuations. Therefore, the Nordic TSOs are in the process of developing new demands for primary governing. Hydro power plants may have to undergo qualification tests in order to participate in the FCR market. In this thesis, the development of a simulation model based on the Method of characteristics is described as well as the qualification tests for primary governing. Lastly the step response test is presented and analyzed.

**Keywords:** Hydro power, governing, simulation model, Method of Characteristics, frequency fluctuations, qualification tests

---

### **1. Introduction**

The Nordic grid has in the later years expanded to include more renewable energy like wind power and solar. This has caused the Nordic grid to experience several frequency fluctuations, lasting for around 40-90 seconds. In order to compensate for these fluctuations, hydro power needs to be utilized as a reserve to stabilize the grid frequency to normal operation of 50 Hz. The Nordic TSOs are now preparing new demands for delivery of primary governing also known as FCR. Hydro power plants may have to undergo qualification tests in order to participate. The tests contain simulation of step and sinusoidal frequency disturbances in the governor and are performed while the plant is still connected to the grid. If the hydro power plant is qualified, it may give incentives to change the governing parameters in order to deliver more capacity. In this paper, a simulation model based on the Method of Characteristics is described as well as the different qualification tests for FCR delivery.

### **2. Simulation Model**

In order to perform the qualification tests, a simulation model based on the Method of Characteristics is developed. The Method of Characteristics is utilized to calculate transient flow in a conduit system. The method is based on transforming the equation of motion and the equation of continuity into four ordinary differential equations that can be solved numerically.

$$\pm \frac{g}{a} \frac{dH}{dt} + \frac{dV}{dt} + \frac{fV|V|}{2D} = 0$$

$$\frac{dx}{dt} = \pm a$$

The simulation model is based on Songa Hydro Power plant in Norway. This plant has two reservoirs that feeds a Francis turbine with a rated head of 264 m and a rated flow of 52 m<sup>3</sup>/s. The surge shaft, U-chamber and stream intakes are defined as a junction at the lower end of a pipe and surge shaft at the upper end.

$$H_i = \frac{\sum \frac{C_{Pj}}{B_j} + \sum C_{Mk}/B_k}{\sum 1/B}$$

$$H_i = H_{i-1} + \frac{\Delta t}{A_s} Q_{i-1}$$

The draft tube in the hydro power plant must also be simulated correctly. The draft tube is designed to convert the kinetic energy from the runner to pressure energy in the draft tube outlet. The author utilized the continuity and momentum equation for an expanding section to simulate the draft tube. In ‘‘Wylie and Streeter’’ a suggestion on MOC form of an expanding section is described. However, the author of this paper found this suggestion to not work properly in the simulation model and decided to develop a new suggestion based on the same equations. The equations used for simulating an expanding section in this model is:

$$Q_i = \frac{\frac{g}{a}(H_{i-1} - H_{i+1}) + \frac{1}{2}Q_{i+1}\left(\frac{1}{A} + \frac{1}{A_{i+1}}\right) + \frac{1}{2}Q_{i-1}\left(\frac{1}{A} + \frac{1}{A_{i-1}}\right)}{\frac{1}{A} + \frac{1}{2A_{i+1}} + \frac{1}{2A_{i-1}}}$$

$$H_i = H_{i-1} - \frac{a}{g} \left[ \frac{Q}{A} - \frac{Q_{i-1}}{A_{i-1}} - \frac{1}{2}(Q + Q_{i-1}) \left( \frac{1}{A} - \frac{1}{A_{i-1}} \right) \right]$$

The reader is referenced to the authors project or master thesis in order to see the development of this suggestion.

The turbine is simulated using Torbjørn Nielsens turbine model as suggested in [1], [2] and [3]. Here the torque and momentum equations is described as:

$$\frac{T_g}{T_r} = -T_a \frac{d\omega}{dt} + \tilde{q}(\tilde{m}s - \psi\tilde{\omega})\eta_h - R_m\tilde{\omega}^2 - m_d \frac{d\delta}{dt}$$

$$T_{wt} \frac{dq}{dt} = h - \left(\frac{q}{\kappa}\right)^2 - \sigma(\tilde{\omega}^2 - 1)$$

These two equations describe the dynamic behavior of the turbine.  $q$ ,  $h$ ,  $\kappa$  and  $\tilde{\omega}$  are the dimensionless flow, head, opening degree and rotational speed of the turbine.  $T_a$  and  $T_{wt}$  are time constants defining the acceleration time of the rotating masses and inflow time of masses of water.  $R_m$  and  $m_d$  are loss and dampening constants.

In order to perform tests on the system while it is connected to the grid, the generator and grid behavior is simulated as:

$$E = K\phi \omega$$

$$T_g = K\phi I \cos \varphi$$

$$\frac{T_g}{T_r} = \frac{\sin \delta}{\sin \delta_r}$$

$$\frac{d\delta}{dt} = \frac{\text{poles}}{2} \omega_t - \omega_{grid}$$

$\delta$  is the angle between the stator and rotor,  $K\phi$  is the magnetic flux of the generator and  $T_g$  is the generator torque.  $E$  is the voltage,  $I$  is the current and  $\cos \varphi$  is the power factor.

The system is governed by two regulating equations. One describing the voltage regulation on the generator and another describing the speed regulation on the turbine. The turbine is governed by a PID regulator with a gain of  $K_p$ , integral time  $T_i$  and derivation time  $T_d$  on serial form:

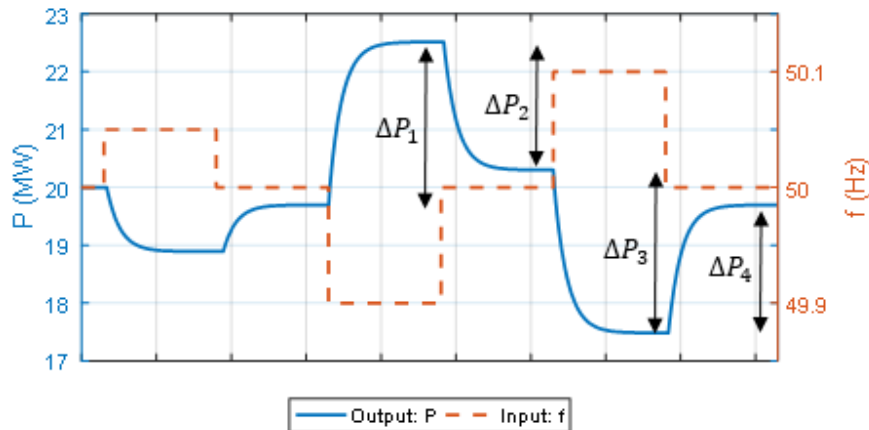
$$\frac{dK\phi}{dt} = -\frac{1}{\delta_{tg}E_r} \frac{dE}{dt} + \frac{1}{\delta_{tg}T_{ig}E_r} \left( E_r + \frac{1}{\delta_{bg}I_r} (I - I_r) - E \right)$$

$$\frac{d\kappa}{dt} = -K_p \frac{d\omega}{dt} + \frac{K_p}{T_i} \Delta\omega - K_p T_d \frac{d^2\omega}{dt^2} - T_f \frac{d^2u_d}{dt^2} + \delta_b \frac{\kappa_r - \kappa}{dt}$$

$T_f$  is the filter time constant, which filters out some of the responses from the derivative term, making the response of the system less noisy.  $\delta_b$  is the droop of the system,  $\delta_{tg}$  and  $\delta_{bg}$  is the transient and permanent droop of the generator.

### 3. Frequency response tests

FCR delivery is divided into two categories: FCR-N and FCR-D. FCR-N is the normal containment reserve and is activated at frequency deviation  $\pm 0.1$ Hz from the nominal frequency of 50 Hz. FCR-D is the disturbance frequency containment reserve which again can be divided into upwards and downwards regulation. This reserve is activated at frequencies from 50.1-50.5 Hz for upwards regulation and 49.9-49.5 Hz for downwards regulation. Both categories are subjected to step response tests at maximum and minimum loading where FCR is provided. These tests are performed to show the possible effect of backlash or other nonlinearities. FCR-N is tested at a range between 49.9-50.1 and is used to determine the capacity of the normal reserve.



From the step response, the total backlash and capacity can be obtained:

$$2D = \frac{|\Delta P_1 - \Delta P_2| + |\Delta P_3 - \Delta P_4|}{2}$$

$$C_{FCR-N} = \frac{|\Delta P_1| + |\Delta P_3| - 2D}{2}$$

For setpoints in between these maximum and minimum, the capacity can be found through interpolation:

$$C(P_{sp}) = C_{min} + (C_{max} - C_{min}) \frac{P_{sp} - P_{min}}{P_{max} - P_{min}}$$

The capacity will change with the set point and is limited by the minimum and maximum values for FCR. Therefore, the capacity need to be recalculated to reflect the actual value at different set points:

$$C_{FCR-N} = \max[\min(P_{max} - P_{sp}, P_{sp} - P_{min}, C(P_{sp})), 0]$$

For the sinusoidal tests performed later, a normalization factor, e, is utilized. In order to find this factor, the average of active power, without backlash, is calculated as follows:

$$\Delta P_{no-backlash} = \frac{|\Delta P_1| + |\Delta P_3|}{2}$$

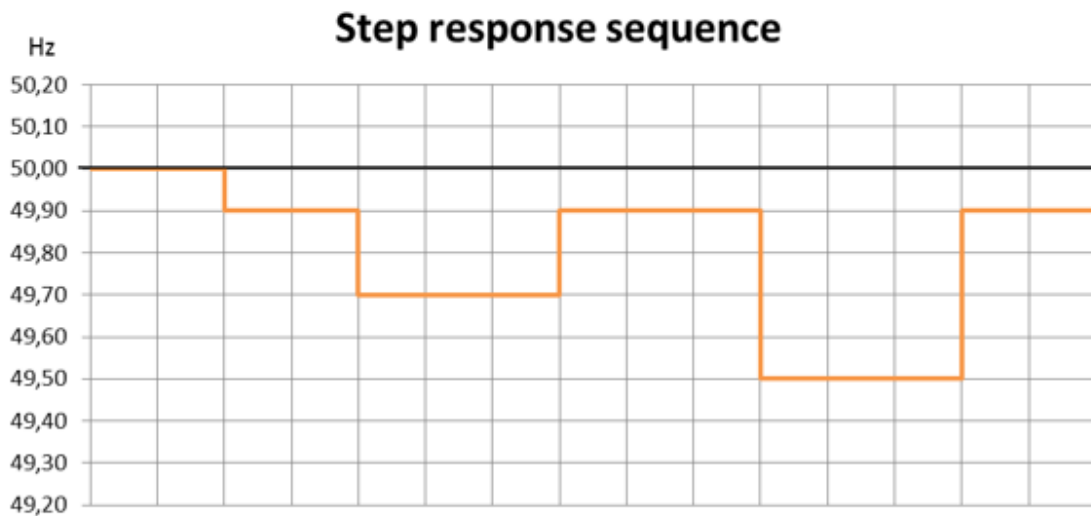
Then the total backlash per unit is:

$$2D_{pu} = \frac{|\Delta P_1 - \Delta P_2| + |\Delta P_3 - \Delta P_4|}{2 \Delta P_{no-backlash}}$$

The total backlash is not allowed to be over 0.3 pu. Based on the value above, the backlash-scaling factor, h, can be obtained from tables. Then the normalization factor e is:

$$e = h \Delta P_{no-backlash}$$

For FCR-D the step response test depend on whether the unit is utilized for upwards or downwards regulation. The upwards regulation is utilized as follows:



The sequence for the downwards regulation mirrors the upwards one.

The maintained capacity of the FCR-D provider can be calculated using the maximum and minimum power of the generating source and the capacity of FCR-N of the unit:

$$C_{FCR-D,upward} = \max \left[ \min(P_{max} - P_{sp} - C_{FCR-N}, C(P_{sp})), 0 \right]$$



$$C_{FCR-D,downward} = \max \left[ \min(P_{Sp} - P_{min} - C_{FCR-N}, C(P_{Sp})) , 0 \right]$$

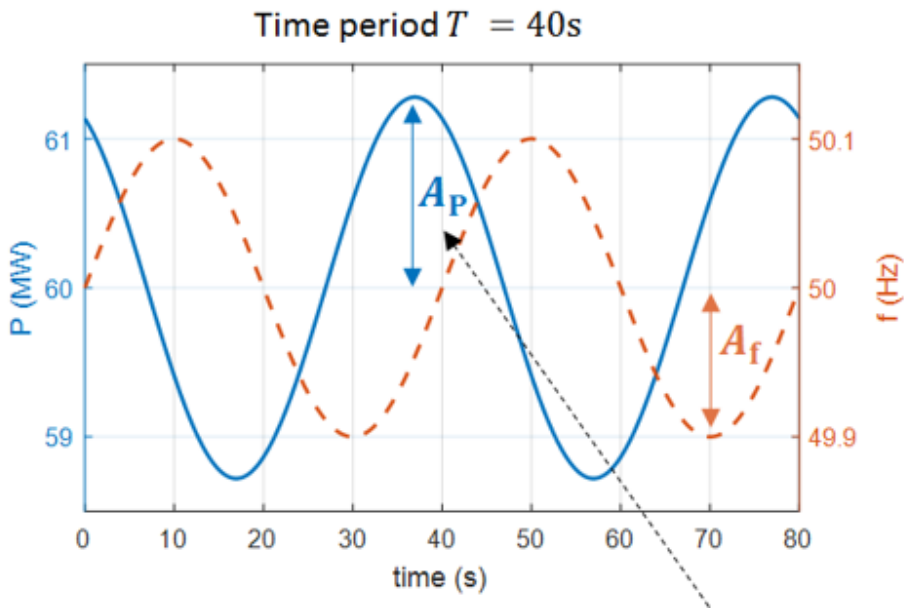
The step response test is used to determine the FCR-N capacity of the unit. In order to test the performance and stability of the plant, a sinusoidal frequency is applied with different time periods. Each time period corresponds to an angular frequency of:

$$\omega = \frac{2\pi}{T}$$

From the tests, the gain and phase angle can be obtained by

$$|FCR(j\omega)| = \frac{A_p}{A_f}$$

Where  $A_p$  is the amplitude of the measured sinusoidal power signal and  $A_f$  is the amplitude of the injected sinusoidal frequency signal.

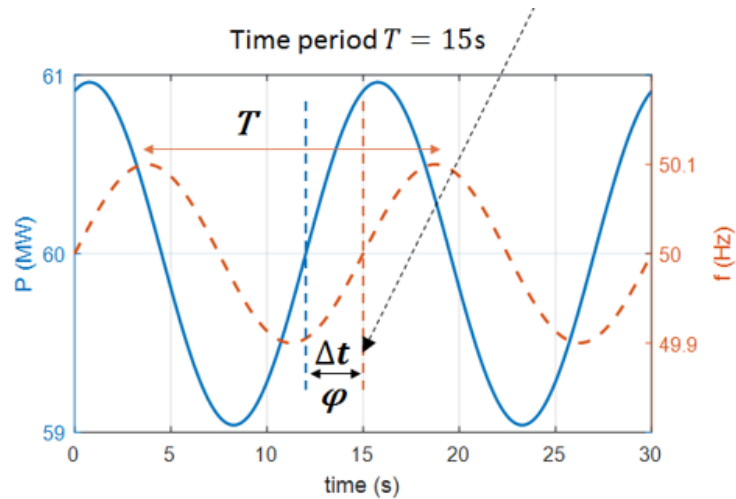


The normalized gain is found by the normalization factor from the step response test:

$$|F(j\omega)| = \frac{|FCR(j\omega)|}{e}$$

The phase shift is obtained by using the time difference between the two signals

$$\varphi = \Delta t \frac{360^\circ}{T}$$



The gain and phase can be plotted in a Bode diagram and analyzed, and as such, the phase and gain margin can be found. The expression can, however, be developed further to find the FCR-vectors of the unit at different time periods. The vectors describe the behavior of the unit when subjected to a sinusoidal frequency and are plotted in the complex plane, where the x-coordinate and y-coordinate is a function of the gain and phase:

$$x = |F(j\omega)| \cos \varphi$$

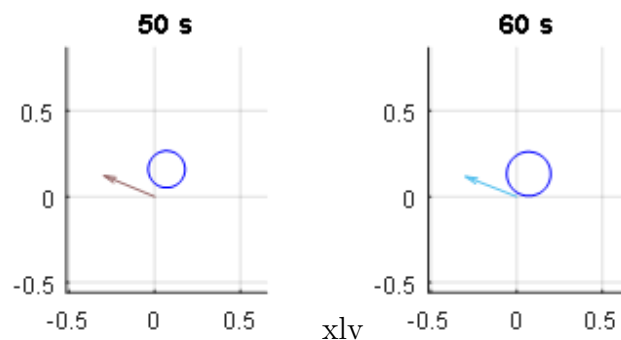
$$y = |F(j\omega)| \sin \varphi$$

For the FCR-unit to be qualified as an FCR- provider, a number of technical requirements have to be met in order to guarantee that the plant will have sufficient stationary and dynamic performance.

The stationary performance requirement states that the activated power reserve shall be linear with respect to the frequency deviation. This is also known as droop:

$$b_b = \frac{|\Delta f| P_r}{f_n \Delta P}$$

For FCR-N the dynamic performance requirement is specified by a number of pre-defined performance circles who corresponds to the time periods utilized in the sinusoidal tests. The circles are plotted with the FCR-Vectors in the imaginary plane. In order for the unit to comply with the requirement, the FCR-Vector has to point outside the corresponding requirement circles.



The power system is required to have sufficient stability margins in order to guarantee a stable system operation. Therefore, a number of predefined stability requirement circles have been predefined. As the performance requirement, the FCR-Vector needs to point outside these circles.

In addition to the step response tests as described earlier, a frequency ramp of  $\pm 0.9$  Hz with a slope of  $\pm 0.3$  Hz/s is applied to the FCR-D provider to find the capacity of the plant:

$$C_{FCR-D} = \min \left[ \frac{\Delta P_{5s}}{0.93}, \frac{E}{1.8}, \Delta P_{SS} \right]$$

Where  $\Delta P_{5s}$  is the activated power 5 seconds after the start of the ramp and E is the activated energy from the start of the ramp to five seconds after the ramp:

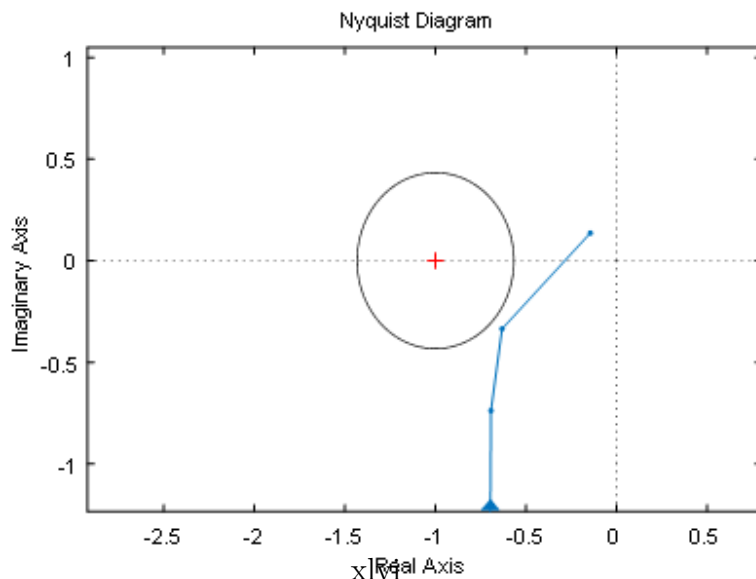
$$E = \int_t^{t+5s} P(t) dt$$

$\Delta P_{SS}$  is the steady-state FCR-D activation when the unit is subjected to a frequency step of 49-9-49.5 Hz for upwards regulation and 50.1-50.5 Hz for downwards regulation.

The stability requirement for FCR-D is similar to FCR-N, but is presented in a different manner. The FCR-Vector is multiplied with the transfer function:

$$\frac{\Delta P_{SS} 1450 MW f_0}{C_{FCR-D} 0.4 Hz S_n} \frac{1}{2Hs + K_f f_0}$$

$f_0$  is the nominal frequency of 50 Hz,  $S_n$  is 23 000 MW, H is 120 000 MWs/ $S_n$ ,  $K_f$  is 0.005 and s is the laplace variable. This multiplication gives a Nyquist curve, where the stability requirement is fulfilled if the curve does not encircle the point  $(-1, j0)$  and does not enter the circle around this point with a radius of 0.433.

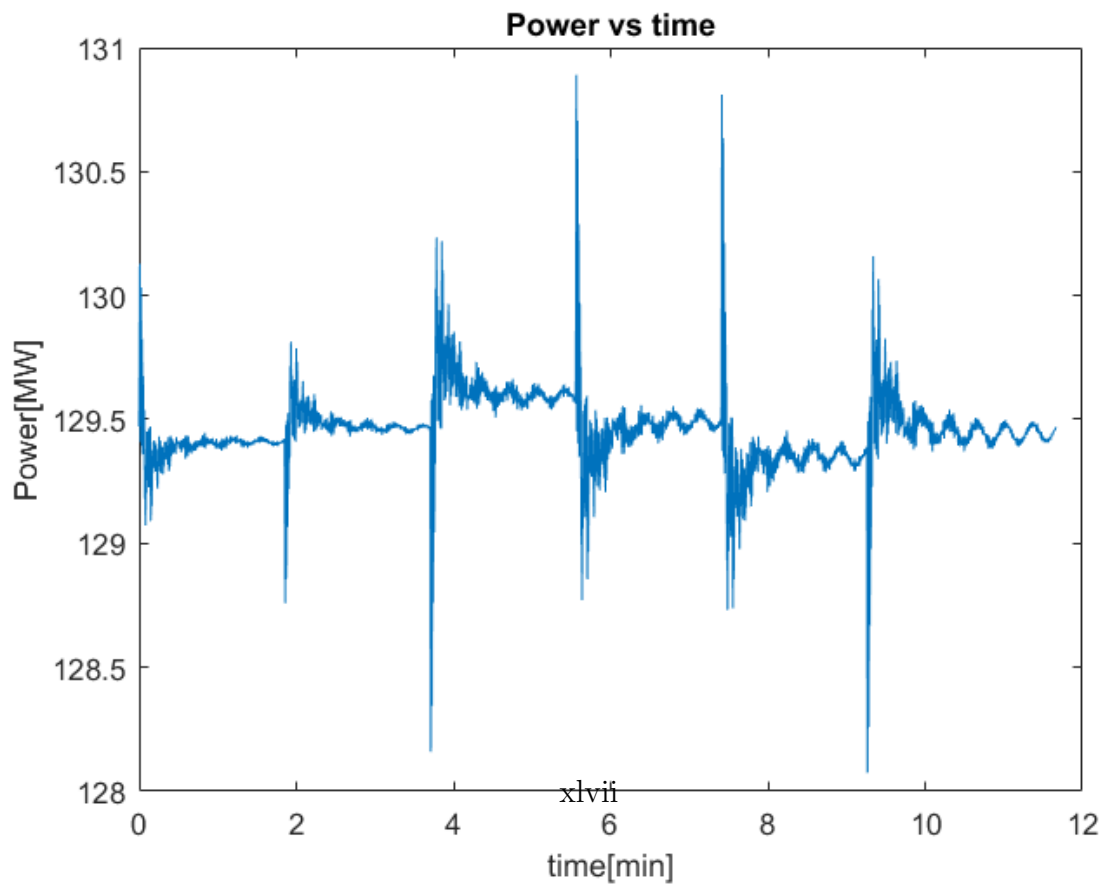


#### 4. Results and discussion

A step response sequence for FCR-N capacity is tested as described above. The parameters on the turbine is:

Test start time	0 min
Test end time	12 min
Start set point generator	129.5 MW
P-term, $K_p$	1.5
I-term, $T_i$	40 s
D-term, $T_D$	2.67 s
Filter term, $T_f$	4 s
Droop	6 %

A frequency change is applied at time 0.002 min,  $t = 1.85$ ,  $t = 3.7$ ,  $t = 5.56$ ,  $t = 7.4$  and  $t = 9.26$ .



$\Delta P_1$	$129.45\text{MW} - 130.23 \text{ MW} = -0.78 \text{ MW} = 0.78$
$\Delta P_2$	$130.23\text{MW} - 129.52\text{MW} = 0.71 \text{ MW}$
$\Delta P_3$	$129.52 \text{ MW} - 128.73 \text{ MW} = 0.79 \text{ MW}$
$\Delta P_4$	$128.73 \text{ MW} - 129.46 \text{ MW} = -0.73 \text{ MW} = 0.73$

The backlash is found through the equations described above:

$$2 D = \frac{0.07 + 0.06}{2} = 0.065 \text{ MW}$$

And the capacity in MW

$$C_{FCR-N} = \frac{0.78 + 0.79 - 0.065}{2} = 0.7525 \text{ MW}$$

Then the normalization factor is found via the average of the active power response without the contribution from the backlash and the total backlash from the unit:

$$\Delta P_{No \text{ backlash}} = \frac{0.78 + 0.79}{2} = 0.785$$

$$2 D_{PU} = \frac{0.07 + 0.06}{2 \cdot 0.785} = 0.082$$

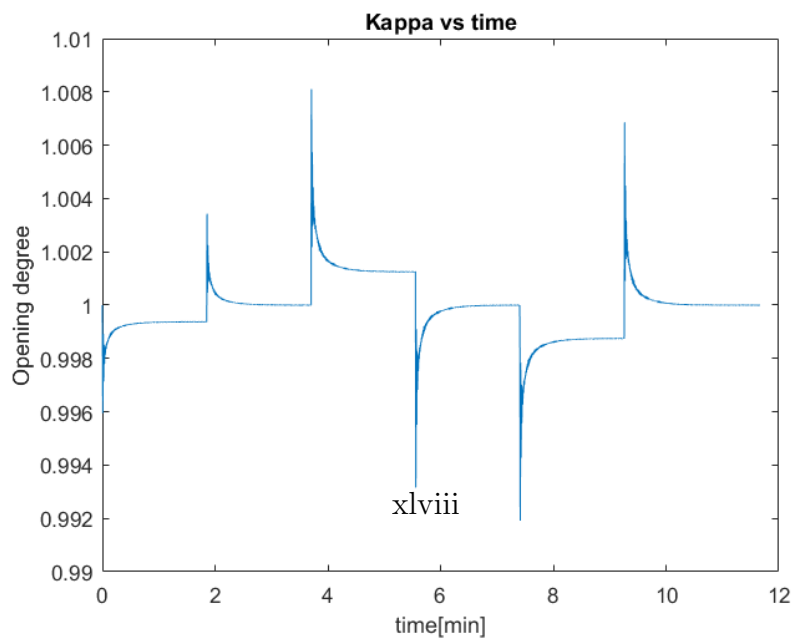
The scaling factor, h, can now be obtained from tables:

$$h = 0.988$$

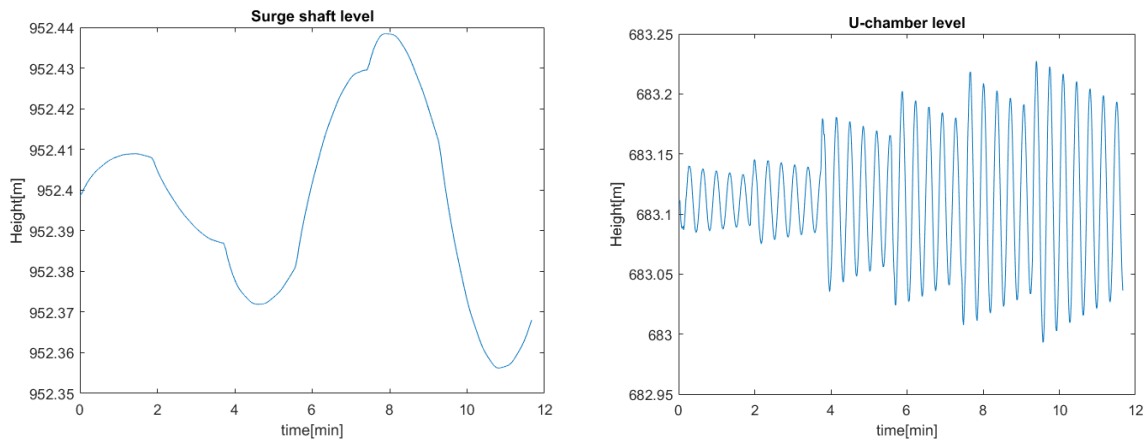
And then the normalization factor is:

$$e = 0.988 \cdot 0.785 = 0.776$$

Plot of opening degree



Plot of Surge shaft and U-chamber



## 5. Conclusion

The capacity of the unit at maximum load where FCR is provided is 0.7525 MW and the normalization factor, used for the sine sweep tests is 0.776. As the total backlash, does not exceed the value of 0.3, the system can be viewed as stable. The system seems to respond per theory to the frequency change applied, however, the power seems to oscillate quite a lot before settling. This may be due to the governor settings on the turbine, that may not provide a fast and stable enough regulation. However, looking at the height of the surge shaft and u-chamber, neither of them are outside the stability limits and there is no danger in air getting sucked into the system or flooding. Step response test for minimum loading as well as sine sweep tests must be performed to accurately decide whether this hydro power plant can be used for FCR. FCR-D capacity must also be tested. The author could also consider performing the test over a shorter amount of time as the system took less time to stabilize than expected.

## Acknowledgement

I would like to thank my supervisor Pål-Tore Storli and my co-supervisors Jørgen Ramdal and Petter Lie.

## References

- [1] Nielsen, Torbjørn, "Simulation model for Francis and Reversible Pump Turbines", NTNU 2015
- [2] Nielsen, Torbjørn, "Dynamic behavior of governing turbines sharing the same electrical grid", NTNU 1996
- [3] Nielsen, Torbjørn, "Analytical model for dynamic simulation of francis turbines – Implemented in MOC", NTNU 1992
- [4] Prequalification Working Group, entsoe, "Technical requirements for Frequency Containment Reserve Provision in the Nordic Synchronous Area", January 2017
- [5] Prequalification Working Group, entsoe, "Supporting Document on Technical requirements for Frequency Containment Reserve Provision in the Nordic Synchronous Area", January 2017

# Appendix F Risk assessment

NTNU	<b>Hazardous activity identification process</b>			Prepared by	Number	Date
 HSE				HSE section	HMSRV2601E	09.01.2013
		Approved by		Replaces		
		The Rector		01.12.2006		



**Date: 07.06.2017**

**Unit:** Department of Energy and Process Engineering

**Line manager:**

**Participants in the identification process** (including their function):

**Short description of the main activity/main process:** Master project for student Anna Afret.

**Project title:** Simulation and analysis of FCR operation of a Francis turbine

**Is the project work purely theoretical? YES**  
 requiring risk assessment are involved in the work. If YES, briefly describe the activities below. The risk assessment form need not be filled out.

*Answer "YES" implies that supervisor is assured that no activities*

**Signatures:** Pål-Tore Storli



**Student:** Anna Afret



ID nr.	Activity/process	Responsible person	Existing documentation	Existing safety measures	Laws, regulations etc.	Comment
	Numerical simulation	Anna Afret				